THERMAL AND LIGHT INDUCED METASTABILITIES IN PHOSPHORUS AND LITHIUM DOPED HYDROGENATED AMORPHOUS SILICON

by

PRATIMA AGARWAL

DEPARTMENT OF PHYSICS

INDIAN INSTITUTE OF TECHNOLOGY KANPUR

JULY, 1995

Thermal and Light Induced Metastabilities in Phosphorus and Lithium Doped Hydrogenated Amorphous Silicon

A Dissertation Submitted
in Partial Fulfillment of the Requirements
for the Degree of
DOCTOR OF PHILOSOPHY

By
PRATIMA AGARWAL

To the

Department of Physics
Indian Institute of Technology, Kanpur—208 016, INDIA
July 1995

TO MY PARENTS

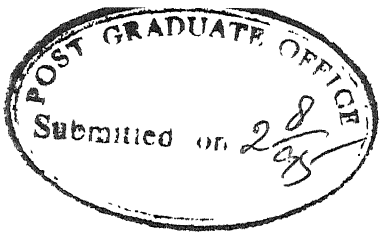

Certificate

It is certified that the work contained in this thesis entitled *"Thermal and Light Induced Metastabilities in Phosphorus and Lithium Doped Hydrogenated Amorphous Silicon"* is an original research work carried out by *"Pratima Agarwal"* under my supervision, and in my opinion it is fully adequate, in scope and in quality, as a dissertation for the degree of *"Doctor of Philosophy"*, and that this work has not been submitted elsewhere for the same.

(Dr. S. C. Agarwal)
Department of Physics
Indian Institute of Technology, Kanpur—208 016, INDIA
July 1995

Synopsis

Hydrogenated amorphous silicon (a-Si:H) is the most important and widely studied material among the disordered semiconductors. It can be made in thin film form by the glow discharge of silane (SiH_4). Unlike many other amorphous and glassy semiconductors, a-Si:H films have very low density of states ($\approx 10^{15}\ cm^{-3}eV^{-1}$) at the Fermi level ($E_f$) and can be doped by adding phosphine or diborane in silane during deposition or by in-diffusion of lithium after deposition. The material is of great interest both from physics and technological point of views, because of its potential use in fabricating devices such as photovoltaic cells, photoconductors, thin film field effect transistors, etc.

These films, however, appear to be in a metastable state, as their properties change when subjected to external perturbations. For example, exposure to light decreases conductivity (σ) of these films (Light Induced Metastability). Also, fast quenching from high temperatures ($T \geq T_E$) increases the σ of doped a-Si:H films for $T < T_E$ (Thermal Induced Metastability). T_E is identified as the equilibration temperature and varies with dopant and doping concentrations. Above T_E, σ is independent of the thermal history of the sample. Below T_E, the metastable states, obtained after fast quenching (FQ) and light soaking (LS), slowly approach the slow cooled (SC) state following a stretched exponential with thermally activated relaxation time.

The changes introduced by FQ and LS are usually reversible in nature and can be annealed at high temperatures. Since SC state can not be recovered by exposure to infra-red light, some atomic movement or structural changes are believed to be associated with these metastabilities. The cooling rate dependence of $\sigma(T)$ and slow relaxation below T_E of a-Si:H resemble the behaviour observed in glasses. The a-Si:H, therefore, has been proposed to be a Hydrogen Glass, where the movement of hydrogen is responsible for the observed metastability. The light induced metastability is also believed to be assisted by the hydrogen motion.

Although, numerous studies have been done, the origin of these metastabilities still remains unclear. Most of the studies on thermal induced changes are limited to the phosphorus doped a-Si:H (a-Si:H(P)), as the effect is large on these films. On the other hand, light induced metastability has been widely studied on undoped a-Si:H, for the same reason. Very few reports exist in literature, where both are studied on the same a-Si:H sample. Further, these studies focus mostly on the density of states measurements by sub-gap absorption, transient spectroscopy and ESR. There are a few reports which suggest a change in structure of these films after light soaking. The structural changes are, however, very small and are therefore difficult to measure.

In a-Si:H, hydrogen is distributed non uniformly, in a dilute monohydride phase and a clustered hydride phase. This may result in a spatial variation of the band gap. In addition, the charge centers may also be inhomogeneously distributed. The heterogeneities caused by the inhomogeneous distribution of hydrogen and charge centers give rise to long range potential fluctuations. These potential fluctuations play an important role in transport properties of a-Si:H.

The aim of the present study is to understand the thermal and light induced metastabilities in a-Si:H and to investigate whether the structural changes involved are similar in the two cases. We have chosen lithium doped films (a-Si:H(Li)), for the

present study, as the effect of both fast quenching and light soaking is clearly seen on these films. In addition, we have also studied undoped a-Si:H and a-Si:H(P) for comparison with literature.

Our results on undoped and P-doped a-Si:H are in agreement with the literature. Our studies show that effect of thermal and light induced metastabilities on a-Si:H(P) and a-Si:H(Li) are qualitatively similar. We also observe that in a given a-Si:H(Li) sample, T_E is the same for FQ and LS state.

The isothermal relaxation of metastable state gives the information about the barrier encountered by hydrogen during relaxation. We find that both FQ and LS states relax following a stretched exponential. However, the relaxation parameters and their temperature dependence are different in the two cases.

Thermopower (S) is sensitive to any changes in long range potential fluctuations arising from random distribution of charge centers or structural inhomogeneities. The measurement of σ and S can give an estimate of the magnitude of potential fluctuations in the material. Thus, the structural changes upon fast quenching or light soaking of a-Si:H should be reflected in $S(T)$ measurements.

Thermopower measurements $S(T)$ alongwith $\sigma(T)$ in SC, FQ and LS states have been used to obtain the information about the magnitude of long range potential fluctuations present in our a-Si:H(P) and a-Si:H(Li) films. These measurements show that both $\sigma(T)$ and $S(T)$ change after FQ and LS; however, no change in the magnitude of potential fluctuations is detected after fast quenching these films. An increase in the magnitude of potential fluctuations is observed after light soaking.

We conclude that heterogeneities play an important role and that fast quenching and light soaking affect a-Si:H in different ways. In particular, we find that FQ does

not change the magnitude of long range potential fluctuations, whereas, LS increases them.

Organization of the Thesis

The present thesis is divided in to seven chapters. A brief literature survey of metastabilities in a-Si:H and the motivation behind the present study is given in the first chapter. The theory of conductivity and thermopower is given in Chapter 2. The potential fluctuations and their influence on transport properties is also discussed in this chapter. In Chapter 3, we have summarized the existing models for the thermal and light induced metastabilities. The experimental details about the a-Si:H films preparation and characterization along with the measurement details about the conductivity and thermopower in annealed and slow cooled state and metastable FQ and LS states are included in Chapter 4. In Chapter 5, we have presented our results on the thermal and light induced metastabilities in undoped, P-doped and Li-doped a-Si:H. The measurements on conductivity, thermopower and isothermal relaxation from FQ and LS states are used to understand and compare thermal and light induced metastabilities in a-Si:H. These results have been discussed in Chapter 6. Finally Chapter 7 summarizes our results and conclusions. Some unanswered questions are raised and some further experiments which may help to understand the observed metastabilities better,are suggested in this chapter.

Acknowledgements

It is a great pleasure to express my deep sense of gratitude to Prof. S.C. Agarwal for his sincere interest, constant encouragement and invaluable guidance during the course of the present investigation.

I am indebted to Dr. Enakshi Bhattacharya for her help, guidance and encouragement during her stay at IIT Kanpur and Dr. Satyendra Kumar for taking constant interest, fruitful discussions and useful suggestion throughout the present work.

It is also a great pleasure to acknowledge

- Dr. R. Prasad and Dr. Vijay A. Singh for many helpful discussions, suggestions and keen interest in my work.
- Dr. R. Bhattacharya and Dr. P.N. Dixit for providing me a few samples, used in the present studies. I am also benefited by many helpful discussions with Dr. Dixit during his visits to IIT Kanpur.
- Dr. T.M. Srinivasan for his invaluable suggestions and tips about the fine aspects of experimental physics.
- Prof. A.K. Majumdar, Prof. D.C. Khan and Prof. O.P. Katyal for their interest in the progress of the work.
- Dr. Ramesh Chander and his associates at SSPL, New Delhi for carrying out the SIMS measurements in lithium doped samples.
- Prof. S.M. Pietruszko for helpful discussions during his visit to IIT Kanpur.

I am thankful to Mrs. Agarwal for her affection and care.

I am also thankful to Prof. B.N. Patnaik for his interest in my work and its progress and also going through a part of the manuscript.

I take this oppotunity to thank my lab-mates: Dr. A.K. Agnihotri, Dr. S.K. Tripathi Dr. Santosh Kumar, Dr. G.S. Narayana, Anil, Manju, Nazrul, Pankaj, Alok, and Joginder for their co-operation.

I am especially grateful to Dr. Tripathi for his help in sample preparation, Nazrul for the computer automation of the long relaxation measurements and Alok for sparing his set-up for the thermopower measurements. Thanks are also due to Dr. Rambilas and Mr. Rajinder for their help, whenever needed.

I am thankful to the members of Physics Work-Shop, Glass-Blowing section and Liquid-Nitrogen plant for their help in fabrication of set-up and providing me liquid nitrogen to carry out the experiments. The members of Physics department office are also duly acknowledged for their help.

My thanks are due to Mr. B.N. Srivastava for neat tracings.

It is also a great pleasure to acknowledge all my friends: Rita, Beena, Sobha, Queeny, Amitabh, Prabha, Jagdish and J.J. Das, who helped me in many ways and made my stay at IIT Kanpur a pleasant memory. I also acknowledge Ranjul and Sailaja for providing me a nice company in the hostel. The memories of Sangeeta will always be there in my heart.

A word of special appreciation to Alok, Manish and Himanshu for their interest and involvement in preparation of the manuscript in the present form and Sudhakar, Sujoy, Manish, Alok and Nazrul for carefully going through the thesis and making suggestions.

The work carried out here would not have been possible without the emotional support and constant encouragement from my parents, brothers, sister, sister-in-law and brother-in-law. I am also thankful to my nephews, whose, innocent talks and affection always relieved me from tension. It is impossible for me to express my feelings for them in words. I wish to express my deep regards to all of them.

Pratima Agarwal

Contents

List of Tables

List of Figures

Chapter 1

Introduction

Hydrogenated amorphous silicon (a-Si:H) is a promising material in amorphous semiconductor technology. The material finds its application in fabricating devices like photovoltaic cells [1], photoreceptors, photoconductors, thin film field effect transistors and many more [2]. Table 1.1 summarizes the commercially available amorphous silicon products. There are many more proposed applications of the material [2].

The main feature which distinguishes an amorphous material from its crystalline counterpart is the long range periodicity of atomic structure of the latter and the lack of this long range periodicity of the former [3]. The short range order is, however, preserved in amorphous material, which results in a similar overall electronic structure like band gap, as compared to the equivalent crystal. However, the slight variation in bond angle and bond length results in the tailing of band edges in the forbidden gap (Anderson localization). Also electronic states within the gap arise from departure from the ideal network, such as coordination defects (like dangling bonds). These defects determine many electronic properties by controlling trapping and recombination.

The presence of localized states due to disorder (band tails) and defects (dangling bonds) give rise to the density of states in the gap (see Fig. 1.1) [4]. Because of the

Table 1.1: a-Si:H Products commercially available(1989)

Device	Product
Photovoltaic cell	Calculators,watches, battery chargers, etc.
Photoreceptor	Electrophtography,LED printers.
Photoconductor, image censors and position sensitive dectors	Colour censors, light censors, contact-type image censors, electronic white boards, spatial light modulators, computor paint-brush table, etc.
Heat control layer	Heat reflecting float glass.
Thin film field effect transistors (FETs)	Displays, televisions, logic circuits for image censors.
High voltage thin-film transistors	Printers.

existence of these localized states, the energy gap loses its meaning in amorphous semiconductors. The disorder also affects the mobility of the charge carriers, which is drastically reduced in the localized states, and thus instead of energy gap, we talk of the mobility gap in amorphous semiconductors. The mobility edges demarcate the localized states and the extended states.

One of the main features, which restricts the use of amorphous semiconductors in making devices, is the presence of a large density of states in the gap ($\approx 10^{20}$ cm^{-3} eV^{-1} near Fermi level), that pin the Fermi level (E_f). Also lack of topological constraints makes the material insensitive to the impurities. The impurity atoms satisfy their natural bonding requirement as prescribed by Mott's 8-N rule and doping seems to be impossible in these materials.

The discovery in 1970s, that unlike other semiconductors, a-Si:H films prepared by glow discharge process, possess a lower density of localized states (DOS) [5] ($\approx$

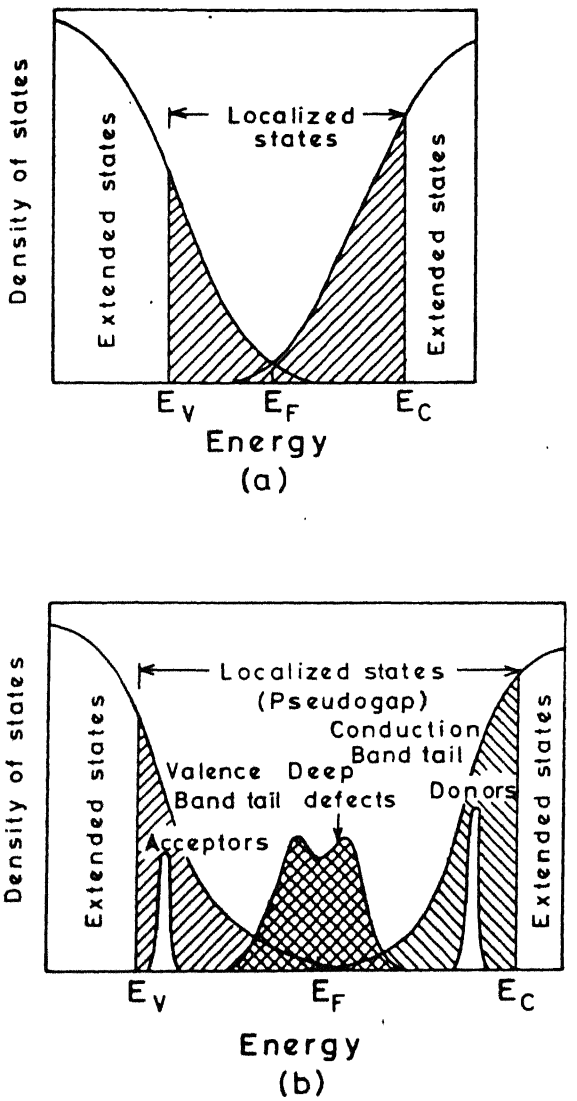

Figure 1.1: Schematic Density of States distribution in the gap (**a**) CFO Model (**b**) real amorphous semiconductors [9].

10^{15} cm^{-3} eV^{-1} near E_f) and the conductivity of the a-Si:H can be controlled over a very large range by substitutional doping from the gas phase [6,7], was a major breakthrough in the semiconductor technology. These properties of a-Si:H attracted the world wide attention of both physicists and technologists. It is believed that the presence of large concentrations of hydrogen ($\approx$ 8-10 at %) in a-Si:H passivates some of these dangling bonds and reduces the DOS near Fermi level. The Fermi level is now no longer pinned and a-Si:H can be doped.

The doping in a-Si:H remained a puzzle for a long time, as the lack of topological constraint allows impurity atoms to go in their natural coordination and thus prevent them from acting as dopants, until in 1982, Street [8] gave a modified 8-N rule. According to this, ionized phosphorus and boron atoms have a coordination number 4 and act as dopants. The doping efficiency is, however, very low and only a very small part of the total impurity atoms act as dopant. Doping increases the density of charged dangling bonds. The donor and acceptor levels are in the band tail regions. A more realistic density of state distribution is shown in Fig. 1.1 [9]. In this figure, the Fermi level drawn corresponds to the case of a perfectly compensated sample. In general, the Fermi level is situated in the upper half (lower half) of the mobility gap for n-type (p-type) samples.

1.1 Metastability

Amorphous semiconductors are prepared by rapid quenching from the vapour or liquid phase and are therefore expected to be in a state of metastable equilibrium. The electronic properties of a-Si:H *e.g.* , conductivity (σ) depend sensitively upon the external perturbations *viz.* exposure to strongly absorbing light [10], high energy electrons [11,12], ions [13] and rate of cooling from high temperatures [14]. The changes are usually reversible in nature and the metastable state introduced by any of these external perturbations can be annealed out at high temperatures. Among these metastabilities, the most important and the widely studied is the light induced

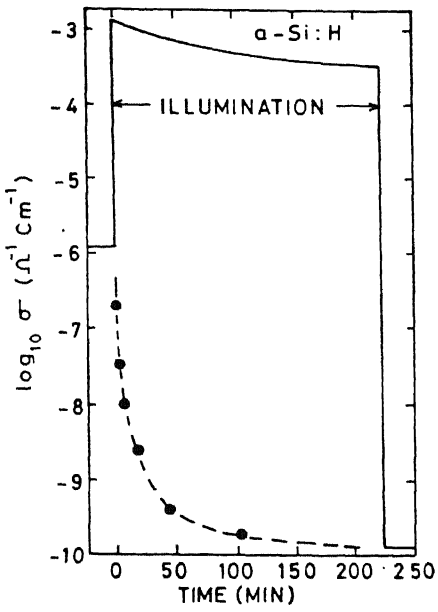

Figure 1.2: Decrease in photoconductivity (——) and dark conductivity (- - -) of a-Si:H upon light soaking [15].

metastability. The effect was first reported by Staebler and Wronski [10], who observed a decrease in dark and photoconductivity (σ and σ_{ph}) of a-Si:H films upon exposure to light (see Fig. 1.2) [15]. The decrease in σ is accompanied by an increase in activation energy (E_σ) and increase in the ESR signal and subgap absorption. This limits the use of the material as a stable photovoltaic device. Although the effect was discovered about two decades ago, its origin is not yet very clear and a lot of research is going on around the globe even today.

Another metastability, which has also attracted wide attention is the thermal induced metastability. It is observed that electronic properties of a-Si:H near room temperature depend upon the rate of cooling from high temperatures ($T \geq 450K$) (see Fig. 1.3) [16]. The observation of thermal induced metastability was first made by Ast and Brodsky [17], but it remained unexplored till Street *et al.* [14] reported on it in 1986. It is found that the effect is seen only for $T < T_E$ and for $T \geq T_E$, electronic

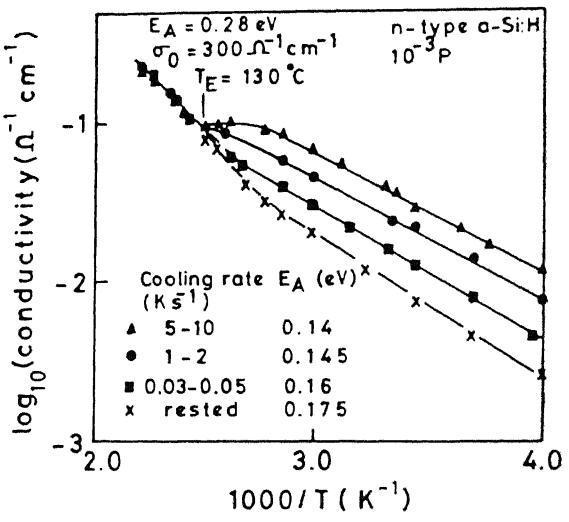

Figure 1.3: Effect of cooling rate on conductivity of P-doped a-Si:H [16].

properties are independent of thermal history of the material. The temperature T_E is identified as the equilibration temperature and depends upon the dopant and doping concentrations. For boron doped a-Si:H, $T_E \approx 90°C$, and increases to $\approx 130°C$ for P-doped and $\geq 200°C$ for undoped a-Si:H. It is generally believed that T_E depends upon hydrogen concentration in a-Si:H [18], however, there are some reports, which show that it is independent of the amount of hydrogen [19]. The effect is also observed in other a-Si:H alloys such as a-Si:Ge:H [20,21], a-Si:C:H [22] and in a-Ge:H [23].

Many models have so far been proposed to explain the thermal and light induced metastabilities and are summarized in Chapter 3. These models are based on two microscopic mechanisms i. e. , the breaking of weak Si-Si bonds **[24-27]** and the trapping of charge carriers [28] in the gap states. All the models suggest an increase in the density of states in the gap, thus limiting the use of a-Si:H in fabricating stable devices.

It has been proposed that the movement of hydrogen in rigid silicon network is responsible for observed metastabilities. Hydrogen atom hops from one bonding configuration to the other separating the defects created, which results in an increase

in the defect density. Furthermore, the cooling rate dependence of the properties of a-Si:H resemble those of glasses [29]. It has been proposed that a-Si:H is a Hydrogen Glass [30]. The dispersive nature of hydrogen diffusion and a thermally activated diffusion constant explain stretched exponential type of relaxation and a thermally activated relaxation time [30] and thus supports Hydrogen Glass model to be valid in a-Si:H (see Section 3.4). However, differential scanning calorimetry curves do not show a clear glass transition for a-Si:H [31]. Matsuo *et al.* [32] observe a peak (not a step) in DSC curve in their P-doped a-Si:H samples after fast quenching.

a-Si:H films grown by the glow discharge of Silane are not homogeneous. Proton resonance experiments by Reimer *et al.* [33] showed that in a-Si:H, $\approx$ 4 at. % hydrogen is present in a dilute monohydride phase and the rest is in a clustered hydride phase with 5-7 H atoms per cluster, which resembles a di- or trivacancy whose internal surface is dressed with hydrogen. The microstructure also depends upon the deposition conditions and dopants [34]. Phosphorus causes larger hydrogen clusters to form, whereas, boron seems to reduce clustering in these films [34]. The variation in hydrogen content in a-Si:H results in a spatial variation of the band gap [35] from 2eV in clustered phase to 1.3eV in the dilute phase. In addition to the non-uniform distribution of hydrogen (density and compositional variation), the charge centers (dopants) may also be distributed non-uniformly. These inhomogeneities modify the mobility edges and cause long range potential fluctuations in the material. These fluctuations may be both antisymmetric (density fluctuation) and symmetric (charge centers) in nature. The symmetric part of these fluctuations are shown in the Fig. (1.4) [36].

1.2 Motivation Of The Present Work

In literature, both thermal and light induced metastabilities have been ascribed to the movement of hydrogen in a-Si:H. If hydrogen is responsible for the two metastable effects, the changes introduced are expected to be the same in both fast quenched

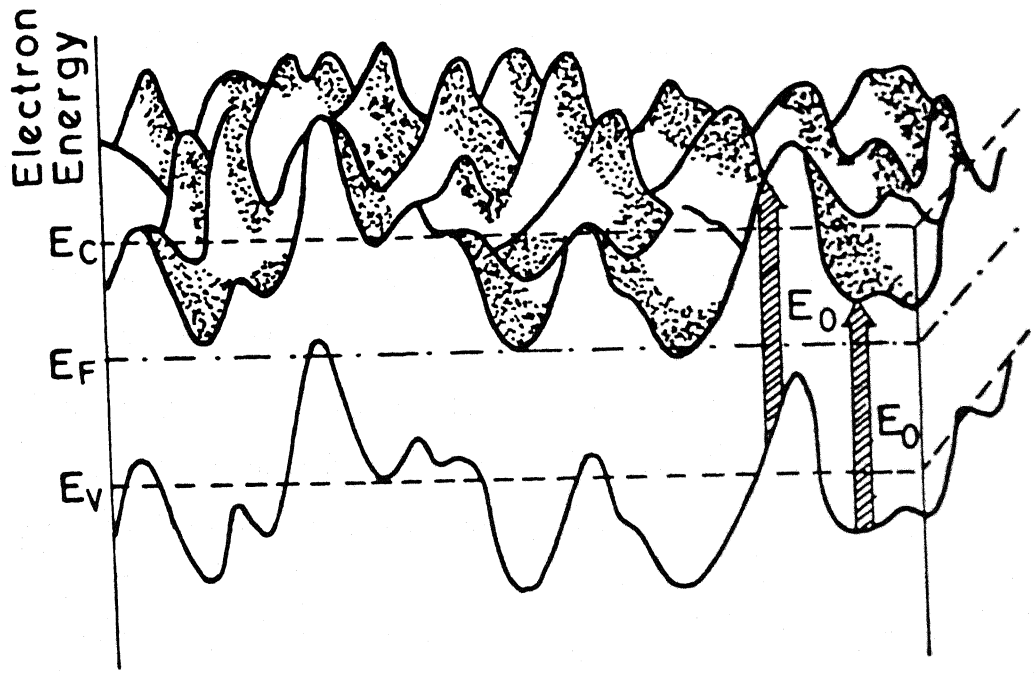

Figure 1.4: Fluctuations of mobility edges in amorphous semiconductors [36].

and light soaked state. We have already pointed out that hydrogen is distributed non uniformly in a-Si:H [33]. It is not clear, whether the metastable changes take place in the dilute or clustered phase. Since the local diffusion of hydrogen is different in dilute and clustered phases [37], it is expected that the effect of metastabilities should be different in the two phases. Street *et al.* [38] have suggested that all hydrogen atoms participate equally in the diffusion process, which means that the dissociation energies of hydrogen from a clustered or from an isolated Si-H site are the same. However, Kondo and Morigaki [39] have shown that clustered hydrogen is responsible for the light induced metastability.

A number of studies have been conducted to understand and explain the observed metastabilities (see for example the papers in the proc. of International Conference on Amorphous Semiconductors 1993, 1991, 1989 and Proc. of (annual) Material

Research Society Meeting 1990 to 1994). Most of the studies on thermally induced changes are limited to the P-doped a-Si:H (a-Si:H(P)) as the effect is large on these films. On the other hand, light induced metastability has been studied widely on undoped a-Si:H for the same reason. Very few reports exist in literature, where both are studied on the same a-Si:H films. The reports by Smith *et al.* [40] and McMahon and Tsu [41] for undoped and by Kakalios and Street [42] on doped a-Si:H suggest that the defect centers created by light and those formed during thermal equilibration process are identical. On the other hand, ESR studies by Stutzmann [43], $C-V$ and ICTS measurements by Okushi *et al.* [44,45], and photocapacitance studies by Leen *et al.* [46] show that these are independent of each other for P-doped a-Si:H. Konnenkamp and Wild [47] have shown that for P-doped a-Si:H, light soaked state relaxes slowly as compared to the fast quenched state. Thus there is disagreement in the literature.

So far we have seen that the origin of thermal and light induced metastabilities is not clear. Since both the effects are clearly visible in lithium doped a-Si:H [48], we have chosen lithium doped a-Si:H (a-Si:H(Li)) for the study of thermal and light induced changes. Lithium is an efficient interstitial donor in a-Si:H [49]. Even small changes in Li bonding configurations due to the lithium motion might be expected to result in a large change in concentration of active dopants. The thermal equilibration effects in a-Si:H(Li) might be enhanced or modified compared to those observed in a-Si:H(P).

In our studies, Li is diffused thermally in a-Si:H after film preparation. Therefore, a varying doping concentration of lithium will not result in a change in total hydrogen concentration; however, the bonding configuration may change. The thermal and light induced effects related to the bonding configurations can thus clearly be seen on these films.

Further, since H is distributed non-uniformly, the effect of fast quenching and light soaking should be different in the two phases, which may result in a structural

change in these films. It is possible that the structural changes introduced by light are different from those introduced thermally. Takada and Fritzsche [50,51] have reported a light induced increase in disorder and thus the slope of the conduction band tail, whereas, in FQ state a decrease in slope or at least a fewer states in the tail are expected.

Thermopower (S) is sensitive to any change in long range potential fluctuations arising from random distribution of charge centers or structural inhomogeneities [52]. The slope E_Q of function $Q(T)$ is a measure of the long range potential fluctuations and is sensitive to structural changes [52]. Thus, the structural changes upon fast quenching or light soaking, which may be too small to be observed directly but large enough to affect the electronic properties of a-Si:H, can be seen as a change in E_Q. These measurements, thus, can help us to separate the effect of these metastabilities on electrical properties because of change in potential fluctuations from those due to a shift in E_f as a result of the change in the density of states alone.

Recently Zhao *et al.* [53] have reported an increase in concentration of Si-H bonds after light soaking. On the basis of some other experimental observations, Fritzsche [54] has suggested photoinduced structural changes, which are in addition to the creation of dangling bonds. However, no reports on any change in structure after fast quenching are yet available. Thermopower measurements in metastable states, which can give information on long range potential fluctuations, may throw some light on these structural changes.

1.3 Organization of the Thesis

The next chapter presents the general formulation of conductivity and thermoelectric power in amorphous semiconductors. This chapter discusses the observation of kinks in the $\sigma(T)$ and $S(T)$ curves, the linear and non-linear shift of the Fermi level and potential fluctuations model to explain the difference between E_σ and E_S (E_S is

the slope of S vs. $1/T$). Some experimental evidence which support the potential fluctuation model are also discussed.

In Chapter 3, we have discussed the thermal and light induced metastabilities in a-Si:H and the models to explain them. The weak bond breaking model and charge trapping model are discussed. The role of hydrogen in the observed metastabilities and the Hydrogen Glass model for a-Si:H is also presented.

Chapter 4 describes the preparation of undoped and doped a-Si:H films by glow discharge method and doping by lithium. The characterization of these films for amorphous nature, thickness, transmission and absorption, band gap, dark and photoconductivity is also discussed. A description of the conductivity and thermopower set up, the introduction of thermal and light induced metastabilities in a-Si:H in vacuum and the measurement of conductivity and thermopower in slow cooled, fast quenched and light soaked state is given.

In Chapter 5, the effect of thermal and light induced metastabilities on conductivity and thermopower of undoped, phosphorus and lithium doped a-Si:H are presented. The results of isothermal relaxation of the slow cooled state after light soaking and fast quenching are also given. It is seen that light soaking reduces the conductivity of undoped and lithium doped a-Si:H, whereas, fast quenching increases the conductivity of both phosphorus and lithium doped a-Si:H. A decrease in photoconductivity of undoped a-Si:H is also observed as a result of fast quenching, whereas, the dark conductivity of these films does not show any measurable change. Both light and thermal induced metastable states in a-Si:H(Li), slowly relax to the slow cooled state at temperature below equilibration temperature and relaxation time is thermally activated. Further, the light and thermal induced states relax at different rates although a common transition temperature T_E is observed for the two states. The activation energy for relaxation for the two states is also observed to be different and is higher for light soaked state. The low lithium doped films have a higher T_E and a larger relaxation time and thus have a similarity with the reported results

for a-Si:H(P). Our results show that both phosphorus and lithium act as donors in a-Si:H. It is further observed that both the magnitude and slope of thermopower change upon light soaking as well as fast quenching.

In Chapter 6, the results of conductivity, isothermal relaxation and thermopower have been discussed in the light of the existing models. It is seen that both P and Li doping show similar quenching and light soaking effects. Thus, models for the observed metastable effects in a-Si:H(P) have been used to explain the results of a-Si:H(Li). Further, it is observed that light soaking and fast quenching are independent of each other. Thermopower results show that light soaking causes an increase in potential fluctuations whereas no effect of fast quenching is found on them for both phosphorus and lithium doped a-Si:H.

Chapter 7 summarizes the results and conclusions of the present study. Directions for further work, which may help in understanding the light and thermal induced metastabilities is also suggested in this chapter. Finally, the references from the literature are listed at the end of the thesis.

Chapter 2

Theory

The lack of long range periodicity gives rise to the localized states in amorphous semiconductors. This leads to the tailing of the bands. In addition, localized defect states, *e.g.* , dangling bonds are also present in the middle of the gap. The mobility edges E_c and E_v for electrons and holes separate the localized states from those that are extended. The transport processes can be divided in several categories [3,55].

1. Conduction in extended states.
2. Conduction in band tail states via phonon assisted hopping.
3. Conduction near Fermi level.

However, in a-Si:H, in the temperature range of interest to us ($200K \leq T \leq 500K$), electrons in conduction band are the majority carriers and process (1) is dominant.

2.1 Kubo–Greenwood Formula

The general expression for conductivity (σ), assuming conduction by either electrons or holes, can be written as [3,56]

$$\sigma = \int \sigma(E)\,dE = e\int g(E)\,\mu(E)\,f(E)\,[1 - f(E)]\,dE \tag{2.1}$$

where $g(E)$ is the density of states, $\mu(E)$ is the mobility and $f(E)$ is the Fermi distribution function. For electrons in the conduction band

$$\sigma = \sigma_0 \exp\left(-\frac{E_c - E_f}{kT}\right) = \sigma_o \exp\left(-\frac{E_\sigma}{kT}\right) \tag{2.2}$$

where 'k' is the Boltzmann constant. E_c and E_f are the conduction band mobility edge and Fermi level respectively. E_σ $(= E_c - E_f)$ is the activation energy for conductivity. The prefactor σ_0 depends upon the mobility (μ) of charge carriers and the density of states at mobility edge (N_c).

2.2 Thermopower

The conductivity (σ) measurements alone can not give information about the type of charge carriers and the conduction mechanism in semiconductors. In crystalline semiconductors, the Hall Effect is an important probe to determine the type of charge carriers, whereas, in amorphous semiconductors, because of the observed sign anomaly, the Hall effect is not a reliable tool [57,58]. Here the conductivity (σ) and thermopower (S) measurements together can provide the information about the type of majority charge carriers and the dominant conduction mechanism.

Fritzsche [56] in 1971 gave a general expression for the thermopower for the case when no inelastic scattering process occurs. In this case, it is assumed that the contributions to the current from states at different energies are independent of each other. Thermopower (S) is related to the Peltier coefficient 'Π' as [59]

$$S = \frac{\Pi}{T} \tag{2.3}$$

where Π is the energy carried by the electrons per unit charge. The energy carried is measured relative to the position of the Fermi energy E_f. Each electron contributes

to Π in proportion to its relative contribution to the total conductivity. Thus Peltier energy (Π) and thermopower (S) can be written as [56]

$$\Pi = -\frac{\int (E - E_f)\, \sigma(E)\, dE}{e \int \sigma\, (E)\, dE} \tag{2.4}$$

$$S = -\frac{k}{e\, k\, T\, \sigma} \int (E - E_f)\, \sigma(E) dE \tag{2.5}$$

where e is the electronic charge. The sign of S is such that $S \leq 0$ for electrons at energies $E \geq E_f$. In the case of extended band conduction, Eq. (2.5) gives

$$S = -\left(\frac{k}{e}\right)\left[\frac{(E_c - E_f)}{kT} + A\right] = -\left(\frac{k}{e}\right)\left[\frac{E_S}{kT} + A\right] \tag{2.6}$$

E_S is the characteristic energy associated with the thermopower. The heat of transport term 'A' is related to the average energy of charge carriers and is determined by the carrier scattering process. If $g(E)$ and $\mu(E)$ in Eq. (2.1) are constant, i.e. , independent of energy, then $A = 1$. For temperature dependent scattering processes, A will depend upon temperature [56].

Eqs. (2.2) and (2.6) are valid if electrons are the majority charge carriers. Similar expressions can be written for the case when holes are the majority carriers and conduction takes place in valence band. The sign of S for this case will be positive.

2.3 Kink in $\sigma(T)$ and $S(T)$

From Eqs. (2.5) and (2.6), it appears that $\log \sigma$ vs. $1/T$ and S vs. $1/T$ will yield straight lines with equal slopes $E_\sigma = E_S = E_c - E_f$. However, it is often observed [60–65] that the $\log \sigma$ vs. $1/T$ and S vs. $1/T$ for the a-Si:H films exhibit a kink. The slopes of the two curves above and below the kink temperature are different.

Various reasons are given in the literature for the kink. Among these, the main reasons are:

1. a change in conduction path [3] at the kink temperature,

2. shift of band edges with temperature [66] and

3. statistical shift of the Fermi level [7,60,64].

The possibility of any change in the conduction path is ruled out in a-Si:H as no drastic change in the drift mobility of the charge carriers around the kink temperature is observed, when measured using Surface Acoustic Wave technique [51]. The temperature dependence of band edges is also very small [67]; and it cannot account for the observed changes in slopes of the $\log \sigma$ vs. $1/T$ and S vs. $1/T$ curves. However, the statistical shift of the Fermi level can account for the kink. Since the density of states (DOS) below and above the Fermi level is not symmetric in a-Si:H [68], it is expected that at high temperatures, the Fermi level will move towards mid gap and might be reflected as a kink in the $\log \sigma$ vs. $1/T$ curve.

It can be easily shown that a linear shift of E_f with temperature will not give a kink. For a linear dependence on T, E_f can be written as

$$E_f(T) = E_f(0) - \gamma T \tag{2.7}$$

$E_f(0)$ is the value of E_f extrapolated to $0K$ and γ is the temperature coefficient.

Substituting Eq. (2.7) in Eq. (2.2) and Eq. (2.6), we get the expression for σ and S as

$$\sigma = \sigma_0 \exp\left(-\frac{\gamma}{k}\right) \exp\left(-\frac{E_c - E_f(0)}{kT}\right) \tag{2.8}$$

$$S = -\left(\frac{k}{e}\right)\left[\frac{E_c - E_f(0)}{kT} + \frac{\gamma}{k} + A\right] \tag{2.9}$$

Thus we see that the observed slopes of $\ln \sigma$ vs. $1/T$ and S vs. $1/T$, $(E_c - E_f(o))$ will differ from the actual slopes $(= E_c - E_f(t))$ by a magnitude γ. It is also expected that the intercepts at $1/T = 0$ obtained from Eq (2.8) and Eq(2.9) will not be the true values of σ_0 and A. However, no kink should be observed in $\sigma(T)$ or $S(T)$. Thus, even if there is a statistical shift of the Fermi level, the observation of the kink

cannot be explained if the shift is linear with temperature. Therefore, we examine if the observed kink can be due to a non linear statistical shift of the fermi level with temperature. Beyer and Overhof [52] approximated the non linear shift of E_f with T by

$$E_f(T) = E_{f,i}(0) - \gamma_i T \tag{2.10}$$

where i = 1,2,3 with three different values of γ_i and $E_{f,i}(o)$ in three different temperature regimes. Inserting Eq. (2.10) in Eq. (2.8) we get,

$$\sigma = \sigma_0 \exp\left(-\frac{\gamma_i}{k}\right) \exp\left(-\frac{E_c - E_{f,i}(0)}{kT}\right) \tag{2.11}$$

giving

$$\sigma_{0,i} = \sigma_0 \exp\left(-\frac{\gamma_i}{k}\right) \tag{2.12}$$

and

$$E_{\sigma,i} = E_c - E_{f,i}(0) \tag{2.13}$$

Thus we see that a non linear shift of E_f with temperature can account for the observed kink in the $\ln\sigma$ vs. $1/T$ and S vs. $1/T$ plots.

2.4 Difference between E_σ and E_S : The Q function

From the above discussion 2.3, it is expected that any shift of E_f with temperature must give the same slope in both the measurements. As already mentioned, it is often observed that the slopes E_σ of $\ln\sigma$ vs. $1/T$ and E_S of S vs. $1/T$ in the same temperature range are not identical. A difference between E_σ and E_S implies that the characteristic energy associated with the thermopower is not exactly the same as

the activation energy of conductivity [29]. This may result when conduction takes place in the localized band tail states via hopping [56] or the thermally activated mobility [56] ($\mu = \mu_o \exp(-E_\mu/kT)$). The conductivity in both the cases is given as

$$\sigma = \sigma_o \exp\left(-\frac{E_\mu}{kT}\right) \exp\left(-\frac{E_c - E_f}{kT}\right) \tag{2.14}$$

On the other hand, in the general expression for S (Eq 2.5), any energy independent term appearing in the expression for σ will cancel out. Thus, the thermopower (S) is still given by Eq(2.9). Comparing Eq(2.14) and Eq(2.9), we see that E_σ will be more than E_S, such that

$$E_\sigma - E_S = E_\mu \tag{2.15}$$

There can be several other reasons for a difference between E_σ and E_S [69] such as

1. both electrons and holes are conducting, in which case, these contribute to the thermopower with opposite sign, but have the same sign in conductivity. This effect may be important in undoped a-Si:H, where Fermi level is near the middle of gap, but does not contribute in doped material, when one sign of carriers completely dominate.
2. conduction is assisted by polarons, however, it does not get much support in a-Si:H [69].
3. mobility edge is not very sharp [70]
4. conductivity is not spatially homogeneous. This may be due to the heterogeneities in the material, such as, the growth inhomogeneities, density potential or random distribution of charge centers [36], which may give rise to the potential fluctuations in the material.

In order to eliminate the effect of statistical shift of E_f or band gap shrinkage on transport properties, Beyer *et al.* [71] defined a function 'Q' which is a linear combination of $\ln\sigma$ and S.

$$Q = \ln \sigma + \frac{e\,S}{K} \tag{2.16}$$

Substituting for σ and S from Eq (2.2) and Eq (2.6), we get, for $E_\sigma = E_S$

$$Q = \ln \sigma_0 + A \tag{2.17}$$

If E_σ and E_S are different

$$Q = \ln \sigma_0^* + A^* - \left(\frac{E_\sigma - E_S}{kT}\right) \tag{2.18}$$

or

$$Q = Q_0 - \frac{E_Q}{kT} \tag{2.19}$$

where $E_Q = E_\sigma - E_S$.

We see that Q is independent of the position of the Fermi level. Thus Q is expected to remain unaffected due to the statistical shift of the Fermi level or shift in E_f due to any other agency, *e.g.* , doping. Any structure present in σ(T) and $S(T)$ should, therefore, be washed out in $Q(T)$ if movement of E_f with T is responsible for it. For many cases [52], it is indeed observed that the kink does not appear in $Q(T)$.

The temperature dependence of Q can come only from σ_0^* or A^* or both (Eqs 2.2 and 2.6). Physically, this could mean a temperature dependent mobility $\mu(T)$ which might indicate the presence of the potential fluctuations.

In order to explain the observed difference between E_σ and E_S, Dohler [70] proposed a model based on the assumptions of a soft mobility edge. In this model, σ(E) is expected to vary by orders of magnitude with temperature. It is also assumed in this model that the density of state picture remains the same irrespective of doping. This model is capable of explaining the difference between E_σ and E_S and thus a nonzero value slope of E_Q, but the shape of $Q(T)$ is very sensitive to σ(E) and thus to the doping, which is not experimentally observed. This extreme sensitivity of $Q(T)$ on σ(E) makes this transport model rather unsuitable [52]. This leaves us with

the only possibility, that the observed difference between E_σ and E_S is due to the presence of potential fluctuations in the material.

2.5 Potential Fluctuations Model

In order to explain the observed difference between E_σ and E_S, Overhof and Beyer [72] proposed a model based on the presence of the long range potential fluctuations in the material which modify the mobility edges. These potential fluctuations can arise from the local density fluctuations, growth inhomogeneity and electric field due to charged centers [36]. The local variation in density and composition will produce amongst the other things, spatial variation or the so called 'elastic fluctuations' in the band gap [3]. In addition, the spatial variation of charge density due to the presence of the charged voids and the impurity atoms (dopants) may result into the potential fluctuations of electrostatic nature (see Fig. 2.1) [3].

In this model [72], it is assumed that the transport is due to the electrons in the conduction band above the mobility edge. The energy of this mobility edge, however, is taken to fluctuate in space owing to the presence of long range disorder. Model calculations for σ and S are done both for two- and three-dimensional cases. In these calculations, the sample is sub-divided into small cells. In each cell, the mobility edge is at constant energy and is determined by the mean disorder potential within the cell. The calculations are done for two different limiting cases [72]:

1. disorder in neighbouring cell is purely uncorrelated,
2. disorder is due to the long range part of the Coulomb potential of charged centers distributed at random in the material, thus disorder in neighbouring cells is not uncorrelated.

It is found [72] that in the first case, for the experimentally observed value of $E_Q = (E_\sigma - E_S) \approx 0.2eV$, the fluctuations of E_c of at least $1eV$ is required for

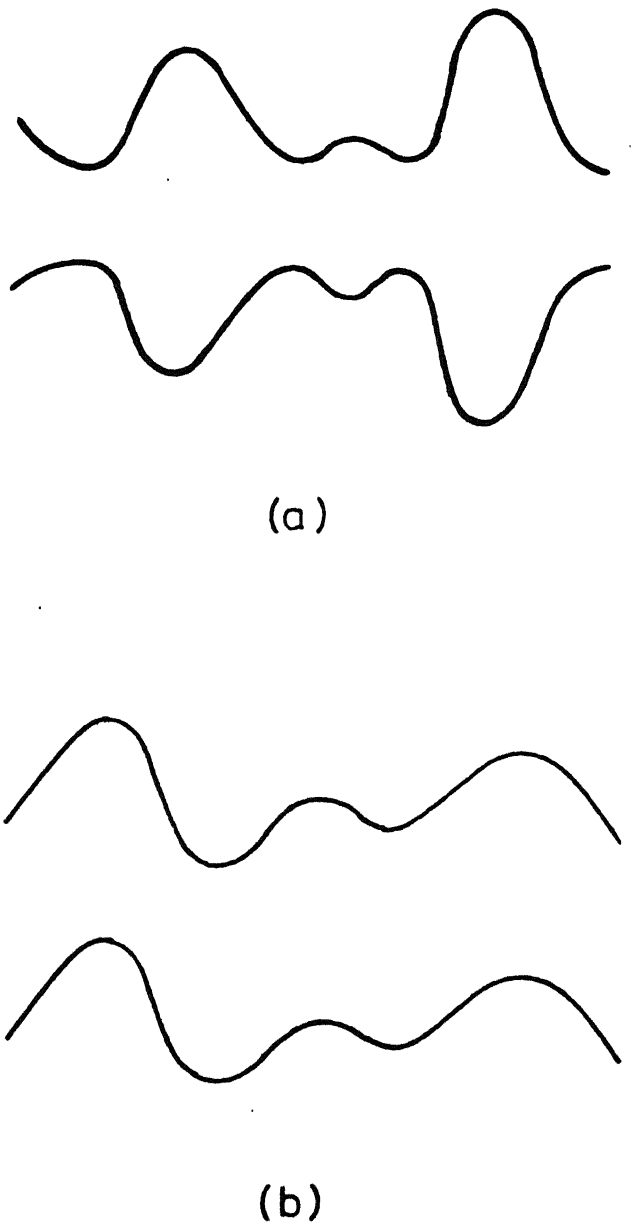

Figure 2.1: Possible forms of spatial fluctuations in the band edges of amorphous semiconductors: (a) Elastic; (b) Electrostatic [3].

all three dimensional models. This value is unreasonable, as the width of the potential fluctuations must be small compared to that of the pseudo-gap [72]. However, in the second case, where the fluctuations in E_c arise due to the random distribution of charge centers, the calculations show that the resulting distribution function $p(E_c)$, for E_c is asymmetric. The width of the $p(E_c)$ increases with the density of charge centers. The calculated E_Q is approximately equal to the half width of $p(E_c)$, thus giving reasonable values of the required fluctuations necessary for the observed difference between E_σ and E_S [72].

The potential fluctuations due to a random distribution of point charges can be calculated as follows [72]. If N_c is the charge density, then within a volume of dimension L, the average charge will be $N_c L^3$. A statistical deviation (ΔN_c) from the average

$$\Delta N_c = \left(L^3 N_c\right)^{1/2} \tag{2.20}$$

will give rise to the potential fluctuation of magnitude

$$\Delta V = \frac{\Delta N_c\, e}{4\pi\epsilon\epsilon_0 L} \tag{2.21}$$

Putting ΔN_c from Eq. (2.20), Eq. (2.21) becomes

$$\Delta V = \frac{e\,(LN_c)^{1/2}}{4\pi\epsilon\epsilon_0} \tag{2.22}$$

The calculated values of E_Q, when plotted against $(N_c)^{1/2}$ yield a straight line except for small N_c values and fit to the equation [72]

$$E_Q = 0.83eV(LN_c)^{1/2} \tag{2.23}$$

At low N_c values, the deviation from the average becomes smaller and causes a smaller value of E_Q than that expected from Eq. (2.23).

It appears from Eq. (2.22) that potential fluctuations will increase indefinitely with the size of the volume considered, which is, of course, unphysical. The fluctuations are limited by the screening from the mobile carriers and the size of the cell is determined by the screening length [69,72]

$$L_{screen} = \left(\frac{8\pi\epsilon\epsilon_0}{ne}\right)^{1/2} \tag{2.24}$$

where n is the density of the mobile carriers. Combining Eq (2.23) and (2.24), we get

$$\Delta V = \left(\frac{2N_c^2 e^3}{(4\pi\epsilon\epsilon_0)^3 n}\right)^{1/4} \tag{2.25}$$

The potential fluctuations, therefore, increase with increasing the density of the fixed charges, but decrease with the increasing density of the free (mobile) charges. Overhof and Beyer [73] showed that the function $Q(T)$ can be fitted to a straight line for $\Delta \geq 3kT$, as

$$Q(T) = \ln \sigma_0(T) + A(T) + 1.8 - 1.25\Delta/kT \tag{2.26}$$

where $Q(T)$, $\ln \sigma_0(T)$ and $A(T)$ are obtained from the model calculations. Comparing Eq. (2.26) and Eq. (2.19), we see that

$$E_Q = 1.25\Delta \tag{2.27}$$

In the high temperature limit, where $\Delta < 3kT$, E_Q is found to be zero and E_σ approaches E_S. In a similar way for $\Delta \geq 3kT$, one can approximate [73]

$$\ln\left(\frac{\sigma}{\sigma_0}\right) = -\frac{(E_c - E_f)}{kT} - 0.2 + 0.25\frac{\Delta}{kT} \tag{2.28}$$

and

$$\frac{cS}{k} = \frac{(E_c - E_f)}{kT} + A + 2 - \frac{1.5}{kT} \tag{2.29}$$

From Eqs. (2.28) and (2.29), we see that the effect of potential fluctuations are more on S than on σ.

It is further shown that the potential fluctuations arising due to the charge centers can account for the experimentally observed difference between E_σ and E_s for the phosphorus doped, boron doped and compensated a-Si:H films [52]. The magnitude of potential fluctuations Δ is expected to be in the range of $0.05 \leq \Delta \leq 0.20eV$. It has also been observed that the general shape of $Q(T)$ remains unaffected by the doping and only E_Q changes.

The above calculations were performed for the case when charged centers are present in a-Si:H films. However, a-Si:H films can grow in an inhomogeneous way [74] with hydrogen distributed randomly. These growth inhomogeneities are the main reason for the potential fluctuations in undoped and lightly doped a-Si:H. For highly doped samples, however, the charged donors (acceptors) will cause additional fluctuations to occur [73].

2.6 Evidence for Potential Fluctuations in a-Si:H

Goldie *et al.* [75] used potential fluctuations to explain the decrease in drift mobility of the charge carriers in compensated a-Si:H as compared to the undoped a-Si:H. Howard and Street [76] also measured the electron and hole drift mobilities and the optical absorption in compensated a-Si:H and found that the drift mobilities of both type of carriers decrease with increasing doping concentrations. The drift mobility and optical absorption data are not consistent with disorder induced band tail broadening as suggested by Marshall *et al.* [77], but agree with the prediction of a model of long range potential fluctuations arising from the charged donors and acceptors states.

The difference between the light induced annealing behaviour of deposition induced and photocreated defects can also be explained, if the band gap fluctuations are taken into consideration [78]. The photogenerated electron-hole pairs are expected to move in the narrow band gap region where the probability of their recombination is more and hence the creation of new defects. This may give rise to an inhomogeneous distribution of photocreated defects, unlike a more probable uniform distribution of deposition induced defects and therefore, the annealing kinetics of these two defects may be different [78].

An investigation of inhomogeneities in a-Si:H films by scanning with laser probes has also been reported [79]. Andrinova *et al.* [79] measured the transverse and planer conductivities and photoresponse of these films. These authors [79] have attributed the peculiarities in the conductivity and optical absorption to the fluctuations of hydrogen content in these films.

Chapter 3

Metastabilities in a-Si:H

Electrical and optical properties of a-Si:H films (both doped and undoped) are altered by the application of external perturbations such as

1. exposure to strong illumination (Staebler-Wronski effect or light induced metastability) [10,15,26,80,81],
2. fast quenching from a high temperature (thermal induced metastability) [14,16,82]
3. irradiation with ions [13], electrons [11], x-rays [83] and
4. charge injection [84,85] etc.

These changes can be reversible or irreversible. For reversible changes, the original state can usually be brought back by annealing. Out of the various reversible metastable effects, light and thermal induced metastabilities have attracted wider attention and we discuss these in the following.

3.1 Light Induced Metastability

In 1977, Staebler and Wronski [10] reported that the dark conductivity (σ) and photoconductivity (σ_{ph}) of a-Si:H films decrease upon exposing these films to strongly

absorbing light (Fig. 1.2). The decrease in σ is accompanied by an increase in its activation energy (E_σ). The effect is reversible and the original state can be brought back by annealing at high temperatures ($\approx$ 150-200^{0}C, 1-2 hours). It is observed that the changes in σ and σ_{ph} depend upon the intensity of illumination and exposure time [26]. This effect is commonly known as the Staebler Wronski Effect. The decrease in σ is fast in the beginning and slows down as time of exposure is increased and a steady state is obtained after prolonged illumination [86]. Metastable changes, introduced by light, give rise to an increase in the density of states ($g(E)$) as indicated by the sub-gap absorption measured by photothermal deflection spectroscopy (PDS) [87] and constant photocurrent measurements (CPM) [88], space charge limited currents (SCLC) [89,90]. In undoped a-Si:H, it has been observed [91] that the light soaking causes an increase in the density of neutral dangling bonds (Si_3^0) characterized by an increase of electron spin resonance (ESR) signal corresponding to g = 2.0055. The results on PDS [87] and time of flight are also consistent with an increase in the density of dangling bonds. Pankove *et al.* [24] find an increase in 0.95eV defect luminescence (PL) band upon light soaking (LS) which can be associated with the increase in Si_3^0 bond density as observed by ESR.

The sign and magnitude of change in conductivity upon LS depend upon the dopant and doping concentration. An increase in σ and σ_{ph} is also observed in some cases [92]. Sometimes, surface is found to play an important role [93]. This is particularly true in case of the a-Si:H doped with boron [94]. Most of the light soaking studies are on undoped and P-doped a-Si:H and we discuss only these here. In case of these films, the SWE is normal, i.e. , σ and σ_{ph} decrease upon light soaking. Metastable changes upon exposure to light are more pronounced in the lightly doped a-Si:H films as compared to heavily doped films which show smaller effects. The sub-gap absorption for P-doped a-Si:H films also shows an increase in the absorption coefficient (α), which implies an increase in the density of deep defect states in the gap [87]. If no other changes take place, an increase in sub-gap absorption would result a downward movement of E_f, which means the density of band tail state (n_{bt})

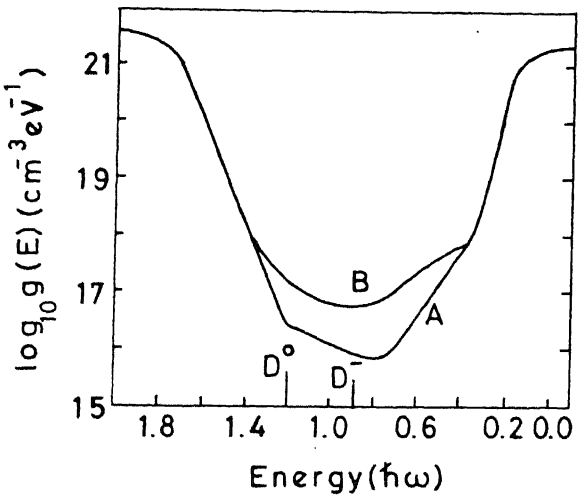

Figure 3.1: The schematic density of states picture in annealed (A) and light soaked (B) states [99].

should decrease. ESR measurements show a decrease [43] in n_{bt} corresponding to g = 2.0044 and an increase in the density of four fold coordinated neutral donors (P_4^0, in phosphorus doped a-Si:H). An increase in P_4^0 and a small decrease in E_f suggest that both donor density and dangling bond density (N_{DB}) increase upon light soaking. Capacitance studies by Leen *et al.* [46] on P-doped a-Si:H also show a decrease in n_{bt} and increase in N_{DB}. Furthermore, transport and capacitance studies on P-doped a-Si:H have indicated that in addition to the dangling bond creation via bond breaking, new metastable electronic levels closer to the mobility edge are also created during illumination [24,44,95,96].

A number of spectroscopic studies have been carried out to find the location of the new states in the gap. Based on the studies of SCLC, transient and steady state photoconductivity, it has been shown that the new states are created in the upper half of the gap [97]. However, diffusion length and sub-gap absorption measurements show that the new defects are created in the lower half of the gap as well [98]. A schematic

representation of the gap state distribution in annealed and light soaked state as proposed by Guha [99] is shown in Fig. 3.1. Han and Fritzsche [100] have observed that the anneal rates of the σ_{ph} and sub-gap absorption are different, indicating that at least two types of defects are created upon light soaking. It has been proposed by Morigaki and Yonezawa [101] that the light creates two types of dangling bonds, one is the normal Si_3^0 and the other is a H-related dangling bond. Similar propositions are made by Hikita *et al.* [102] upon deconvolution of ESR spectra. Shepard *et al.* [103] suggest that the light creates a distribution of gap states, which anneal at different rates.

It has been observed that steady state photoconductivity σ_{ph} is not a single valued function of dangling bond defect concentration [104] and that the decrease in σ_{ph} of a-Si:H is much more by the light exposure than by the same number of native defects as produced by the light exposure [105]. It has been suggested [54] that in addition to creation of dangling bond defects, light causes a change in structure of a-Si:H films. The experimental observations such as an increase in Si-H stretching mode at wave number 2000 cm^{-1} [53], a reversible shift of about 0.1eV of the Si 2p X–ray photoelectron spectroscopy to lower binding energy [106], changes in 1/f noise spectrum of a-Si:H [107] and in proton NMR dipolar spin lattice relaxation time [108] also can not be explained by a simple increase in dangling bond defects but require some additional changes in structure of a-Si:H upon light soaking.

3.1.1 Microscopic Mechanism for Creation of Light Induced Defects

Several explanations have been proposed for the creation of light induced defects in a-Si:H [15,24,26,28]. These models are based upon two microscopic mechanisms:

1. Weak-bond breaking [26]
2. Charge trapping [28].

Both models explain most of the experimental data. In particular, they all predict an increase in the Si_3^0 upon light soaking, along with a decrease in σ and σ_{ph}, in agreement with the experiments. We shall be discussing these two models in the following sections.

3.1.1.a Weak-bond Breaking Model

The model based on the breaking of weak bonds proposes that the energy released by recombination of photogenerated carriers during light soaking results in the formation of new defects, which act as additional traps and recombination centers. The observation that these defects can not be removed by exposure to infrared light and require annealing at high temperatures, suggests that some atomic motion is involved in the process. This model is able to explain the lowering of diffusion length, decrease in σ_{ph} and PL at 1.2 eV, increase in $g(E)$, sub-gap absorption and ESR signal.

However, there are some difficulties with this model [28]. For example, the energy available to create the defects ($\approx 1.6eV$) is extremely small compared to that needed to break a Si-Si bond and create a pair of defects. Also, these defects are to be separated by $\approx 10\mathring{A}$ in order to prevent the recombination.

These can be taken care of, if we take into account the possibility of involvement of hydrogen in creation of the light induced defects. It has been pointed out that a-Si:H films contain $\approx 10at\%$ of hydrogen, which is much more than that required to passivate the silicon dangling bonds ($\approx 10^{19} cm^{-3}$). Thus, a lot of hydrogen is expected to be loosely bound and may be free to move. Furthermore, molecular dynamics calculations [109] show that Si-Si bonds in the neighbourhood of Si-H-Si bond is a weak bond and only $\approx 0.04eV$ is needed to break this bond. This supports the weak bond breaking model.

Muller *et al.* [110] proposed the charge induced breaking of weak bonds. It is shown [111] that through the diffusive re-arrangement of Si-H bonds, the a-Si:H lattice is able to establish thermal equilibrium between the densities of band tail trapped

charge carriers and dangling bond defects. When this equilibrium is disturbed by changes in temperature, carrier injection or illumination, dangling bond defects have to be generated or annealed out via H- diffusion processes. We now discuss, how this model explains the results in undoped and P-doped a-Si:H.

Undoped a-Si:H

Stutzmann *et al.* [26] gave a quantitative analysis for the creation of the light induced defects in undoped a-Si:H assuming that Si_3^0 are the dominant defects created. These authors proposed that the energy released by non radiative recombination of photo-generated electron hole pairs causes weak Si-Si bonds to break. This produces pairs of dangling bonds (Si_3^0)

$$\text{Si-Si} \longrightarrow 2\ Si_3^0$$

Atomic hydrogen from a neighbouring site moves to make a bond with one of these dangling bonds and thus separate them. If N_d is the concentration of defects (dangling bonds) at time t and G is the illumination intensity then quantitative analysis shows

$$N_d(t) = \left(\frac{3C_{sw}}{A^2}\right)^{1/3} G^{2/3}\, t^{1/3} \tag{3.1}$$

Stutzmann *et al.* [26] measured N_d by ESR after light soaking for different intensities and duration and found that N_d obeys Eq. (3.1).

P-Doped a-Si:H

The model is proposed by Stutzmann [43] in order to explain the increase in density of neutral four fold coordinated donors (P_4^0) along with a decrease in n_{bt} , σ and increase in E_σ after light soaking the P-doped a-Si:H, as observed by hyperfine ESR signal [43] and conductivity measurements. The microscopic model suggests that the photon causes a weak Si-Si bond in the neighbourhood of Si-H bond to break and create two dangling bonds (Si_3^0). The hydrogen atom from the neighbouring bond moves and makes a bond with one of the two Si_3^0. Valence alteration then takes place between a three fold coordinated phosphorus atom P_3^0 and a neutral dangling bond Si_3^0 created

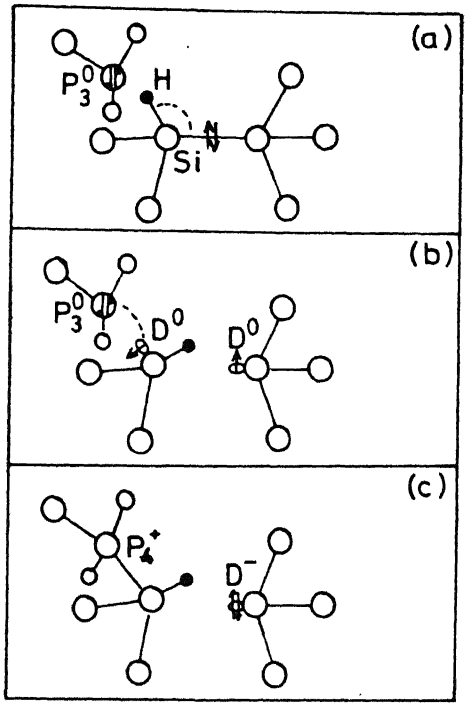

Figure 3.2: Microscopic mechanism for light induced creation of donors and defects

by the movement of hydrogen. Finally, the four-fold coordinated phosphorus atom (P_4^0) donates an electron to become an ionized donor P_4^+ and the electron is taken by the other Si_3^0 created by the photon to become negatively charged Si_3^- (see Fig. 3.2). The whole process is supported by the movement of hydrogen. Since both Si_3^- and P_4^+ increase, a small shift of E_f is expected towards mid-gap, resulting in a decrease in σ and n_{bt}. Furthermore, an increase in P_4^+ causes a simultaneous increase in P_4^0 as observed in ESR.

3.1.1.b Charge trapping Model

Adler [28] proposed an alternative model to explain the light induced changes based on the trapping of charges. During illumination with band gap light, electrons and

holes are created and are trapped on the Si_3^+ and Si_3^- defects respectively. This forms neutral defect centers, but without rehybridization or relocation of the neighboring atoms. Since electronic levels of the trapped carriers are near band edges, these defects are readily thermally ionized back to Si_3^+ and Si_3^- except at low temperatures. However, Si_3^+ and Si_3^- centers, which are close to the mid-gap, do not release these trapped charges quickly and convert into the Si_3^0. Now there is a small probability of rehybridization to make a stable dangling bond. Since the Si_3^+ and Si_3^- have different bond angles than that for Si_3^0, a lattice relaxation is necessary to stabilize the neutral dangling bonds. It is proposed [112] that 15^0 bond angle change is necessary to move the defects electronic level from a near band edge towards mid gap where it functions as a more efficient recombination center and appears as a stable Si_3^0. Thus in this model, no new defects are created by light. The trapping of photogenerated carriers induces excess neutral dangling bonds. These metastable centers are responsible for the increase in N_s, the decrease in σ_{ph} and a shift in E_f etc.

3.1.1.c Comparison of Weak bond breaking and Charge trapping models

From the above discussion, we see that both the models explain the most of the experimental data. For example, these explain the creation of neutral dangling bonds (Si_3^0) in undoped a-Si:H, decrease in σ and σ_{ph}, an increase in subgap absorption and a shift in E_f towards mid-gap. In spite of the partial success of these models, these are unable to explain some of the experimental results. A critical evaluation [113] of these is given below.

The weak bond breaking model assumes that the defects created by the breaking of Si-Si bonds during light soaking are separated by the movement of hydrogen. The hydrogen stabilizes the state with more defects. Therefore, H is directly responsible for the observed light induced metastability. Shimizu *et al.* [114] reported that the density of photocreated dangling bonds increase with the increase in the flexibility

factor F defined as $F = \{4\alpha+4\beta+3\gamma-\delta/(1-\delta)\}^{-1}$, where α, β, γ and δ designate the composition of the film $(Si_\alpha C_\beta N_\gamma)_{1-\delta}H_\delta$ and $\alpha+\beta+\gamma = 1$. The parameter F represents the flexibility of the amorphous structure. Since the density of photocreated dangling bonds is a function of this parameter F alone, it has been argued that H atoms do not play a direct role in producing the light soaking effects, but influence it only indirectly by making the structure flexible. This is consistent with the pulsed ESR experiment of Isoya *et al.* [115], which show that the photocreated ESR center is more than 4.2 $\AA$ away from the closest hydrogen atom. Also the decrease in σ_{ph} is not uniquely determined by the increase in N_s upon LS as explained in the weak-bond breaking model [113].

The charge trapping model for the photocreated spins appears to be inconsistent with the following results:

1. The difference between ESR bulk density (Si_3^0) and CPM defect density (Si_3^0 + Si_3^-) gives the density of Si_3^-. The charge trapping model predicts that Si_3^- should decrease as the exposure time increases. However, it is found to remain constant $\simeq 7 \times 10^{15} cm^{-3}$, irrespective of exposure time [116].

2. Addition of nitrogen in a-Si:H increases the density of Si_3^- in the annealed state, but, in the light soaked state the density of Si_3^0 is independent of the amount of nitrogen. This is in contrast to the charge trapping model, which predicts a higher density of Si_3^0 in light soaked state, as the density of Si_3^- are more in these films [117].

Thus, we see that, although, both the models explain most of the experimental observations, none of them is able to explain all the results and it is difficult to decide which model is better.

3.2 Thermal Induced Metastability

Metastable changes in conductivity (σ) of a-Si:H are also observed, when these films are cooled rapidly from high temperatures, as shown in Fig. 1.3. The effect was first reported by Ast and Brodsky [17] in 1978 and attracted wider attention after Street *et al.* [14] reported in 1986 that σ of P-doped a-Si:H films near room temperature increases and E_σ decreases upon fast cooling from high temperatures and remains unchanged for months. The $\log \sigma$ vs. $1/T$ curves, obtained during heating these films in the fast quenched state meet the corresponding curve obtained after slow cooling, at temperature T_E. For $T \geq T_E$, σ is independent of the cooling rate (see Fig. 1.3). The temperature T_E is identified as the equilibration temperature for these films and varies with dopant [16,82] and the doping concentration [30]. For B-doped a-Si:H films, T_E is the lowest ($\approx$ 80-90^oC) and increases to $\approx$ 130-150^oC for P-doped and $\approx 200^oC$ for undoped a-Si:H. In case of singly doped films, T_E is lowered as the doping concentration is increased [30].

Metastable changes after fast quenching of doped a-Si:H films result in an increase in the density of the band tail carriers (n_{bt}) as measured by charge sweep-out technique [118] and ESR (g = 2.0055) and an increase [16,43] in the density of P_4^0 as measured by hyperfine ESR. The sub gap absorption measurements like PDS [82] do not show any significant change in the density of states ($g(E)$) of doped a-Si:H upon fast quenching. Also, no change is expected in the density of dangling bonds from the $C - V$ measurements and bias annealing experiments [44,46]. The isothermal capacitance transient spectroscopy (ICTS) measurements also do not show no any change in density of state distribution in the mobility gap [45].

Effect of fast quenching is small in case of undoped a-Si:H. An increase in sub-gap absorption (α) of a-Si:H [40], measured by CPM and PDS and a decrease [41] in σ_{ph} has been reported upon fast quenching these films from the deposition temperature ($\approx 300^oC$). These results suggest an increase in density of Si_3^0 of these films in the

fast quenched state. SCLC measurements also show a small increase in $g(E)$ [119]. A small decrease in σ has also been reported [120,121]. All these reports show that the changes introduced are reversible in nature and the original state can be brought back by annealing these films at high temperatures ($T \geq 200^0C$).

The changes observed in σ, E_σ and n_{bt} of doped and undoped a-Si:H films depend upon the rate of cooling [16] and also the cooling conditions, such as, cooling under reverse bias [122,123] and in presence of light [124].

3.2.1 Mechanism for the Creation of Thermal Induced Metastable State

Metastable changes in electronic properties have been observed for both undoped and doped a-Si:H films. However, the changes observed in σ in two cases are in opposite directions. In the following, we discuss the possible mechanism for thermal induced metastability in a-Si:H(P) and undoped a-Si:H.

3.2.1.a P-Doped a-Si:H

Street *et al.* [16] proposed that the a-Si:H films are in thermal equilibrium at high temperature. The Fig. 3.3. shows the density of state picture in the upper half of the mobility gap for a n-type a-Si:H film [68]. The negatively charged dangling bonds (Si_3^-) lie in the middle of the gap and the ionized four-fold co-ordinated donor states (P_4^+) lie close to the mobility edge in the conduction band tail region. The band tail and the dangling bonds are separated by a minimum (E_{min}). In the doping model of Street [8], the Fermi energy (E_f) lies in the minimum, while Si_3^- and P_4^+ states equilibrate reflecting the charge neutrality between Si_3^- and P_4^+. At finite temperatures, the Fermi function is sufficiently extended into the conduction band tail region and in addition to the Si_3^- and P_4^+, the shallow occupied band tail states (n_{bt}) and holes (Si_3^0) in the Si_3^- states are also present. Since density of states rises

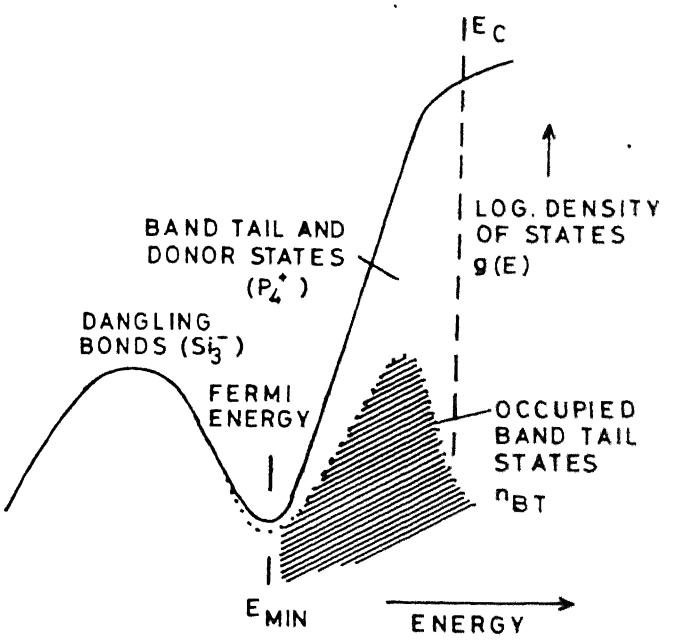

Figure 3.3: Density of States picture in the upper half of the gap for a-Si:H(P).

much more rapidly above E_{min} than below it, $n_{bt} \gg Si_3^0$. The charge neutrality condition can thus be written as

$$n_{bt} = N_{donor} - N_{DB} = P_4^+ - Si_3^- \tag{3.2}$$

where N_{donor} and N_{DB} are the densities of charged donors and dangling bonds. From Eq. (3.2), it is clear that any change in defect structure is reflected in the measurements of n_{bt} . The n_{bt} is related to σ as [125]

$$\begin{aligned} \sigma &= n\, e\, \mu \\ \sigma &= n_{bt}\, e\, \mu_d \\ n_{bt} &= \sigma\, e\, \mu_d \end{aligned} \tag{3.3}$$

where μ and μ_d are the free carrier mobility and drift mobility respectively and n is the density of the free carriers in the extended band.

When no structural change takes place both P_4^+ and Si_3^- are independent of the temperature and so n_{bt} is also constant. The variation of n_{bt} with the thermal history implies that either P_4^+ have increased or Si_3^- have decreased or both of them have changed, i. e. , either or both of P_4^+ and Si_3^- are the equilibrating species. Eq. (3.2) and Eq. (3.3) relate the structural changes to the electronic properties. Thus structural equilibrium is reflected in the transport measurements.

Sub gap absorption measurements like PDS [82] show that in doped a-Si:H, the defect density does not change significantly, after fast quenching. Further, $C-V$ measurements [82,44] show that the junction capacitance increases after quenching. Bias annealing experiments also show an increase in n_{bt} and P_4^+. From all these measurements it is inferred that the fast quenching results in an increase in donor concentration.

3.2.1.b Undoped a-Si:H

Smith and Wagner [126] proposed that at high temperature, the thermally generated electron hole pairs recombine and the energy released in the recombination process breaks some of the weak Si-Si bonds, resulting in the creation of neutral dangling bonds (Si_3^0). The reaction is similar to that proposed by Stutzmann *et al.* to explain the light induced creation of dangling bonds by the recombination of photogenerated electron-hole pairs. At high temperature, these Si_3^0 are in thermal equilibrium because the simultaneous annealing of these dangling bonds also takes place. When the a-Si:H films are fast quenched, the structure is frozen and a higher defect density is observed near room temperature. At room temperature, since annealing is very slow, the frozen-in state seems to be stable.

3.3 Annealing of metastable states

The metastable states obtained after light soaking and fast quenching slowly relaxes to the original slow cooled state [15,127,30,128]. The time of relaxation (τ) is very large (of the order of months) near room temperature and decreases to only a few minutes at high temperatures. Jackson and Kakalios [127] fitted the relaxation of excess defect density ΔN_d as measured by ESR, after light soaking the undoped a-Si:H films, to a stretched exponential of the form

$$\Delta N_d(t) = \Delta N_d(0) \exp\left\{-\left(\frac{t}{\tau}\right)^{\beta}\right\} \tag{3.4}$$

where $\Delta N_d(t)$ is the deviation in defect density from the annealed value at any time t and $\Delta N_d(0)$ is the value of $\Delta N_d(t)$ at $t = 0$ and τ and β are fit parameters. τ is found to be thermally activated [82]

$$\tau = \tau_0 \exp\left\{\frac{E_\tau}{kT}\right\} \tag{3.5}$$

where E_τ is the activation energy for relaxation. Similar behaviour is observed by Street *et al.* [129] for the decay of excess defect density after fast quenching the undoped (40 μm thick) a-Si:H films.

Similar stretched exponential has been fitted to the relaxation of excess n_{bt} and σ obtained after fast quenching the doped a-Si:H films [30,128]. The stretched exponential has been ascribed to the motion of hydrogen present in a-Si:H films [130]. It has been found that the dispersive diffusion of H in these films can explain the observed relaxation kinetics of metastable states. (This has been discussed further in Section 3.4 on Hydrogen Glass Model).

On the other hand, Crandall [131] (see Section 3.5.2) argues that it is not necessary to invoke hydrogen motion to explain the annealing of metastable defects. Using a defect controlled relaxation model for the creation and recovery of metastable states, he shows [131] that the stretched exponential is a natural consequence, if there is a

distribution of activation energies. Such a distribution is possible in a-Si:H, as it is disordered and heterogeneous.

3.4 Thermal Equilibrium and Hydrogen Glass Model

We have mentioned in the earlier sections (Sect 3.2) that a-Si:H films are in thermal equilibrium above T_E. For $T \geq T_E$, the electronic properties, like σ and n_{bt} depend upon the rate of cooling from high temperatures ($T \geq T_E$) [16]. Furthermore, at a fixed temperature, σ and n_{bt} in fast quenched state slowly relax to the slow cooled state following a stretched exponential given by Eq. (3.4). These properties of a-Si:H films resemble the structural properties of conventional glasses [29]. These glasses are prepared by the rapid cooling of the melt and are in thermal equilibrium for $T \geq T_g$ (glass transition temperature). Below T_g, the thermodynamic properties, like volume etc, depend upon the rate of cooling from $T \geq T_g$ and are in metastable equilibrium.

Street *et al.* [16] and Kakalios *et al.* [30,132] have proposed the so called Hydrogen Glass model for a-Si:H. This is based on the movement of hydrogen in these films. According to this model [30], the a-Si:H films consists of two networks, namely,a rigid network of four fold coordinated silicon and a relatively flexible network of hydrogen. Since hydrogen is present in a large concentration, some of it is loosely bound and for $T \geq T_E$ is free to diffuse in the rigid silicon network and establishes an equilibrium fairly quickly. For $T \leq T_E$, the diffusion is slow in comparison of the time scale of measurements and a metastable state is observed. In this model, T_E for a-Si:H is analogous to the T_g observed for the conventional glasses.

3.4.1 Evidence in support of Hydrogen-Glass Model

It is suggested that the hydrogen is responsible for the observed thermal equilibrium behaviour of a-Si:H films. In the following, we discuss, a few properties of a-Si:H, which resembles those of glasses and provide supports to the Hydrogen Glass model.

3.4.1.a Dispersive Diffusion of Hydrogen

Carlson and Magee [133] measured the diffusion coefficient of hydrogen in undoped a-Si:H films using secondary ion mass spectrometry (SIMS) with deuterium tracer and found that the hydrogen diffusion constant (D_H) is thermally activated with an activation energy of 1.5eV. The technique was later used by Street *et al.* [38], to measure the D_H in doped a-Si:H. It is observed that D_H is greatly enhanced by doping and increases upon increasing the doping concentration. D_H is found to be higher for B- doped a-Si:H as compared to the P-doped a-Si:H films and is thermally activated over the temperature range examined.

$$D_H = D_0 \exp\{-E_D/kT\} \tag{3.6}$$

It is observed that the diffusion activation energy E_D remains essentially unchanged upon doping and only the prefactor D_0 changes with doping.

It has also been observed [30] that D_H is time dependent and varies as

$$D_H(t) \propto (\omega t)^{-\alpha} \tag{3.7}$$

where ω is the attempt to diffuse frequency.

From Eq. (3.7), it is clear that the D_H is not uniquely defined and should be referred to a particular annealing time. Commonly, it is measured by varying the annealing time at each temperature, so that, the deuterium concentration profile will extend to a fixed distance L in to the a-Si:H layer.

Kakalios *et al.* [132] have shown that the time dependence of D_H arises from an exponential distribution of trapping sites. These authors [132], further suggest that the hydrogen atom is excited from a Si-H bond to an interstitial band, leaving a dangling bond behind. It is now free to move in to the silicon network until it is trapped either at a weak Si-Si bond or at a dangling bond. In both the cases, it forms a Si-H bond. The hydrogen atom trapped in to a weak Si-Si bond might get re-excited to the interstitial band and move freely. The process of excitation and trapping can go until the hydrogen is trapped into a deep bond. At longer times, the probability that a hydrogen will fall in to a Si-Si state with high binding energy increases and thus, D_H is expected to decrease. In analogy with the dispersive transport model suggested by Scher and Montroll [134], if the weak bonds are exponentially distributed in energy as $\exp(-E/kT_0)$, where kT_0 is the width of the trap distribution then D_H will decrease as a power law in time. The dispersive model [134] also predicts the dispersion parameter α to be given by $\alpha = 1 - T/T_0$, where T is the temperature at which the diffusion is taking place. Measurement of diffusion coefficient of hydrogen in a-Si:H fits to $\alpha = 1 - (T/T_0)$ with $T_0 \approx 600K$.

3.4.1.b Slow Relaxation Below T_E

A characteristic of glasses [29] exhibited by a-Si:H is the slow non exponential relaxation below T_E. The slow decay of σ and n_{bt} in a-Si:H at a fixed temperature $T < T_E$ follows a stretched exponential time dependence

$$\Delta(t) = \Delta(0) \exp\left\{ -\left(\frac{t}{\tau}\right)^{\beta} \right\} \tag{3.8}$$

where $\Delta(t)$ is the deviation of σ or n_{bt} from the slow cooled state at time t and $\Delta(0)$ is the initial deviation at $t = 0$. This form of equation can be related to the hydrogen diffusion. For small departure from equilibrium, the relaxation will be given by the linear equation

$$\frac{d\Delta(t)}{dt} = -k(t)\Delta(t) \tag{3.9}$$

where $k(t)$ is the rate constant. Shlesinger and Montroll [135] showed that if $k(t)$ has a time dependence of the form $k(t) \propto t^{-\alpha}$, then the Eq. (3.8) is the solution of Eq. (3.9) with $\beta = 1 - \alpha$. Substituting $k(t) = At^{-\alpha}$ in Eq. (3.9)

$$\frac{d\Delta(t)}{dt} = -at^{-\alpha}\Delta(t) \tag{3.10}$$

Integrating above equation and putting the boundary condition that at $t = 0$, $\Delta(t) = \Delta(0)$ we get

$$\ln\left\{\frac{\Delta(t)}{\Delta(0)}\right\} = -\frac{At^{-\alpha+1}}{(1-\alpha)}$$

$$\text{or} \qquad \Delta(t) = \Delta(0)\exp\{-(t/\tau)^{\beta}\}$$

which is same as Eq. (3.8) with parameters τ and β as

$\tau = (1-\alpha)/A^{1/\beta}$ and $\beta = 1 - \alpha$

We see from Eq. 3.7 that the hydrogen diffusion coefficient has a similar power law time dependence as required by Shlesinger and Montroll [135] to explain the stretched exponential. We will now see, how τ and D_H are related.

3.4.1.c Viscosity at the Glass Transition Temperature

For conventional glasses, the glass transition temperature (T_g) is defined as the temperature at which the viscosity of the super cooled liquid attains a value $\approx 10^{13}$ poise [29]. Viscosity (η) is related to the self diffusion coefficient (D) through the Stokes-Einstein relation

$$\eta D = \frac{kT}{6\pi R} \tag{3.11}$$

where R is the effective radius of the self diffusing species. For the equilibration temperature $T \approx 100^0 C$ and $R \approx 3\text{Å}$, Eq. 3.11 gives $\eta D = 10^7$ dyne. This is the value reported in literature for many glasses for which both η and D can be

measured. Using Eq. (3.11), we can now express the glass transition temperature as the temperature for which $D_H \approx 10^{-20}\, cm^2\, s^{-1}$. It has been observed [30] that upon extrapolating the data of diffusion coefficient of hydrogen (log D_H vs. $1/T$ curve) to $D_H \approx 10^{20}\, cm^2\, s^{-1}$ the corresponding value of the temperature is equal to the observed equilibration temperature (T_E) for n and p type a-Si:H films. The changes in D_H upon varying doping concentration results in the different values of T_E. This observation, further, supports the hydrogen glass model.

3.5 Unifying models for Creation and Annihilation of Thermal and Light Induced Metastable Defects

We have seen in the previous sections that the metastable defects can be introduced in a-Si:H by light soaking as well as fast quenching and can be removed by annealing at elevated temperatures. It has also been reported [136] that the relaxation is fast when annealing is done in presence of low intensity light. Several models have so far been proposed to explain the creation and annihilation of these metastable defects. These can be divided into two categories : (a) based on movement of hydrogen (SJT and RB models) and (b) defect controlled model(DCR).

3.5.1 SJT and RB Models

Stutzmann *et al.* [26] (SJT) were first to give a quantitative analysis for the creation of light induced defects. As described in Section 3.1.1.a, metastable defects are created by breaking of weak Si-Si bonds. The proposed defect reaction for the creation of metastable defects is given as

$$dN_d/dt = C_{sw}\, n\, p \tag{3.12}$$

where C_{sw} is a constant describing the creation probability and n and p are the free electron and hole concentrations. It is assumed here, that Si_3^0 are the only defects that are responsible for S-W effect in undoped a-Si:H. The recombination is quite complicated, but for high illumination intensity (G), the carrier densities n and p at the conduction and valence band edges are given, to a fair approximation, by

$$n = p = \frac{G}{A N_d} \tag{3.13}$$

where, A is an average recombination constant. Stutzmann, [137] further, introduced an annealing term in the rate equation and the net equation is given by

$$\frac{dN_d}{dt} = C_{sw}\, n\, p - r_{ann}\, N_d \tag{3.14}$$

where r_{ann} is the anneal rate. Under strong illumination, annealing term is negligible near room temperature and the solution of Eq. (3.14) gives

$$N_d^3(t) - N_d^3(0) = 3\, C_{sw}\, G^2\, t\, /A^2 \tag{3.15}$$

here, $N_d(0)$ is the initial equilibrium defect density. For sufficiently long illumination times, such that $N_d(t) \geq 2N_d(0)$, excess defect density follows a power law time dependence

$$N_d(t) = \left(3\, C_{sw}/A^2\right)^{1/3}\, G^{2/3}\, t^{1/3} \tag{3.16}$$

Smith and Wagner [126] also proposed a similar rate equation for the higher frozen-in defect density after fast quenching the a-Si:H films, suggesting that a common rate equation can be written for the creation of metastable defects.

A stretched exponential time dependence for the creation of metastable defects has been obtained by Redfield and Bube (RB) [138,139]. The kinetic model proposed by these authors [140,139] takes into account both thermal and light induced creation and annealing of metastable defects. The rate equation in this case is given as

$$\frac{dN_d(t)}{dt} = C_r\,(N_s - N_d) - A_r\,N_d \tag{3.17}$$

where N_s is the saturated defect density and C_r and A_r are the creation and annealing rate coefficients, which include both thermal and light induced terms. For a dispersive process, both C_r and A_r are time dependent and the metastable defect density is given as

$$N_d(t) = N_s - (N_s - N_0)\,\exp\left\{-\left(\frac{t}{\tau}\right)^{\beta}\right\} \tag{3.18}$$

These authors have shown that the stretched exponential yields a better agreement with the experimental data than the power law dependence as obtained in the SJT model. Meaudre *et al.* [124,136] have also considered a similar rate equation as proposed by Redfield and Bube (Eq. 3.17) and have shown that the annealing in dark as well as under illumination follows a stretched exponential.

A discrepancy between the SJT model (power law time dependence) and RB model (stretched exponential time dependence) has been removed by considering the exponential nature of the band tails and a saturation of defect density [141]. In this case, the creation of metastable defect density follows a stretched exponential, as suggested by Redfield and Bube [139].

Redfield and Bube [139], however, do not propose any particular dispersive mechanism. Later Kakalios *et al.* [132] proposed that the dispersive diffusion of hydrogen is the rate controlling mechanism for the stretched exponential behaviour of annealing of metastable defects.

Recently, some new kinetic models have been proposed for creation and annihilation of metastable defects. These include, 1) a model by Abdulhalim [142], based on the existence of short range large energy fluctuations, which include transition traps for carriers that release their energy and enhance the creation or annihilation of metastable defects. The general form of the kinetic equation is based on that proposed originally by Redfield and Bube [139] and explains the experimentally observed

dependence of metastable defect density on the material and external parameters. 2) a model by Schumm [143] based on the thermodynamic equilibrium between free carriers, defects and defect free configuration. The suggested chemical reaction in this case maintains the reversibility. During the forward reaction, an electron-hole pair is destroyed under both equilibrium and non-equilibrium conditions. However, in the backward reaction, an electron-hole pair is created. The thermodynamic picture predicts that light induced forward rate is much higher than the thermal backward rate near room temperature and thus a large number of defects are created. However, both thermal forward rate and light backward rates are small and thus a large change in metastable defect density is seen upon light soaking, while annealing of these defects is slow.

3.5.2 Defect controlled model

Crandall [131] proposed a model for creation and annealing of metastable state based on defect controlled relaxation (DCR). The main hypotheses of the model are as follows:

1. A metastable state can be either in state A or in state B. The energy barrier for transition from state A to state B is E_{A-B} and that for the transition from state B to state A is E_{B-A} (see Fig. 3.4).
2. In amorphous materials, disorder produces a variation in barrier height and energy minima among different sites. So a distribution of barrier heights E_{A-B} and E_{B-A} is present, however, each individual defect has a well defined energy barriers. These defects have an exponential distribution given by $N_d = N_0 \exp(-E/kT_0)$, where kT_0 is the characteristic energy of the distribution.
3. Defects with highest barrier have lowest formation energy. The i^{th} defect in the ensemble is characterized by a barrier energy E_i.

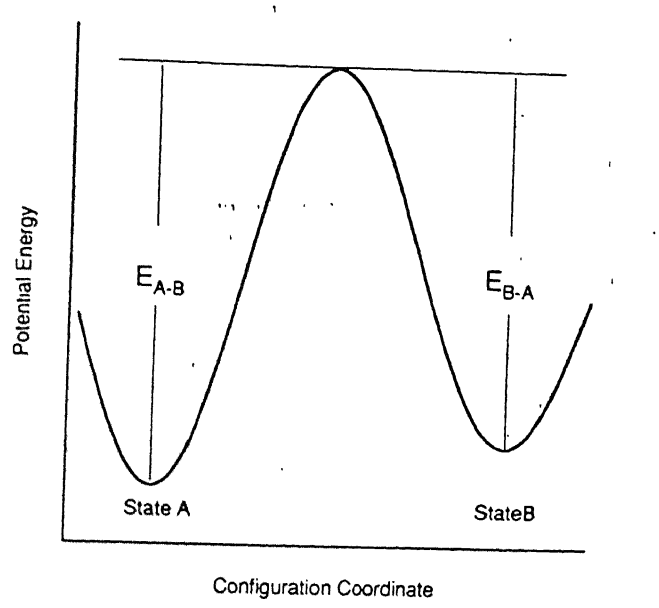

Figure 3.4: Configuration coordinate diagram for metastable defects. Energies are defined in the text.

The first order rate equation is considered for the time rate of defect conversion. If $n_A(E_i)$ and $n_B(E_i)$ are density of defects per unit volume per unit energy at energy E_i in state A and state B respectively, then

$$\frac{dn_A(E_i)}{dt} = -\frac{dn_B(E_i)}{dt}$$

$$= -n_A(E_i)\,W_{A\to B}(E_i) + n_B(E_i)\,W_{B\to A}(E_i) \tag{3.19}$$

where $W_{A\to B}(E_i)$ and $W_{B\to A}(E_i)$ are the transition probabilities per unit time per defect from state A to B and from state B to A respectively. Total population in state A and B are

$$N_A(t) = \sum_i n_A(E_i) \tag{3.20}$$

and

$$N_B(t) = \sum_i n_B(E_i) \tag{3.21}$$

using Eqs. (3.19), (3.20) and (3.21)

$$\frac{dN_A}{dt} = -\frac{dN_B}{dt} \tag{3.22}$$

for a continuous distribution of states in energy, summation can be replaced by integration.The transition rates, for a thermally activated process are given by

$$W_{A\rightarrow B}(E) = k_{ab}\exp(-E/kT) \tag{3.23}$$

$$W_{B\rightarrow A}(E) = k_{ba}\exp(-E/kT) \tag{3.24}$$

k_{ab} and k_{ba} are the transition rate constants, which depend upon the transition mechanism. Since defect formation (A $\rightarrow$ B) is caused by electrons and holes and thus k_{ab} is a function of carrier density. The annealing (B $\rightarrow$ A) rate constant k_{ba} is of the order of a lattice vibration frequency (ω)

Under illumination or during charge injection, $k_{ab} \gg k_{ba}$ and the creation of metastable defects is given as

$$N_B(t) - N_B(0) = (N_B(\infty) - N_B(0))\left(1 - \exp\left\{-\left(\frac{t}{\tau}\right)\right\}\right) \tag{3.25}$$

where $N_B(0)$ and $N_B(\infty)$ are the initial and steady state defect density in state B. The Eq. (3.25) shows that the increase in defect density obeys a stretched exponential.

For defect annealing, the solution of rate equation {Eq. (3.19)} gives

$$N_B(t) - N_B(\infty) = (N_B(0) - N_B(\infty))\exp\left\{-\left(\frac{t}{\tau}\right)^{\beta}\right\} \tag{3.26}$$

where τ is thermally activated, with activation energy E_τ. Crandall [131] obtained an expression for E_τ with the assumption that $k_{ab} \approx k_{ba} \approx \omega$, and showed that since $E_{A-B} \geq E_{B-A}$,

$$E_\tau \approx E_{B-A}$$

This shows that the transition energy is mainly determined by the maximum barrier height (E_{mB}) surmounted during degradation. The model, furthermore, predicts that

the barrier height is related to the time of degradation (t_d) such that

$$E_{mB} = k\,T \ln(k_{ab}\,t_d)$$

which implies that the longer degradation time converts defects with longer anneal time and a higher activation energy (E_τ).

Thus we see that all the models for the creation and annealing of metastable defects predict a stretched exponential time dependence. It is, therefore, difficult to distinguish between these models on this basis.

Chapter 4

Experimental Details

This chapter describes the preparation of both undoped and doped a-Si:H films and their initial characterization for the quality. The details of the measurements set-up and the experimental procedures are also discussed here.

4.1 Preparation

In the following, we describe the preparation of a-Si:H films and electrodes used for the electrical measurements.

4.1.1 Preparation of a-Si:H films

4.1.1.a Undoped Films

Hydrogenated amorphous silicon (a-Si:H) films are prepared on Corning 7059 glass substrates by the standard dc and rf glow discharge techniques [144,90]. The reaction chamber used for the preparation of a-Si:H films is shown in Fig. 4.1. Prior to the film deposition, the reaction chamber is evacuated to a pressure $\leq 10^{-6}$ torr using a turbo-molecular pump and baked for a few hours at temperature (T) $\leq$ 600K. The chamber

Table 4.1: Deposition Parameters for a-Si:H by d.c Glow-Discharge

Gas used	3% SiH_4 + 97% Argon
Pressure	$\approx 1torr$
Flow rate	$\approx 20sccm$
Substrate temperature T_s	$\approx 550K$
Power density	≈ 40 mW/cm^2
deposition rate	$\approx 1A/s$

Table 4.2: Deposition Parameters for a-Si:H by r.f Glow-Discharge

Samples	Undoped a-Si:H	P doped a-Si:H
Gas used	Pure SiH_4	SiH_4 + H + PH_3
Pressure	$\approx 0.5torr$	$\approx 1torr$
Flow rate	$\approx 50sccm$	$\approx 40sccm$
Substrate temperature T_s	$\approx 575K$	$\approx 500K$
Power density	$\approx 40mW/cm^2$	$\approx 40mW/cm^2$
deposition rate	$\approx 5A/s$	$\approx 3A/s$

is then purged with hydrogen followed by cleaning of the substrates with hydrogen plasma. The starting gas Silane (SiH_4) is then introduced into the reaction chamber and glow discharge is produced between the electrodes by applying an electric field to the cathode. Silane (SiH_4) molecules are dissociated through collisions with fast electrons in the plasma, into neutral radicals, atoms and ions. These radicals and atoms generated in the plasma, travel to the growing surface through a gas phase diffusion process resulting in the deposition of the amorphous silicon thin film onto Corning 7059 glass substrates. Externally controllable parameters for plasma CVD process are: starting gas materials (pure SiH_4, H_2 or Ar diluted SiH_4), gas flow rate, gas pressure, power density, electrode separation and the substrate temperature [144]. The deposition parameters are selected so as to get good quality a-Si:H films with low defect density and high photosensitivity. Typical deposition parameters are given in Tables 4.1 and 4.2.

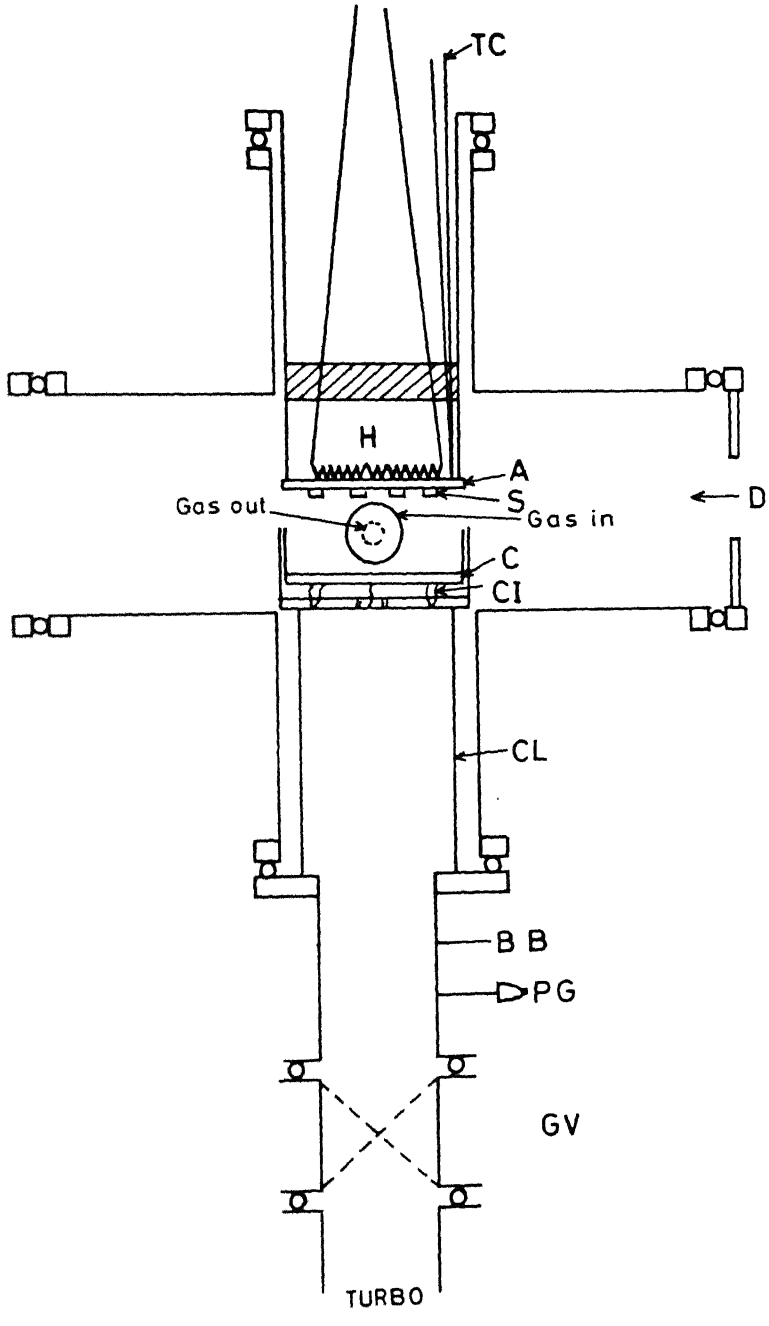

Figure 4.1: Schematic diagram of the reaction chamber used for preparation of a-Si:H. Here, GV is the gate valve, B and PG are beratron and penning gauges, A, H and S are anode, substrate heater and substrate respectively. CI and CL represent ceremic insulators and SS cylinder. D is the view-port.

conductivity increases by 2 orders of magnitude at room temperature. The properties of typical undoped and doped films are listed in Table 4.3.

4.1.2 Electrodes

Evaporated nichrome and aquadac (colloidal graphite solution in organic solvent) are used as electrodes for characterizing the films electrically in a coplanar geometry.

Nichrome is evaporated in vacuum on to the films so as to make coplanar strips $\approx$ 1 cm long and $\approx$ 1mm apart for conductivity measurements and $\approx$ 5 mm apart for thermopower measurements on the top surface of a-Si:H films. Graphite paint is used in the form of dots of $\approx$ 2 mm diameter and with $\approx$ 1mm separation. Both nichrome as well as graphite paint are found to give good Ohmic contact to the films up-to a field of 1000V/cm in the entire measurement temperature range.

4.2 Characterization

In the following, we discuss the initial characterization of the films for the quality.

4.2.1 Structural Characterization

Hydrogenated amorphous films (a-Si:H) so deposited are characterized for their amorphous nature using X-rays . The X-ray diffractogram gives a broad peak, characteristic of amorphous materials.

4.2.2 Optical Characterization

This consists of the measurement of optical transmission (T) in the wavelength (λ) range 400nm - 1200nm and gives the thickness and optical gap of these films, following the analyses of Swanpole [146]. Transmission is measured using a Hitachi

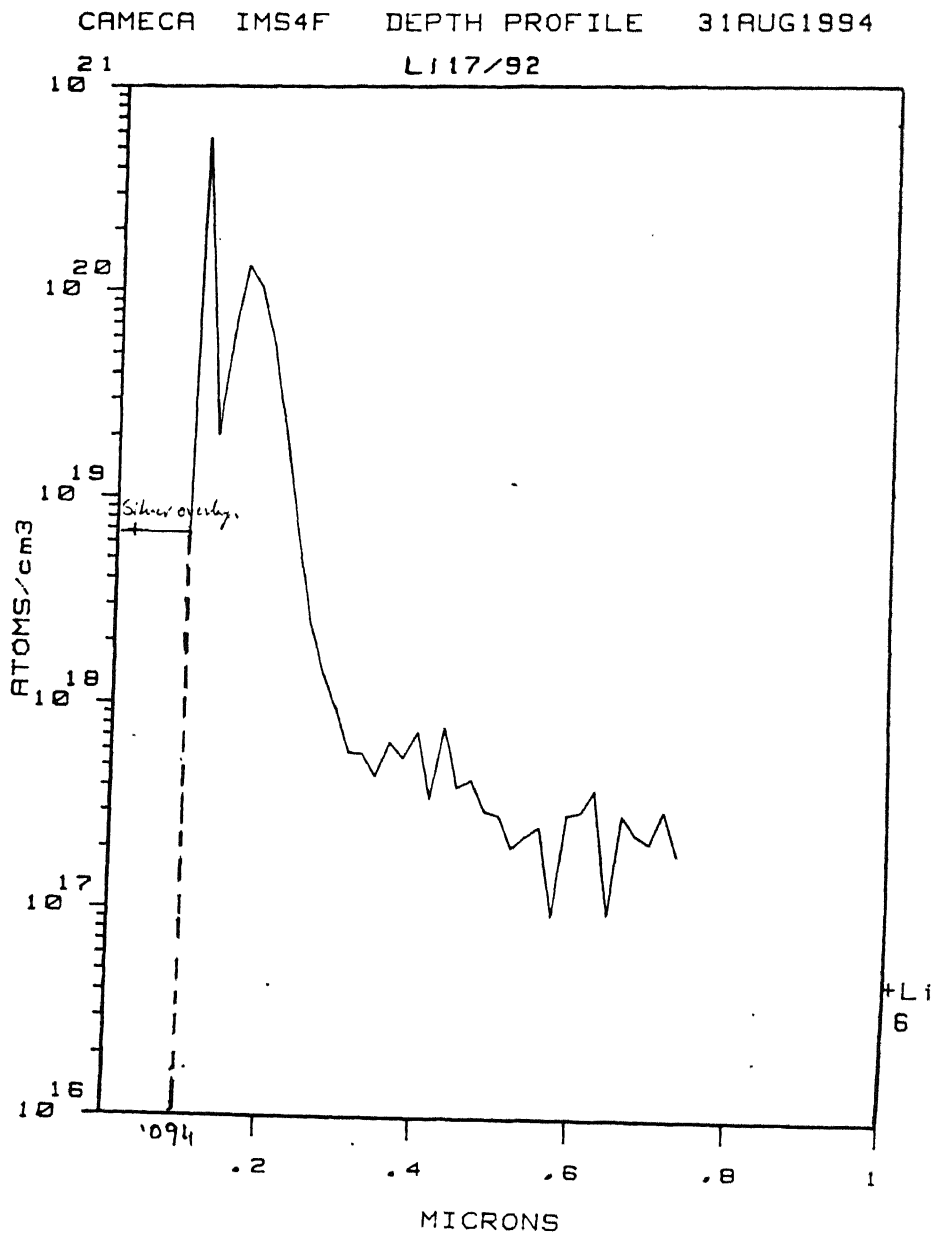

Figure 4.2: Depth profile of lithium in a-Si:H as measured by SIMS. Initial profile upto 0.1μm is because of silver overlayer.

2000 spectrophotometer for 400nm $\leq \lambda \leq$ 900nm and photodiode for 500nm $\leq \lambda \leq$ 1200nm. Similar values of T are obtained in both the measurements.

4.2.2.a Determination of Thickness

Thickness is determined using the $T(\lambda)$ following Swanpole. The transmission (T) for a-Si:H films is a function of the wavelength(λ), refractive index(n), substrate refractive index(s), film thickness(d) and the absorption coefficient(α):

$$T = T(\lambda, s, n, d, \alpha) \tag{4.1}$$

for a known value of 's' (refractive index of substrate Corning 7059), $n(\lambda)$ is calculated from the minimum and the maximum value of T at corresponding λ in the weak and medium absorption regions. The interference condition for a maximum or a minimum is

$$2nd = m\lambda \tag{4.2}$$

where m is an integer for maxima and a half integer for minima. If n_1 and n_2 are the refractive indices at the two adjacent maxima (or minima) at λ_1 and λ_2 respectively, then

$$d = \frac{\lambda_1 \lambda_2}{2(n_2\lambda_1 - n_1\lambda_2)} \tag{4.3}$$

for an adjacent maximum and minimum, the interference conditions are given by

$$2nd = m\lambda_1 \qquad (maxima)$$

$$2nd = (m + 1/2)\lambda_2 \qquad (minima)$$

and thus

$$d = \frac{\lambda_1 \lambda_2}{4(n_2\lambda_1 - n_1\lambda_2)} \tag{4.4}$$

From Eq. (4.4), d is determined, knowing $n_1(\lambda_1)$ and $n_2(\lambda_2)$. The procedure is repeated for all the interference fringes and an average value of d is calculated.

4.2.2.b Determination of absorption coefficient(α) and Optical gap(E_g)

A plot of $n(\lambda)$ vs. λ is used to calculate α in the medium and weak absorption regions ($600 \leq \lambda \leq 900$nm). In the strong absorption region ($\lambda < 600nm$), the fringes are not found and hence $n(\lambda)$ could not be calculated using the transmission data. However, $n(\lambda)$ in the interference region is a slowly varying function of λ, and hence, it could be extrapolated to get the fairly accurate value of $n(\lambda)$ in the strong absorption region. Thus α is obtained in this region.

To determine the optical gap of a-Si:H films $(\alpha h\nu)^{+1/2}$ vs. $h\nu$ is plotted for $h\nu \geq 1.5eV$. It is fitted to a straight line [147]

$$(\alpha h\nu)^{1/2} \propto (E - E_g) \tag{4.5}$$

The value of E_g thus obtained is $\approx 1.75eV$ for these films.

4.2.3 Electrical Characterization

All undoped and doped films are characterized for dark and photoconductivity (σ and σ_{ph}) at room temperature, activation energy (E_σ) and the type of majority charge carriers. The characteristic properties are listed in Table 4.3.

4.3 Measurements

This section is divided in two sub sections. First, we give a brief description of the set-up and then we describe our measurements.

4.3.1 Conductivity and Thermopower Set Up

Conductivity (σ) of the undoped and doped a-Si:H films in a coplanar geometry has been measured in an oil diffusion pump vacuum system at a pressure $\leq 10^{-6}torr$.

Table 4.3: Characteristic electrical properties of a-Si:H in annealed and slow Cooled (SC) State.

Sample Name	σ (300K) $\Omega^{-1}cm^{-1}$	σ_{ph} (300K) $\Omega^{-1}cm^{-1}$	E_σ (eV)		T_E °C	$\sigma_0(T > T_E)$ $\Omega^{-1}cm^{-1}$
			$(T < T_E)$	$(T > T_E)$		
a-Si:H #15 (undoped)	2.5×10^{-10}	3×10^{-6}	0.84	0.84		2×10^4
a-Si:H #18 (undoped)	5.3×10^{-8}	6.5×10^{-5}	0.50	0.70	180	2×10^3
a-Si:H(P) #11	2×10^{-4}		0.28	0.34	150	50
a-Si:H(P) #12	7.5×10^{-4}		0.24	0.33	150	80
a-Si:H(Li) (low doping)	8.5×10^{-6}	2.14×10^{-4}	0.35	0.40	170	30
a-Si:H(Li) (high doping)	3.0×10^{-3}	3.3×10^{-3}	0.14	0.23	120	12

The measurement chamber is shown in Fig. 4.3. The samples are kept on a copper block having a heater and a water circulation facility. The top view of the copper block with the sample is shown in the Fig. 4.4. The conductivity measurements are carried out in vacuum as a function of temperature (T), such that $250K \leq T \leq 500K$. The system also enables us to heat or cool the samples at a desired rate. For slow cooling ($\approx 1 - 2K/min$), the heater current is slowly reduced. Cooling rates as high as $400 - 600K/min$ are achieved by switching off the heater at a high temperature ($\approx 450K$) and then circulating chilled water through the copper block. The top plate of the chamber has a quartz window through which light is shone during the photoconductivity (σ_{ph}) measurements as well as for light soaking these films in vacuum. This system facilitates us to do all electrical measurements such as I-V, dark and photo conductivity (σ and σ_{ph}) as a function of temperature in the slow cooled (SC), fast quenched (FQ) and the light soaked (LS) states in vacuum, without disturbing the sample, once it is loaded.

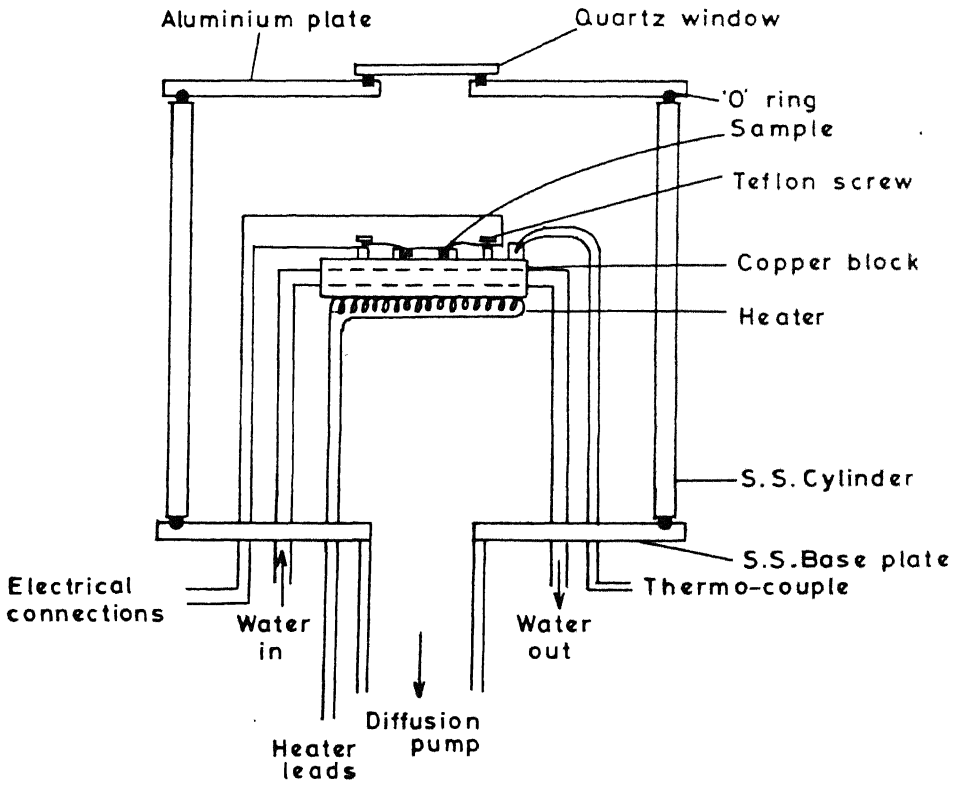

Figure 4.3: Schematic diagram of measurement chamber used for conductivity measurements in SC, FQ and LS states

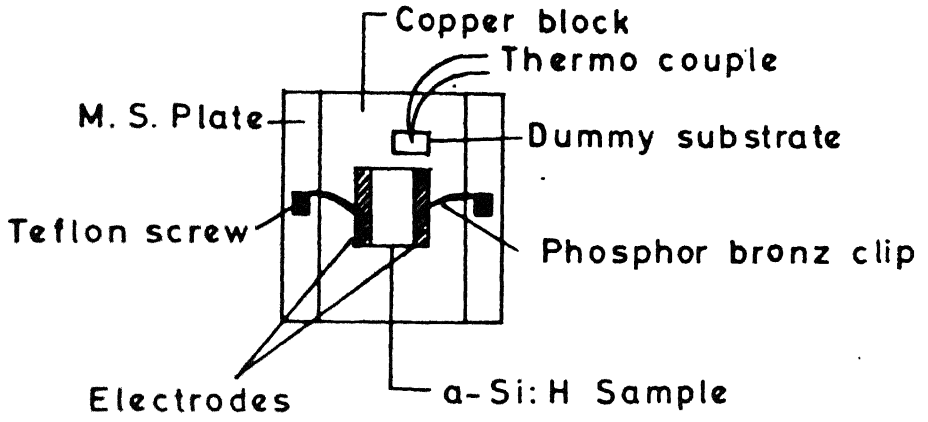

Figure 4.4: Top view of sample holder (conductivity)

For a better thermal contact between the sample and copper block, silver paint has been used. The temperature of the sample has been monitored using a Chromal-Alumel thermocouple placed on the dummy substrate (Corning 7059) mounted next to the sample. The reference junction of the thermocouple is placed in a beaker containing water, whose temperature is measured by a mercury thermometer, to determine the reference temperature accurately.

Thermopower set up is similar to the conductivity set-up [148] except that it has two copper blocks at a separation of $\approx$ 5 mm with separate heaters so that both the ends of the sample can be heated independently and also a desired temperature difference can be maintained between the two ends of the sample. A lateral view of the sample holder is shown in the Fig. 4.5. This system also has a water circulation and a light shining facility similar to the conductivity set-up and thus enables us to do these measurements in SC, FQ, and LS states without disturbing the sample.

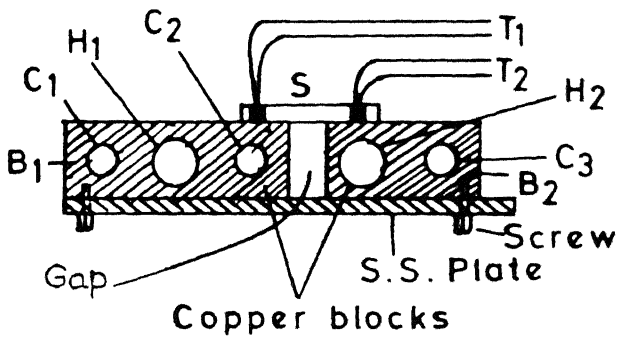

T_1, T_2 Thermo couples
H_1, H_2 Heaters
C_1, C_2, C_3 Water circulation line
S Sample
B_1, B_2 Copper blocks.

Figure 4.5: Lateral view of sample holder (thermopower)

4.3.2 Measurement Details

We have measured the conductivity and thermopower in the SC, FQ and LS states. In addition the relaxation from metastable state at a fixed temperature is also done for both FQ and LS states.

4.3.2.a Conductivity Measurements

Dark conductivity (σ) measurements are done at room temperature as a function of voltage in vacuum using a Keithley 617 electrometer–voltage source. The σ(T) measurements are done in the ohmic range. The samples are annealed at $470K$ for about 1 hour, and then slowly cooled ($\approx 1K/min$) to room temperature. Conductivity ($\sigma(T)$) measurement are done during slow cooling of the sample. Films are then

heated slowly ($1-2K/min$) to $470K$ and the conductivity is measured during heating also. The two $\sigma(T)$ curves (while heating and cooling) are found to be identical.

The photoconductivity (σ_{ph}) of these films is measured at room temperature in vacuum. The films are exposed to $\approx$10mW/cm^2 LO light (at flim surface) from a $200W, 220V$ tungsten lamp using a red filter. For the intensity dependence of photoconductivity, neutral density filters are used. A combination of these filters allow the relative intensity to vary over 4 orders of magnitude. LO light is used for all the photoconductivity measurements to avoid the Staebler-Wronski effect, commonly observed in these films.

In order to study the effect of fast quenching (FQ) on a-Si:H films (Thermal induced metastability), these films are annealed at a high temperature ($\approx 470K$) for 1 hour and then fast quenched by circulating water through the copper block. The water is kept circulating for more than half an hour,so as to bring the entire system to thermal equilibrium near room temperature. The $\sigma(T)$ measurements in the fast quenched state are done while heating it slowly ($1-2K/min$). Changes in σ and E_σ have been observed for doped films after fast quenching.

For the study of light induced metastability, the sample is first annealed at 470K and then slowly cooled to room temperature. HI light from a $360W, 80V$ ENX tungsten halogen lamp (intensity $\approx 150mW/cm^2$) or a LO light from a tungsten lamp is shone through the quartz window. A beaker filled with water is kept on the top of the window, to absorb heat and cut-off infrared light during light soaking at room temperature. Water is circulated continuously through the copper block to avoid any change in sample temperature during light soaking of these films. After light soaking the sample for the required time, the lamp is put off and the window is covered with a black cloth. Water circulation is kept on for another half an hour so as to bring the system into thermal equilibrium at room temperature. Conductivity measurements are then done while heating slowly as described earlier. A change in

$\sigma(T)$ is observed in some of these films after light soaking. An on-line computer is used for σ(T) measurements in the SC, FQ and LS states.

4.3.2.b Isothermal Relaxation

The thermal and light induced metastable states slowly return to the equilibrium slow cooled state, at any temperature $T \leq T_E$. To study the kinetics of recovery of metastable state obtained after FQ and LS, the sample in metastable state is heated quickly ($\approx$ 10-20min) to the measurement temperature and the σ is monitored as a function of time using an on-line computer. The electrical bias is kept on during the σ(t) measurement. The recovery kinetics is studied at different temperatures, after both FQ and LS and the normalized conductivity $Y(t)$ has been fitted a stretched exponential as given by Eq.. (3.8) to obtain the relaxation parameter β and τ. $Y(t)$ is defined as

$$Y(t) = \frac{\sigma(t) - \sigma(\infty)}{\sigma(0) - \sigma(\infty)} \tag{4.6}$$

where σ(t) is the conductivity at any time t, $\sigma(0)$ and $\sigma(\infty)$) are the conductivity values in the beginning i. e. , at $t = 0$ and in the final slow cooled state respectively.

4.3.2.c Thermopower Measurements

For measurement of thermopower S, coplanar nichrome electrodes, about 1 cm long and 0.5 cm apart, are evaporated on the top surface of the film. The sample is placed in the measurement chamber such that the two electrodes are on two separate copper blocks. For a better thermal contact between the sample and the copper blocks, silver paint is used. The temperatures of the two ends (T_1 and T_2) are monitored using Copper-Constantan (Cu-Ct) thermocouples, placed on each electrodes. By varying the heater currents a variable temperature difference ΔT ranging between 0 and $5K$ could be achieved. Thermo-emf ΔV is measured using copper wires of the two thermocouples. Since a-Si:H films are resistive, the signal is often very noisy. To

avoid any electrical pick-up, the thermocouple wires coming out of the chamber are shielded using an aluminium box. It is often observed that, the curve ΔV vs. ΔT does not pass through the origin (see Fig 4.6). This may probably be due to the fact that temperature read by the thermocouple is different than that of the sample. Thus if ΔV is measured only for a few values of ΔT, it could lead to an error in the determination of S, which is the slope of ΔV vs. ΔT. In order to avoid this, we have measured ΔV for 8-10 values of ΔT such that -5K $\leq \Delta T \leq$ 5K for an average temperature T, which may vary, in some cases between T $\pm$ 2K.

It is observed that if these measurements are done in partial pressure of inert gas like helium, the curve ΔV vs. ΔT shifts towards the origin. This may be due to the fact that helium provides a better thermal contact between the thermocouple and sample.

To measure S, the sample is initially annealed at 470K and cooled slowly. All the measurements are done in He atmosphere, while heating the sample. Effects of fast quenching and light soaking on S are also studied. The metastabilities are introduced in the same way as described for the conductivity measurements.

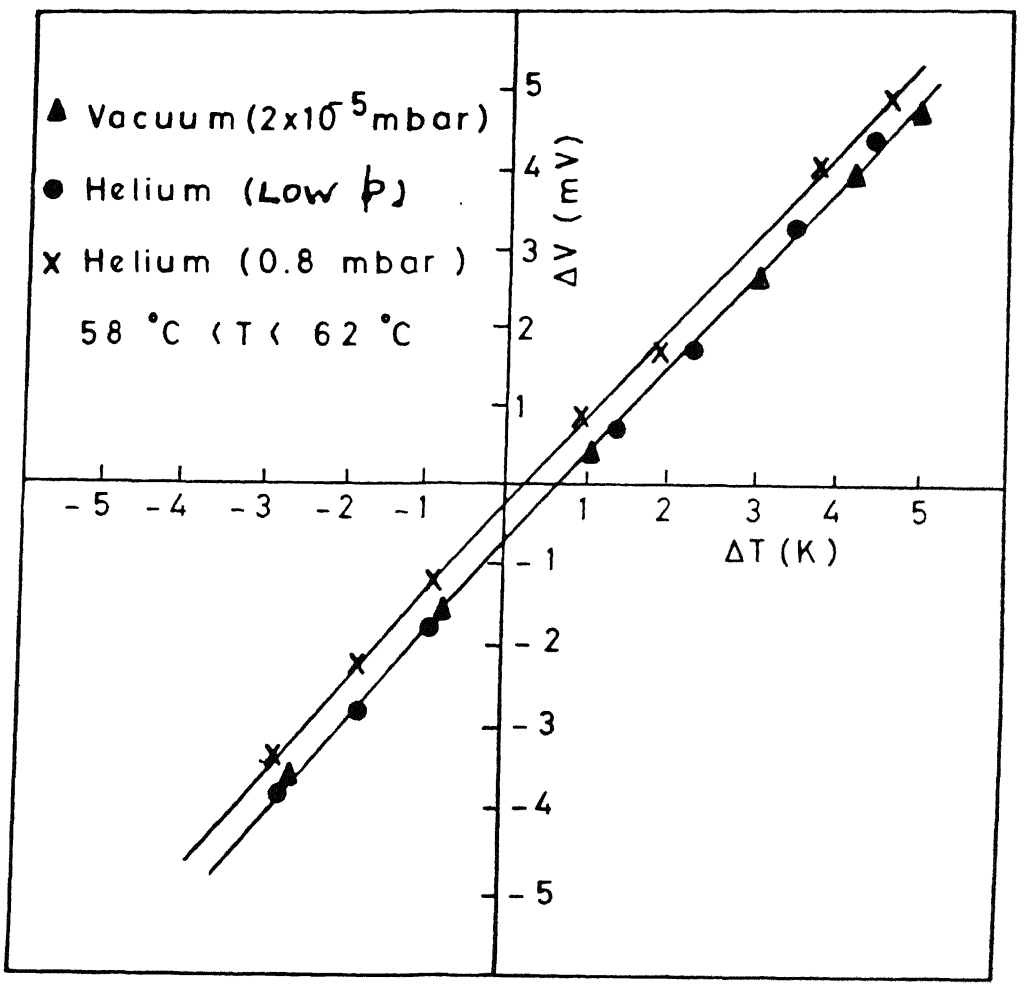

Figure 4.6: Thermovoltage (ΔV) vs. temperature difference (ΔT) in vacuum and He atmosphere.

Chapter 5

Results

In the following, we present our results of the thermal and light induced metastabilities on undoped, P-doped and Li-doped a-Si:H. We have measured the conductivity (σ) and thermopower in the slow cooled (SC), fast quenched (FQ), and light soaked (LS) states. Furthermore, we have also measured the relaxation of metastable state introduced by fast quenching or light soaking a-Si:H films.

5.1 Effect of doping on conductivity of a-Si:H

As discussed in the chapter 2, for extended band conduction, the conductivity of a-Si:H films follows Arrhenius relationship,

$$\sigma = \sigma_0 \exp\left\{-\frac{E_c - E_f}{kT}\right\} \tag{5.1}$$

It is observed that most of these curves show two values of activation energy, E_σ, one below $400K$ and the other above $400K$ (Fig. 5.1). The room temperature conductivity $\sigma(300K)$ is observed to be higher than that determined by extrapolating the high temperature curve. The characteristic properties in the annealed and slow cooled (SC) state of the a-Si:H films are summarized in Table 4.3.

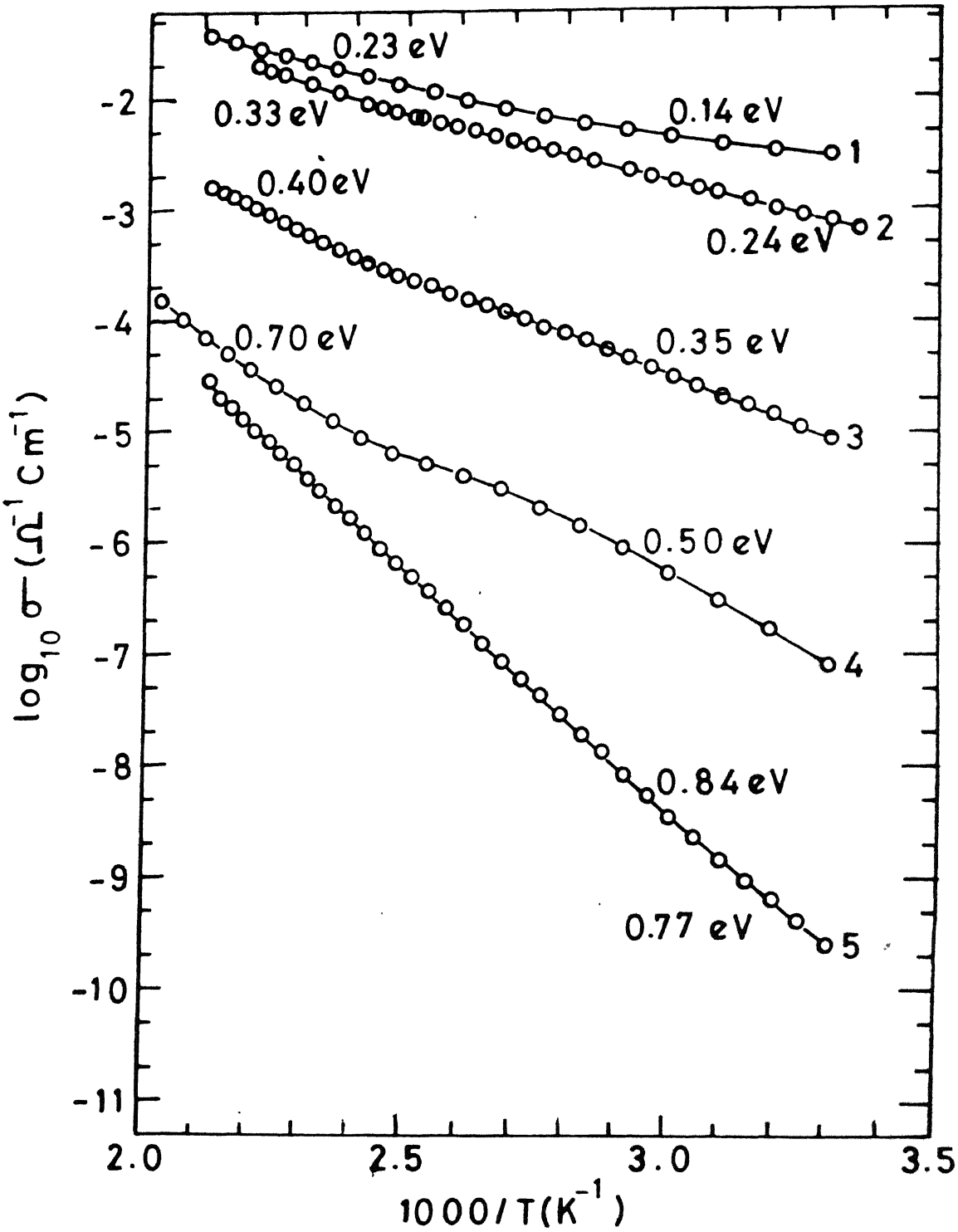

Figure 5.1: $\log\sigma$ vs. $1/T$ for a-Si:H films in SC state. Curves (4, 5) are for undoped, (2) for P-doped and (1, 3) are for Li-doped a-Si:H.

Fig. 5.1 shows the Arrhenius plot of σ for $300K \leq T \leq 500K$ for undoped and doped a-Si:H films in the annealed and slow cooled (SC) state. For the two undoped films (Curve 4 and 5), $\sigma(300K)$ are $9\times10^{-8}\Omega^{-1}cm^{-1}$ and $2.5\times10^{-10}\Omega^{-1}cm^{-1}$ respectively. The photoconductivity, $\sigma_{ph}(300K)$ under $\approx 10mW/cm^2$ light (LO red light) for these films are $6.5 \times 10^{-5}\Omega^{-1}cm^{-1}$ and $3 \times 10^{-6}\Omega^{-1}cm^{-1}$ respectively. The two films are qualitatively similar and the difference in $\sigma(T)$ is because of the different preparation condition.

When these films are doped with phosphorus $\sigma(300K)$ increases and activation energy (E_σ) decreases. Doping with phosphorus changes $\sigma(300K)$ to $2\times10^{-4}\Omega^{-1}cm^{-1}$ and $7.66 \times 10^{-4}\Omega^{-1}cm^{-1}$ respectively for the two slightly different doping concentrations (curve 2). The E_σ values for $T \geq 400K$ are $0.35eV$ and $0.33eV$ respectively. The difference between σ and σ_{ph} for these films is negligible in presence of LO light at room temperature. These results are in agreement with the published results [6].

Doping with Li increases both σ and σ_{ph} [49]. For a-Si:Hfilms with low Li concentration, $\sigma(300K)$ and $\sigma_{ph}(300K)$ (for LO red light) are $\approx 8.5 \times 10^{-6}\Omega^{-1}cm^{-1}$ and $2.14 \times 10^{-4}\Omega^{-1}cm^{-1}$ respectively. For high lithium concentrations, $\sigma(300K) \approx 3 \times 10^{-3}\Omega^{-1}cm^{-1}$ and $\sigma_{ph}(300K) \approx 3.3 \times 10^{-3}\Omega^{-1}cm^{-1}$. The E_σ values for $T \leq T_E$ in these films are to $0.35eV$ and $0.14eV$. For $T \geq T_E$, these values are $0.4eV$ and $0.23eV$ respectively (Curve 1 and 3). All these results are summarized in Table 4.3.

The results for Li doped films are in agreement with those published for P-doped a-Si:H and can be understood as follows. Doping increases the defect density in a-Si:H. These defects act as trapping centers for the photogenerated electrons and holes and thus reduce the photoconductivity. Also the density of photogenerated electrons is comparable to the equilibrium carrier density and thus a small difference is seen between σ_{ph} and σ for heavily doped films as compared to the low doped a-Si:H.

It is also evident from these curves, that $\log\sigma$ vs. $1/T$ has a kink for almost all the films. The activation energies below and above the kink are different and E_σ is higher for the high temperature range. This kink may arise due to a change in

conduction mechanism or due to a non linear statistical shift of the Fermi level (see section 2.3). We have shown in chapter 2, that a non linear statistical shift of the Fermi level is the more likely reason for the observed kink in a-Si:H.

5.2 Undoped a-Si:H

Fig. 5.2 shows the $\log \sigma$ vs. $1/T$ curve for undoped a-Si:H prepared by glow discharge of a mixture of 3% Silane in Argon. $\sigma(300K)$ in SC state is $\approx 9 \times 10^{-8}\Omega^{-1}cm^{-1}$. In presence of LO red light from a tungsten lamp. $\sigma_{ph}(300K)$ is $\approx 6.5 \times 10^{-5}\Omega^{-1}cm^{-1}$ with $\gamma \approx 0.5$, ($\sigma_{ph} \propto G^{\gamma}, G$ the is intensity of light). Qualitatively similar results are obtained for the a-Si:H films prepared by glow discharge of pure Silane. The $\log \sigma$ vs. $1/T$ curve for one of these films is shown in Fig. 5.3.

5.2.1 Thermal Induced Metastability

As is clear from Figs. 5.2 and 5.3, upon fast quenching ($\geq 400K/min$) from 470 to $500K$, undoped a-Si:H films used in the present study, do not show any change in $\sigma(300K)$. The Arrhenius plot of these films remains unchanged in the measurement temperature range after fast quenching. A small decrease in σ_{ph} is, however, observed as a result of fast quenching and is listed in Table 5.1.

5.2.2 Light Induced Metastability

Light soaking these films with LO white light for 2 hours, decreases both σ and σ_{ph}. (See Fig. 5.2 and Table 5.1). In the light soaked (LS) state $\sigma(300K) \approx 2.5 \times 10^{-9}\Omega^{-1}cm^{-1}$. The exponent γ changes to 0.8 in LS state and E_{σ} is now 0.71 eV. The $\sigma(T)$ curve in LS state meets the corresponding SC curve at $\approx 455K$ and for $T \geq 455K$, $\sigma(T)$ is unique. The effect is completely reversible and annealing at $475K$

Table 5.1: σ, σ_{ph} and E_σ of a-Si:H films in SC, FQ, LS and FQ+LS states. Exponent γ for the intensity dependence of σ_{ph} is also shown. The quenching and light soaking conditions are as described in the text. Light used for σ_{ph} is shown in column 1

Sample	State	σ (300K) $\Omega^{-1}cm^{-1}$	σ_{ph} (300K) $\Omega^{-1}cm^{-1}$	E_σ(eV) $(T < T_E)$	γ
a-Si:H #18	SC	9.0×10^{-8}	6.5×10^{-5}	0.50	0.5
Undoped	FQ	9.0×10^{-8}	5.5×10^{-5}	0.50	
LO Red light	LS	2.5×10^{-9}	9.91×10^{-6}	0.71	0.80
	FQ+LS	2.4×10^{-9}	9.25×10^{-6}	0.71	0.73
a-Si:H #15	SC	2.5×10^{-10}	3×10^{-6}	0.84	0.78
Undoped	FQ	2.4×10^{-10}	2.43×10^{-6}	0.84	0.75
LO Red light	LS	2.0×10^{-11}	8.41×10^{-8}	1.01	0.86
a-Si:H(P) #11	SC	2×10^{-4}		0.28	
	FQ	3.5×10^{-4}		0.22	
	LS	2×10^{-4}			
	FQ+LS	3.5×10^{-4}			
a-Si:H(P) #12	SC	7.5×10^{-4}		0.24	
	FQ	1.2×10^{-3}		0.21	
a-Si:H(Li)	SC	1×10^{-5}	6×10^{-4}	0.35	0.35
(low doping)	FQ	7.5×10^{-5}	7.2×10^{-4}	0.20	
LO White light	LS	2.5×10^{-8}	1.36×10^{-4}	0.75	0.77
	FQ+LS	4.0×10^{-8}	1.61×10^{-4}		
a-Si:H(Li)	SC	3×10^{-3}	3.38×10^{-3}	0.14	
(high doping)	FQ	6×10^{-3}	6.8×10^{-3}	0.09	
LO Red light	LS	1.5×10^{-3}	1.84×10^{-3}	0.15	
	FQ+LS	3×10^{-3}		0.09	
a-Si:H(Li)	SC	3×10^{-3}	5.68×10^{-3}	0.14	
(high doping)	FQ	6×10^{-3}	8.35×10^{-3}	0.09	
HI White light	LS	1.5×10^{-3}	4.12×10^{-3}	0.15	
	FQ+LS	3×10^{-3}	6×10^{-3}	0.09	

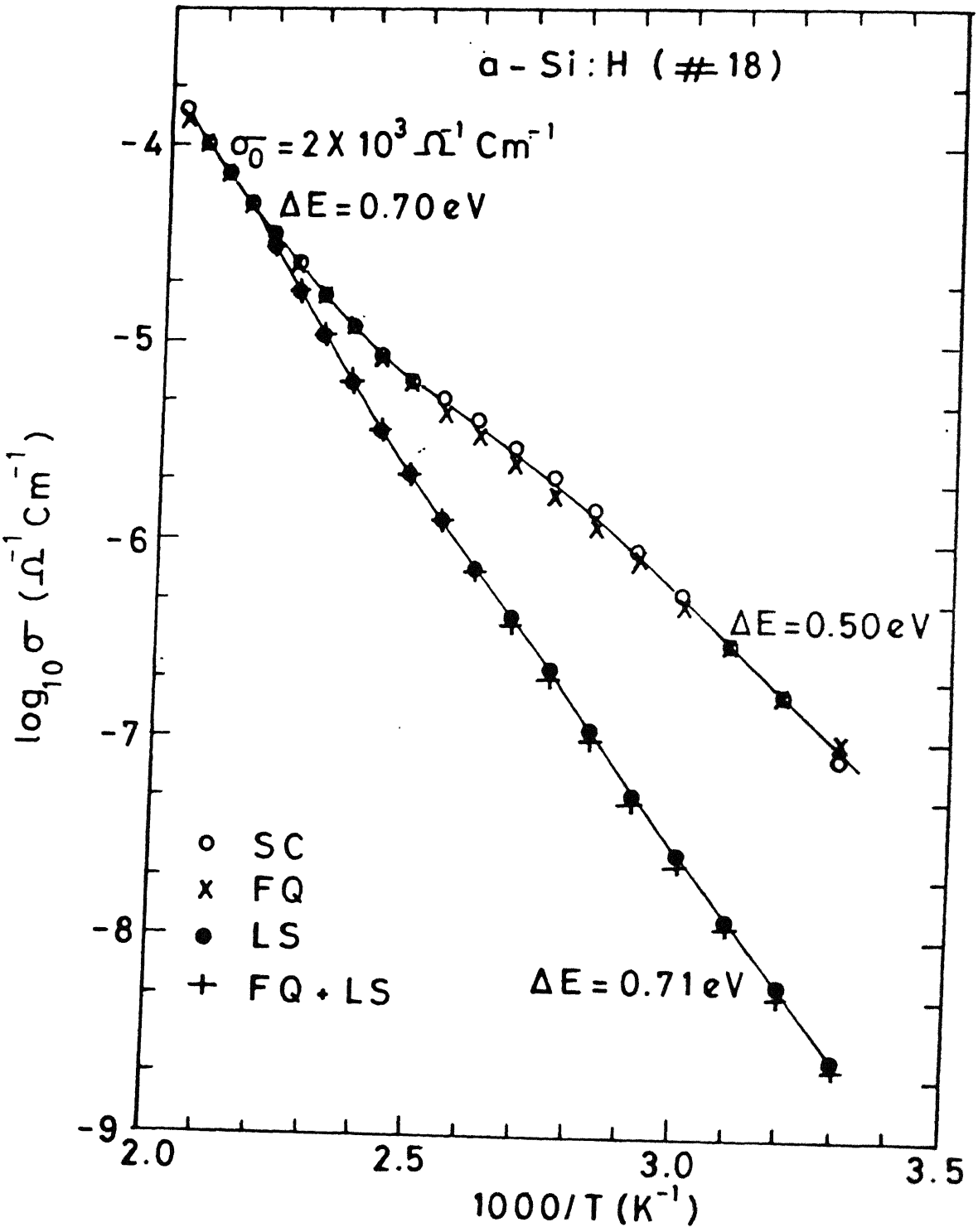

Figure 5.2: $\log \sigma$ vs. $1/T$ for undoped a-Si:H in slow cooled (SC), fast quenched (FQ) and light sokaed (LS) states.

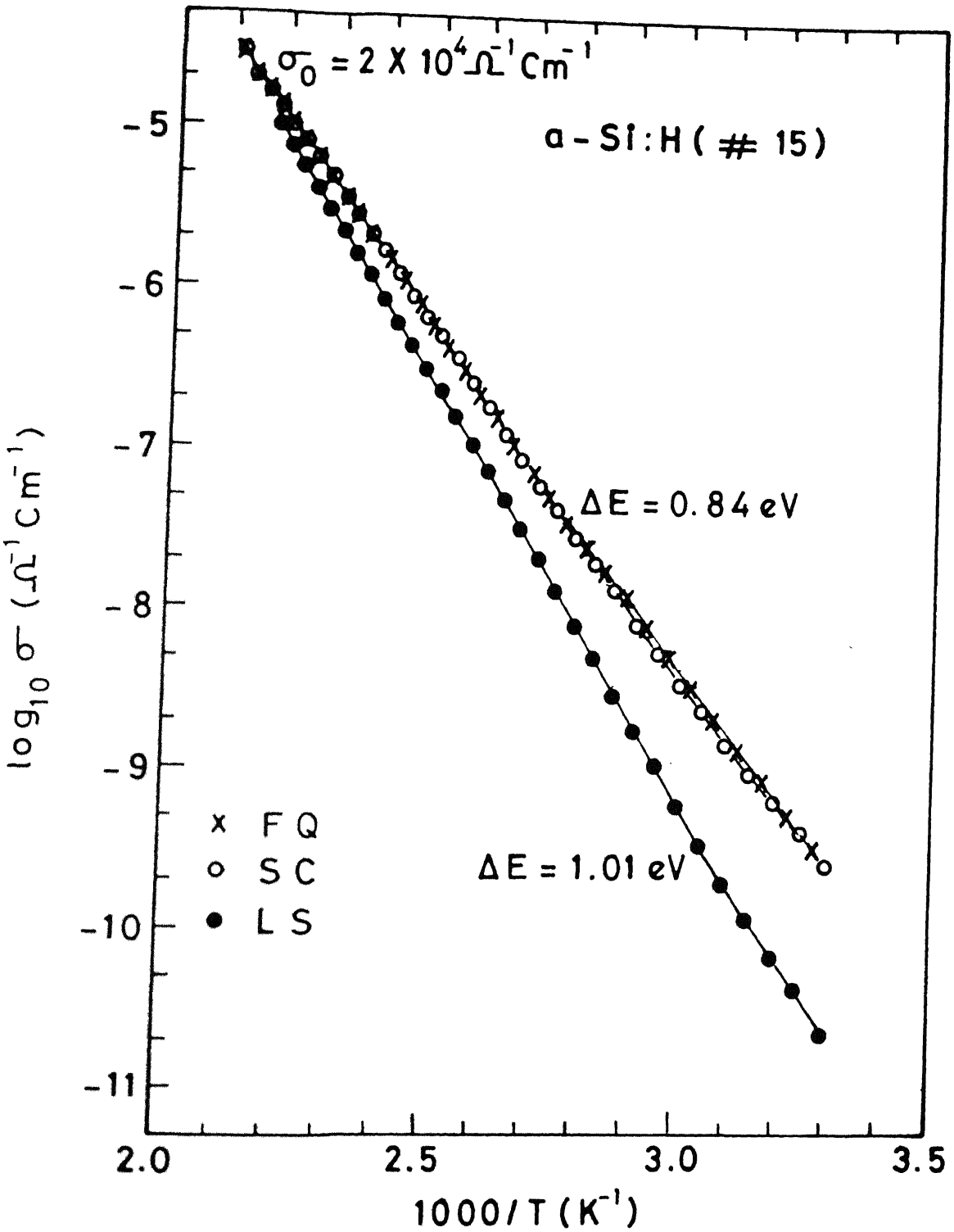

Figure 5.3: $\log \sigma$ vs. $1/T$ for undoped a-Si:H in slow cooled (SC), fast quenched (FQ) and light sokaed (LS) states.

for $\approx 1h$ results in the initial SC state. These results are similar to the reports in literature [10].

Similar effect of light soaking has been observed for undoped films prepared by pure Silane. These film also show a decrease in σ and σ_{ph} upon Light soaking with heat filtered high intensity white light (HI light $\approx 150mW/cm^2$ of incident intensity at film surface) (Fig. 5.3 and Table 5.1). In the LS state, the σ $(300K)$ is $\approx 2 \times 10^{-11}\Omega^{-1}cm^{-1}$ and $E_\sigma is \approx 1.01eV$. The $\sigma(T)$ curve in LS state meets the equilibrium curve at $\approx 470K$. Annealing at this temperature brings back the original state of these films.

5.3 Phosphorus Doped a-Si:H

Fig. 5.4 and 5.5 show $\log\sigma$ vs. $1/T$ curves for the two P-doped a-Si:H (a-Si:H(P)) films. In the SC state, for the two films investigated here, the observed values of $\sigma(300K)$ are $2 \times 10^{-4}\Omega^{-1}cm^{-1}$ and $7.66 \times 10^{-4}\Omega^{-1}cm^{-1}$ respectively. The $\sigma(T)$ curves for both the films show two values of activation energies (Fig. 5.4 and 5.5). For $T \leq 400K$, E_σ for the two films are found to be $\approx 0.28eV$ and $\approx 0.24eV$ respectively. These values of E_σ at $T \geq 400K$ change to $0.35eV$ and $0.33eV$. The prefactor σ_0 is $50\Omega^{-1}cm^{-1}$ and $80\Omega^{-1}cm^{-1}$ for the two films. The two films are qualitatively similar and a small difference in σ might be due to a slightly different doping concentrations.

5.3.1 Thermal Induced Metastability

An increase in $\sigma(300K)$ is observed (see Figs. 5.4 and 5.5) when phosphorus doped a-Si:H films are fast quenched from $450K$. The $\sigma(300K)$ for the two films in FQ state are $3.5 \times 10^{-4}\Omega^{-1}cm^{-1}$ and $1.2 \times 10^{-3}\Omega^{-1}cm^{-1}$ respectively. A decrease in E_σ is also observed in FQ state for both the films. The new values of E_σ in fast quenched state are now $0.22eV$ and $0.24eV$ respectively. The $\sigma(T)$ curves after FQ meet the

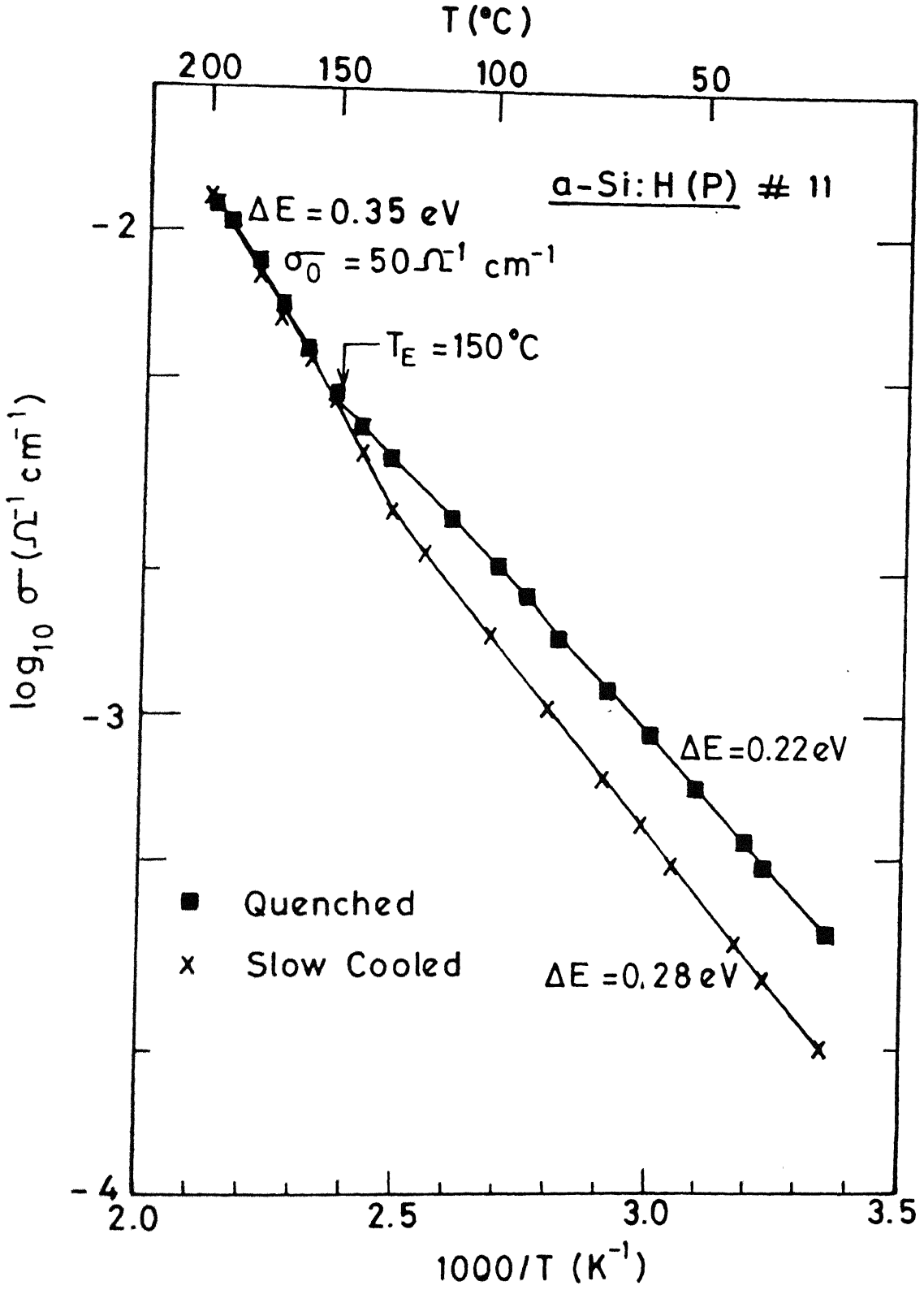

Figure 5.4: $\log \sigma$ vs. $1/T$ for a-Si:H(P) in slow cooled (SC), fast quenched (FQ) states.

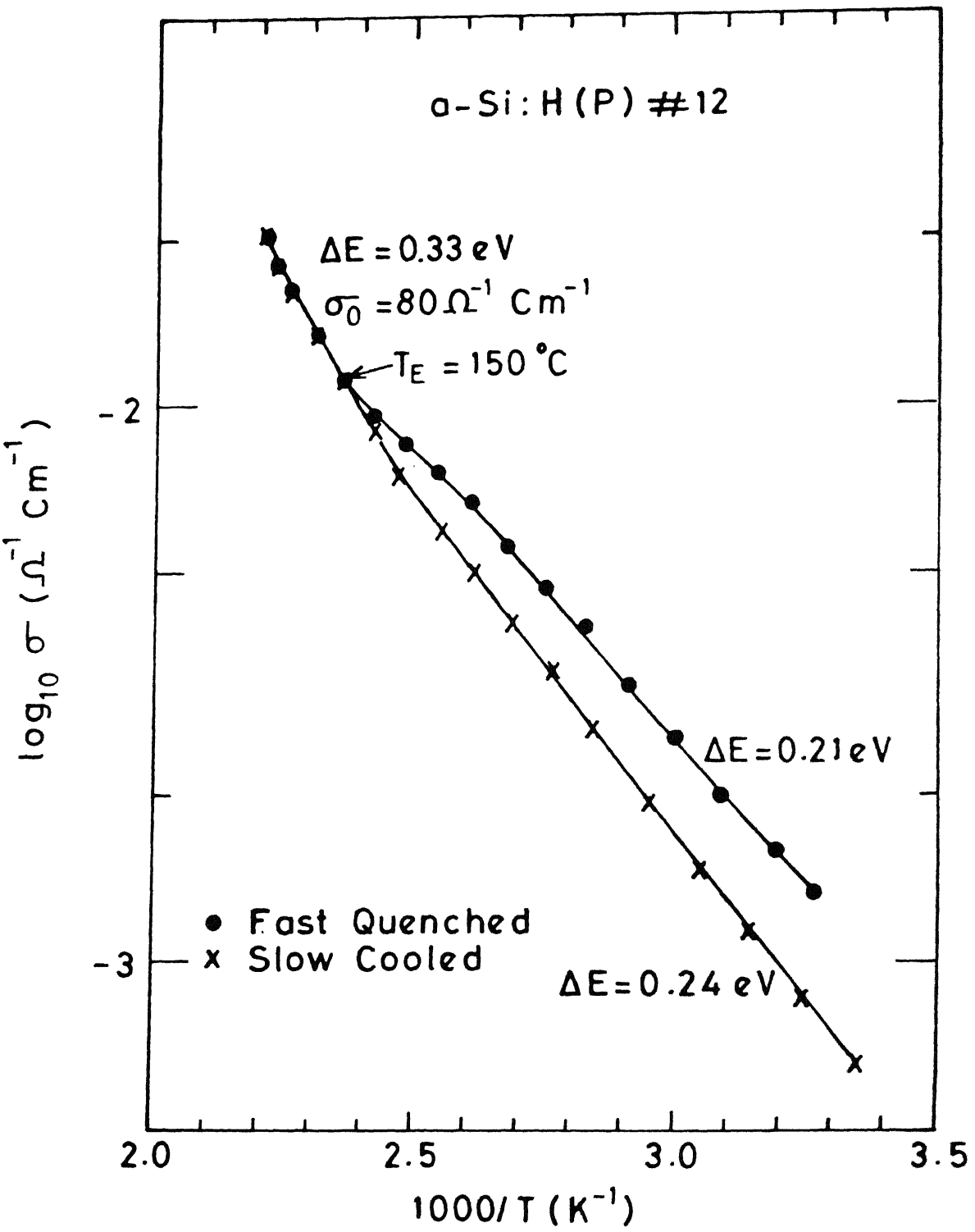

Figure 5.5: $\log \sigma$ vs. $1/T$ for a-Si:H(P) in slow cooled (SC), fast quenched (FQ) states.

corresponding SC curves at $420K$ for both the films. These results are in agreement with those reported by Street *et al.* [16].

5.3.2 Light Induced Metastability

Unlike undoped a-Si:H films, these films do not show any change in $\sigma(300K)$ after exposing them to LO light or heat filtered HI white light. The $\log \sigma$ vs. $1/T$ curve remains unaltered for these films upon light soaking. There are some reports in literature, where a decrease in σ of a-Si:H(P)after light soaking has been reported, however, the effect is small in case of a-Si:H(P)with higher P concentrations

5.3.3 Isothermal Relaxation

The metastable states created by fast quenching from high temperatures or by light soaking, slowly approach the equilibrium value (the slow cooled state) at $T \leq T_E$ following a stretched exponential

$$Y(t) = \exp\left\{-\left(\frac{t}{\tau}\right)^{\beta}\right\} \tag{5.2}$$

where, $Y(t)$ is the normalized conductivity defined in Eq.(4.6). The parameters τ and β are temperature dependent.

Fig. 5.6 shows the Isothermal relaxation curves at different temperatures for a phosphorus doped a-Si:H films after fast quenching these films from $450K$. Similar to the reported results recovery at each temperature follows a stretched exponential time dependence. The relaxation time τ decreases as the measurement temperature is increased and is found to be thermally activated, with an activation energy of $\approx 1eV$(see Fig. 5.7). The exponent β is also a temperature dependent parameter and increases with temperature (Fig. 5.8). Kakalios *et al.* [30] measured the time dependence of excess band tail carrier density and obtained the similar temperature dependence of β and τ for P-doped a-Si:H.

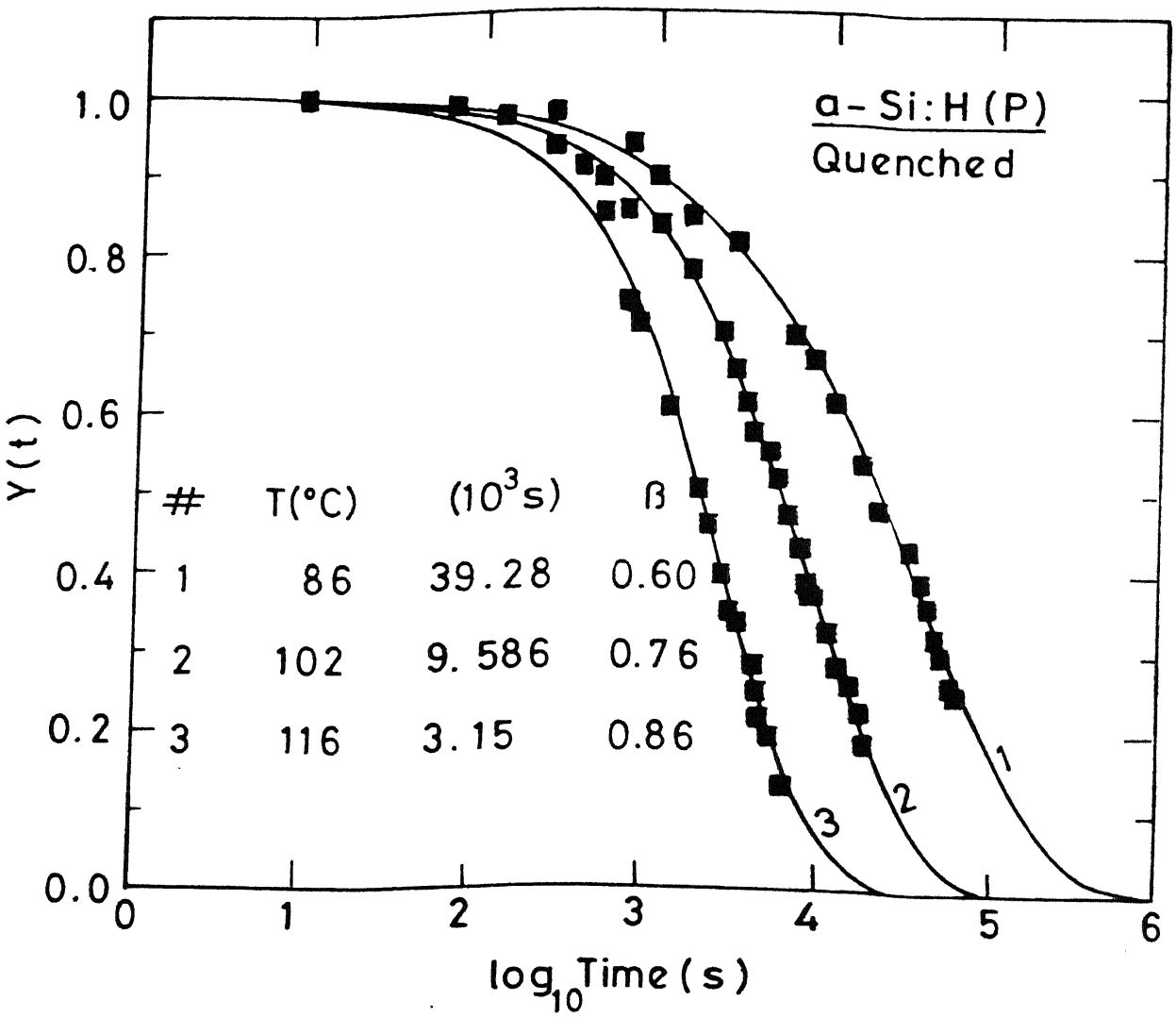

Figure 5.6: Normalised conductivity $Y(t)$ vs. $\log(t)$ for relaxation from FQ state for a-Si:H(P) at different temperatures. Points are actual data, line is fit to the Eq.(3.8). The corresponding fit parameters β and τ are also shown.

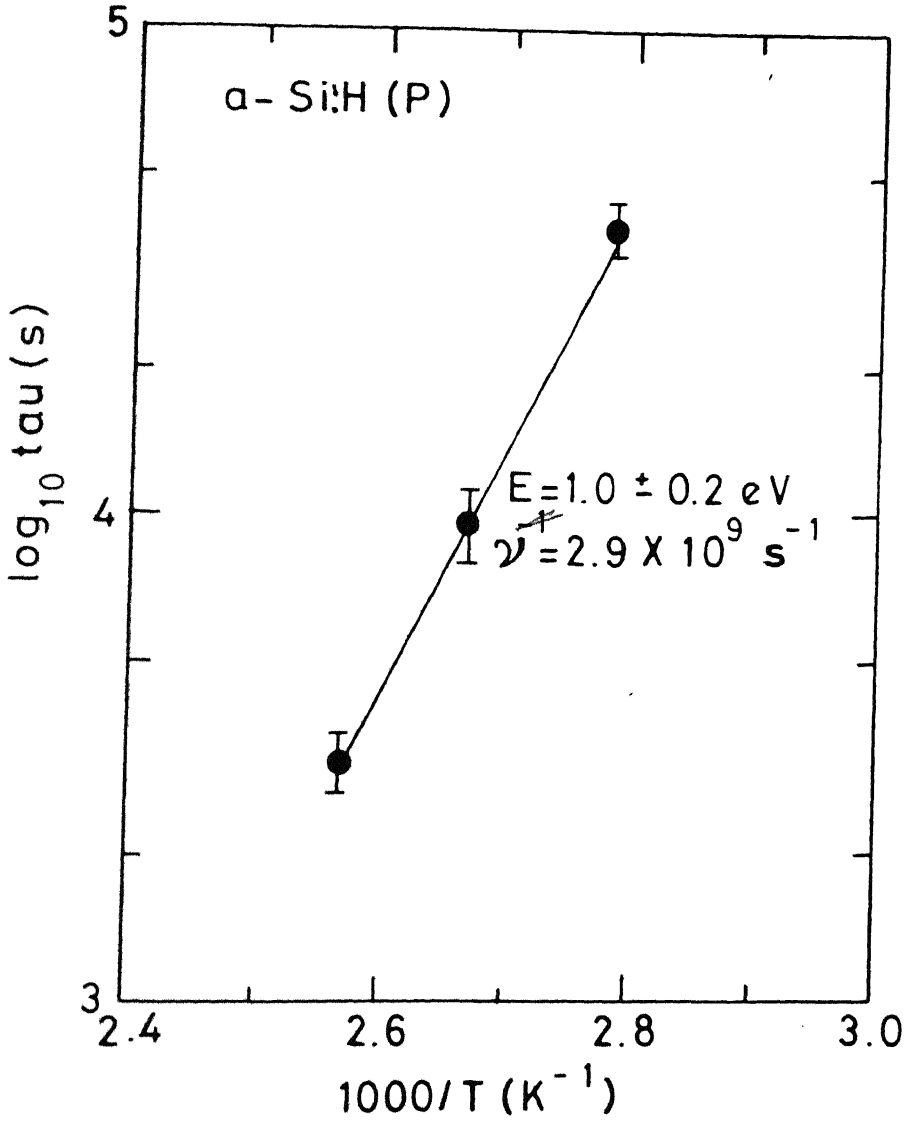

Figure 5.7: $\log \tau$ vs. $1/T$ for a-Si:H(P) for relaxation from FQ state at different temperatures.

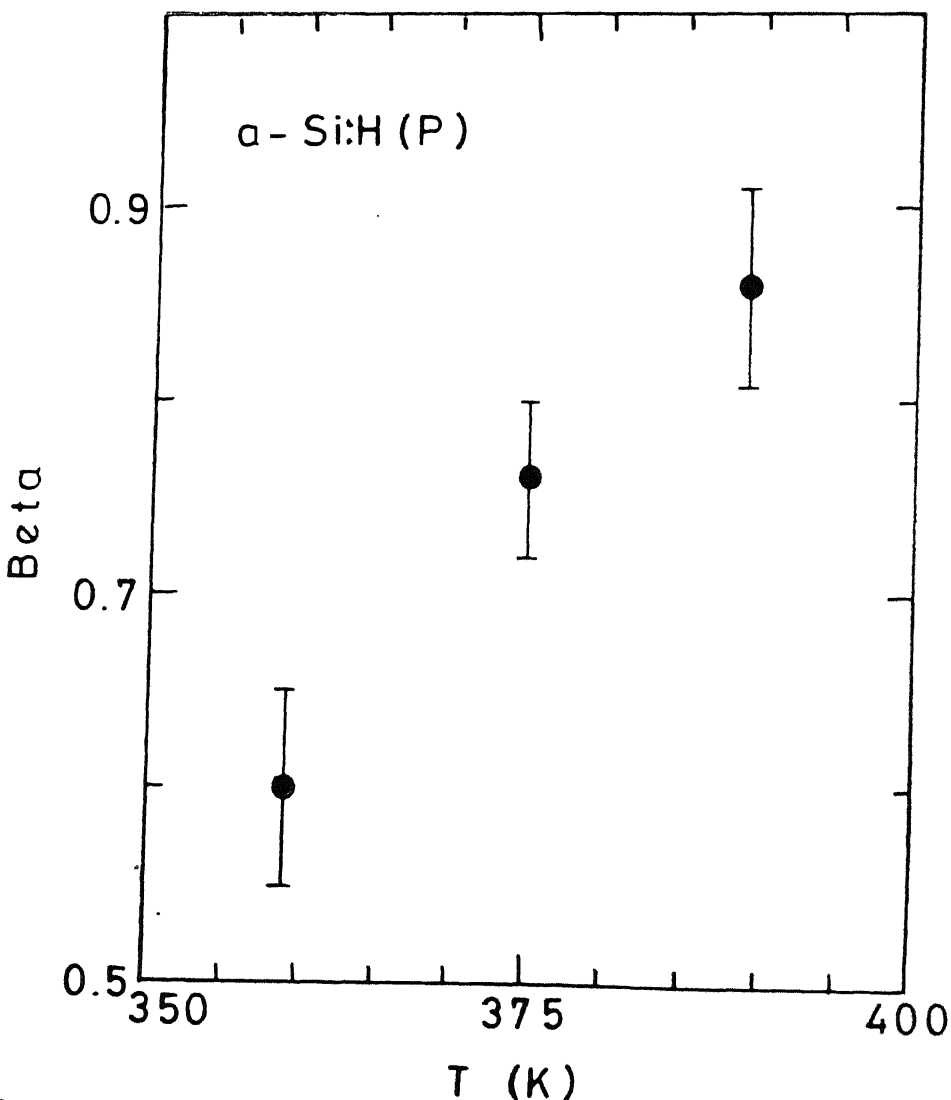

Figure 5.8: β vs. $1/T$ for a-Si:H(P) for relaxation from FQ state

5.4 Lithium Doped a-Si:H Films

Fig. 5.9 and 5.10 show $\log \sigma$ vs. $1/T$ curves for two lithium doped a-Si:H films for different doping concentrations. Doping with lithium causes an increase in $\sigma(300K)$ and decrease in E_σ of these films. We present our results for two doping concentrations in the following.

For a-Si:H films with low Li concentration, $\sigma(300K) \approx 1 \times 10^{-5}\Omega^{-1}cm^{-1}$ which is nearly two orders of magnitude higher as compared to the undoped films. The activation energy E_σ near room temperature for these films is $\approx 0.35eV$ and for $T \geq 400K$ the value of E_σ is $\approx 0.40eV$. The prefactor σ_0 is $\approx 30\Omega^{-1}cm^{-1}$ for the high temperature curve (Fig. 5.9).

For a-Si:H films with high Li concentration, $\sigma(300K)$ changes to $\approx 3 \times 10^{-3}\Omega^{-1}$ cm^{-1}, about 4×10^4 times of the undoped films (See Fig. 5.10; Table 5.1). Activation energy (E_σ) for these films near room temperature is $0.14eV$ in SC state and at $T \geq 400K$, E_σ is nearly $0.23eV$, the prefactor σ_0 for high temperature curve is about $12\Omega^{-1}cm^{-1}$.

5.4.1 Thermal Induced Metastability

Fast quenching lithium doped a-Si:H (a-Si:H(Li)) films with low lithium concentration, from $470K$ at a cooling rate $\geq 500K/min$ results in about an order of magnitude increase in $\sigma(300K)$ (see Fig. 5.9). A small increase in photoconductivity (σ_{ph}) is also seen in the FQ state (Table 5.1). The activation energy E_σ of these films after FQ decreases to $0.20eV$ and $\sigma(T)$ curve in the FQ state meets the corresponding SC curve at $\approx 440K$ which is identified as equilibration temperature (T_E) for these films. For $T \geq 440K$, $\sigma(T)$ curve is unique, independent of the thermal history of the sample. These results are in qualitative agreement with the literature [48].

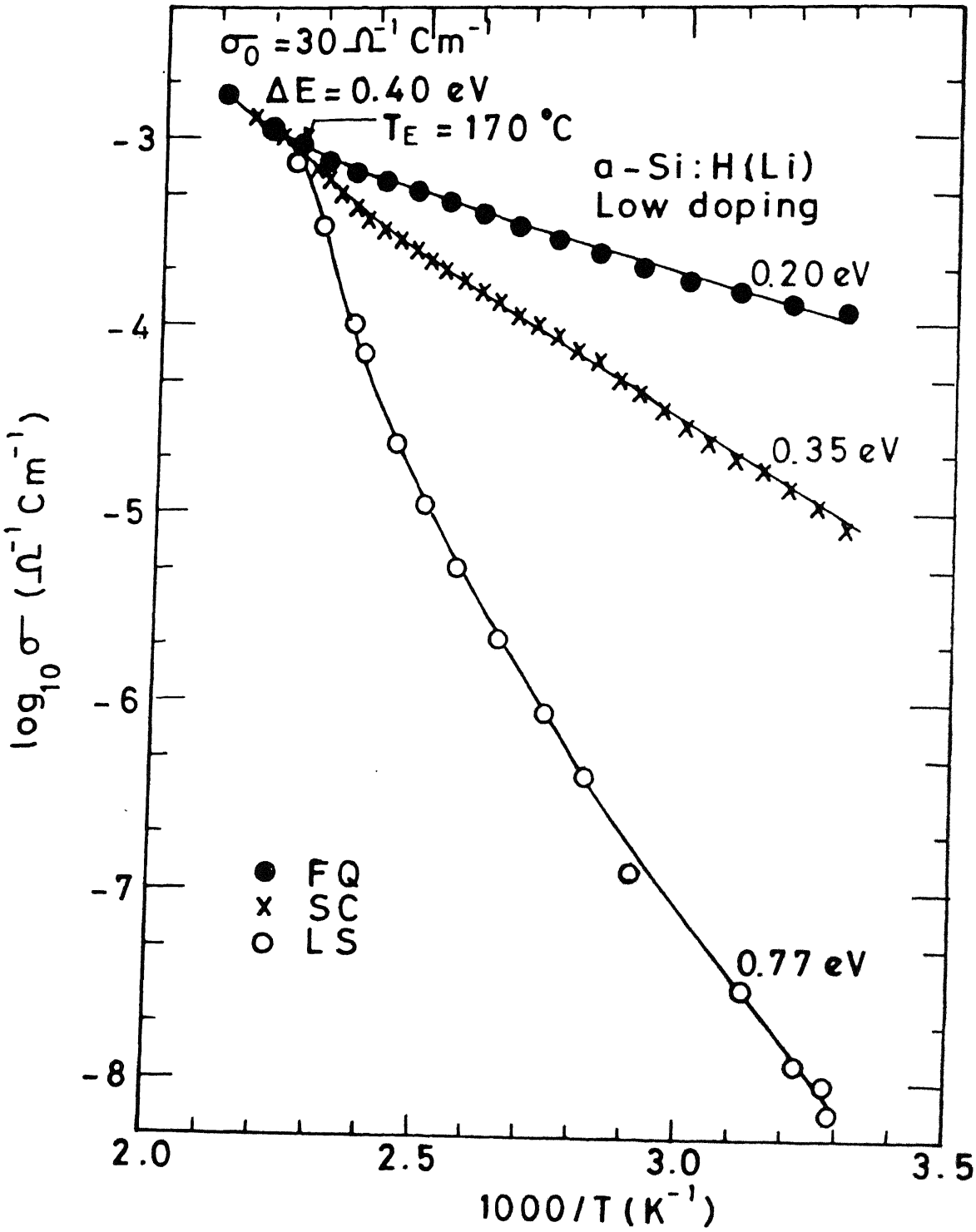

Figure 5.9: $\log \sigma$ vs. $1/T$ for low doped a-Si:H(Li) in slow cooled (SC), fast quenched (FQ) and light sokaed (LS) states.

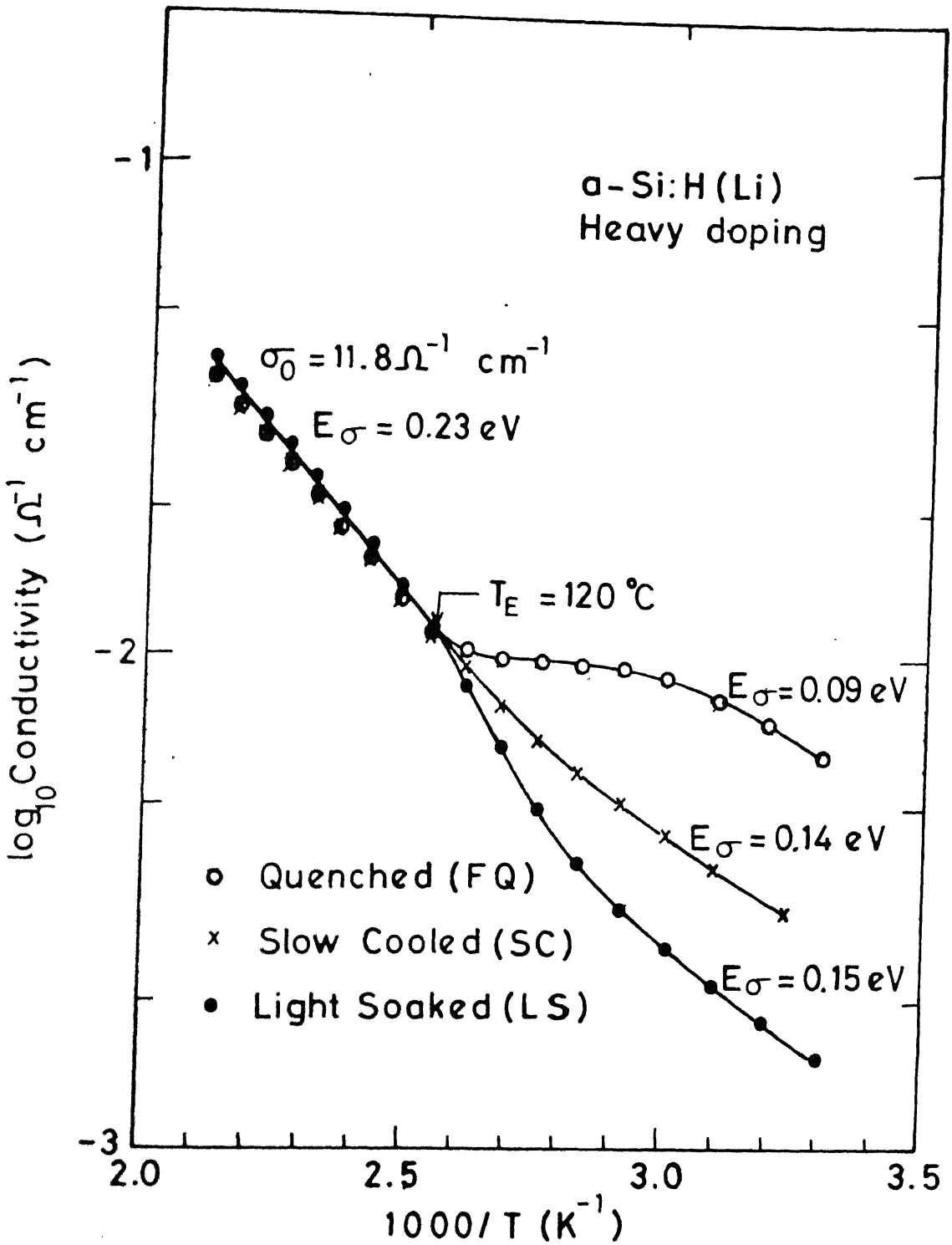

Figure 5.10: $\log\sigma$ vs. $1/T$ for heavily doped a-Si:H(Li) in slow cooled (SC), fast quenched (FQ) and light sokaed (LS) states.

Table 5.2: σ and E_σ for a-Si:H(Li) at 300K after quenching from different temperatures.

State	T_A °C	T_q °C	$\sigma(300K)$ $\Omega^{-1}cm^{-1}$	$E_\sigma(eV)$ $T < T_E$
SC	200		8.50×10^{-6}	0.35
FQ	180	165	5.50×10^{-5}	0.22
FQ	180	180	8.30×10^{-5}	0.20
FQ	200	195	6.25×10^{-5}	0.24
FQ	200	200	1.20×10^{-4}	0.20
T_A	$\Rightarrow$	annealing temperature &		
T_q	$\Rightarrow$	quenching temptrature		

Fast quenching a-Si:H films, with high Li concentration, from $470K$ causes a two fold increase in $\sigma(300K)$ from $3 \times 10^{-3}\Omega^{-1}\,cm^{-1}$ in SC state to $6 \times 10^{-3}\,\Omega^{-1}\,cm^{-1}$ in FQ state and a decrease in E_σ to $0.09eV$ near room temperature (Fig. 5.10). The $\sigma(T)$ curve obtained after FQ meets the curve in the SC state at $393K$ and above this temperature, $\sigma(T)$ is independent of thermal history of these films also. Thus for these films T_E is found to be $393K$. These results are in qualitative agreement with literature for P-doped a-Si:H.

5.4.1.a Effect Of Fast Quenching From Different Temperatures

Fig. 5.11 shows $\sigma(T)$ curve obtained after fast quenching a lithium doped a-Si:H film with low doping concentration from different temperatures (T_q). This doping is chosen as it shows the highest change in σ both after FQ as well as after LS. It is evident from this figure that as the quenching temperature is decreased from $470K$ to $435K$, the difference between $\sigma(300K)$ in SC and FQ states also decreases. E_σ also shows a dependence upon the quenching temperature (T_q). For $T_q \approx 470K$, E_σ is $0.20eV$ but when T_q is decreased to $435K$, which is slightly below the T_E for these films, the E_σ increases to $0.22eV$. It is further observed that for $T_q \geq T_E$, the

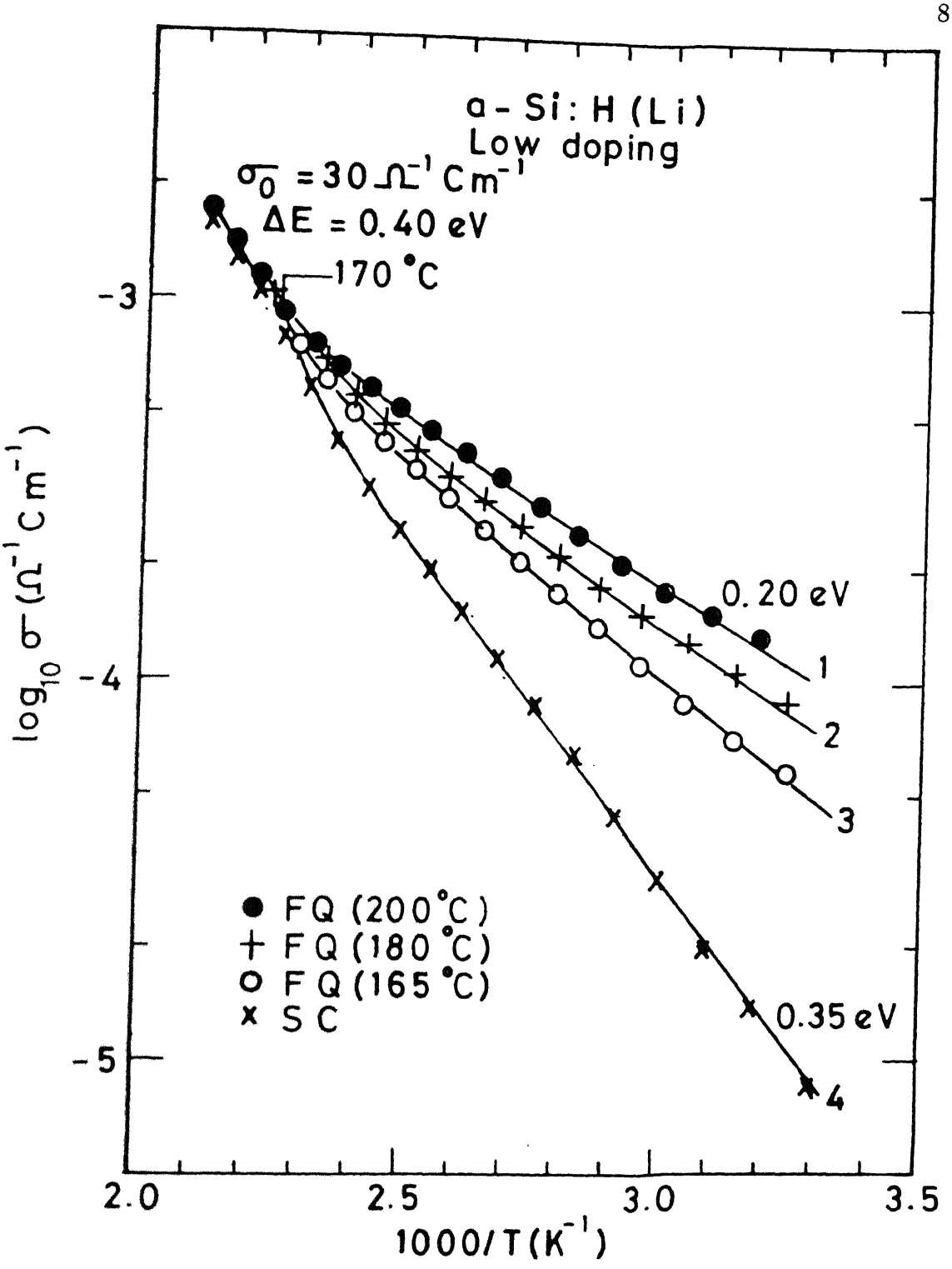

Figure 5.11: $\log\sigma$ vs. $1/T$ for low doped a-Si:H(Li) after quenching from different temperatures (T_Q). Curve in the SC state is also shown.

$\sigma(T)$ curve obtained after FQ meets the SC curve at $440K$, which is nothing but T_E for these films. However, for $T_q < T_E$, the two curves meet at the quenching temperature only. It is also observed that when the cooling rate is decreased the change in $\sigma(300K)$ is less. The results are also summarized in the Table 5.2. A cooling rate dependence on $\sigma(300K)$ has also been reported for P-doped a-Si:H by Street *et al.* [16].

5.4.2 Light Induced Metastability

Illuminating a-Si:H films with low Li concentrations at $300K$ with heat filtered LO ($\approx 15mW/cm^2$) white light for 15 hours results in about three orders of magnitude decrease in $\sigma(300K)$ and an increase in E_σ to $0.77eV$ (Fig. 5.9). A decrease in σ_{ph} is also seen after LS (see Table 5.1). The $\sigma(T)$ curve after LS meets the corresponding SC curve at $440K$ and for $T \geq 440K$, the $\sigma(T)$ curve is independent of the history of the sample. Similar to the undoped films, the effect of light soaking is found to be reversible for Li doped films.

For a-Si:H films with high Li concentration, light soaking at room temperature from heat filtered HI white light for 2 hours reduces the $\sigma(300K)$ to $1.5 \times 10^{-3}\Omega^{-1}cm^{-1}$, which is half of the value obtained after SC. A small change in E_σ is also observed after LS, which is now changed to $0.15eV$ (Fig 5.10). The $\sigma(T)$ curve in LS state meets the SC curve at $393K$ and is independent of initial state for $T \geq 393K$. The effect of light soaking on σ and E_σ for lithium doped a-Si:H is qualitatively similar to that reported in literature for P-doped films [15].

5.4.2.a Effect of Light Soaking on Exposure Time and Illumination Intensities

Fig. 5.12 shows the $\log\sigma$ vs. $1/T$ curve for a lithium doped a-Si:H films with a low doping concentration after exposing it to white light for different exposure times.

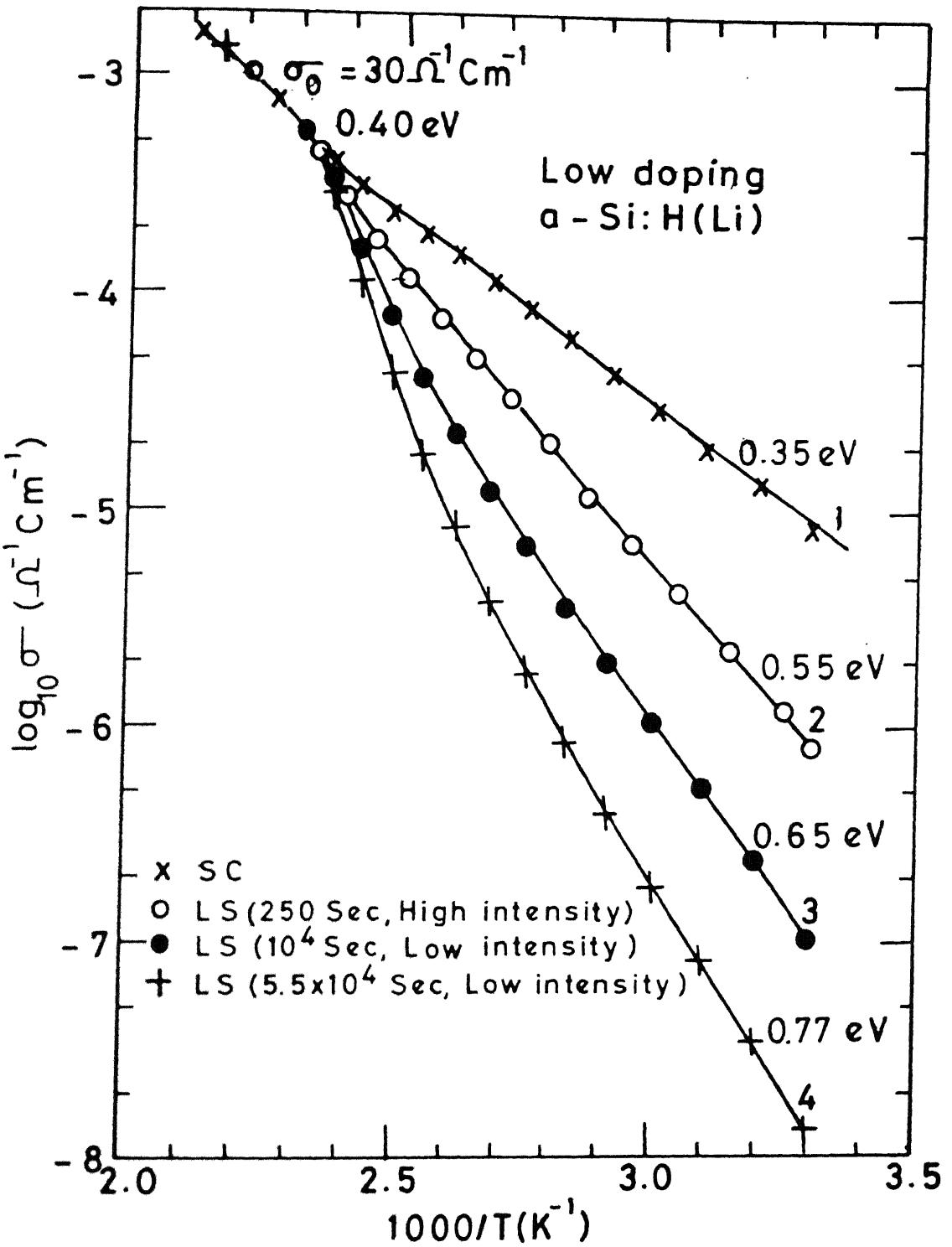

Figure 5.12: log σ vs. $1/T$ for low doped a-Si:H(Li) after different exposure conditions. Also shown is the $\sigma(T)$ curve in the SC state.

Table 5.3: σ and E_σ for a-Si:H(Li) in LS state.

State	Light Soaking Condition			$\sigma(300K)$	E_σ†
	Light	Intensity*	Duration	$\Omega^{-1}cm^{-1}$	eV
SC				8.5×10^{-6}	0.35
LS	White	$15mW/cm^2$	5.5×10^4 s	1.34×10^{-8}	0.76
LS	White	$10mW/cm^2$	1.0×10^4 s	1.02×10^{-7}	0.65
LS	White	$150mW/cm^2$	250 s	8.2×10^{-7}	0.54
LS	Red	$5mW/cm^2$	7200 s	3.9×10^{-6}	

* Approximate values † for $T < T_E$

We see that the effect of increasing the time of exposure is to change $\sigma(300K)$ and E_σ more, but all the $\sigma(T)$ curves meet the SC curve at the same temperature i.e. at T_E. The effect of light soaking does not seem to saturate even after 15 hours of exposure to white light. From the same figure, it is also seen that illumination with a HI light causes a rapid decrease in $\sigma(300K)$ but again the $\sigma(T)$ curve in LS state meets the SC curve at T_E, as observed for the rest of the states. Similar dependence on exposure conditions has been reported for undoped [26] and low P-doped a-Si:H films. Table 5.3 lists the value of conductivity and activation energy in different light soaked states.

5.4.3 Effect Of Light Soaking On Films In Quenched State

To study the effect of light soaking on the initial state of a-Si:H, we have measured the conductivity of a-Si:H films after light soaking them in the initial FQ state (new state is termed as FQ+LS state). Fig. 5.13 shows $\sigma(T)$ curve for a-Si:H film with Low Li concentration in SC, FQ, LS and FQ + LS state. Exposure conditions (*viz.*intensity and duration of light soaking) are kept same for LS and FQ + LS states (LO light for $10^4 s$). It is observed that σ in FQ+LS state is different than that in LS state. Light soaking in SC state decreases $\sigma(300K)$ from $8.5 \times 10^{-6} \Omega^{-1} cm^{-1}$ to $1.2 \times 10^{-7} \Omega^{-1} cm^{-1}$,

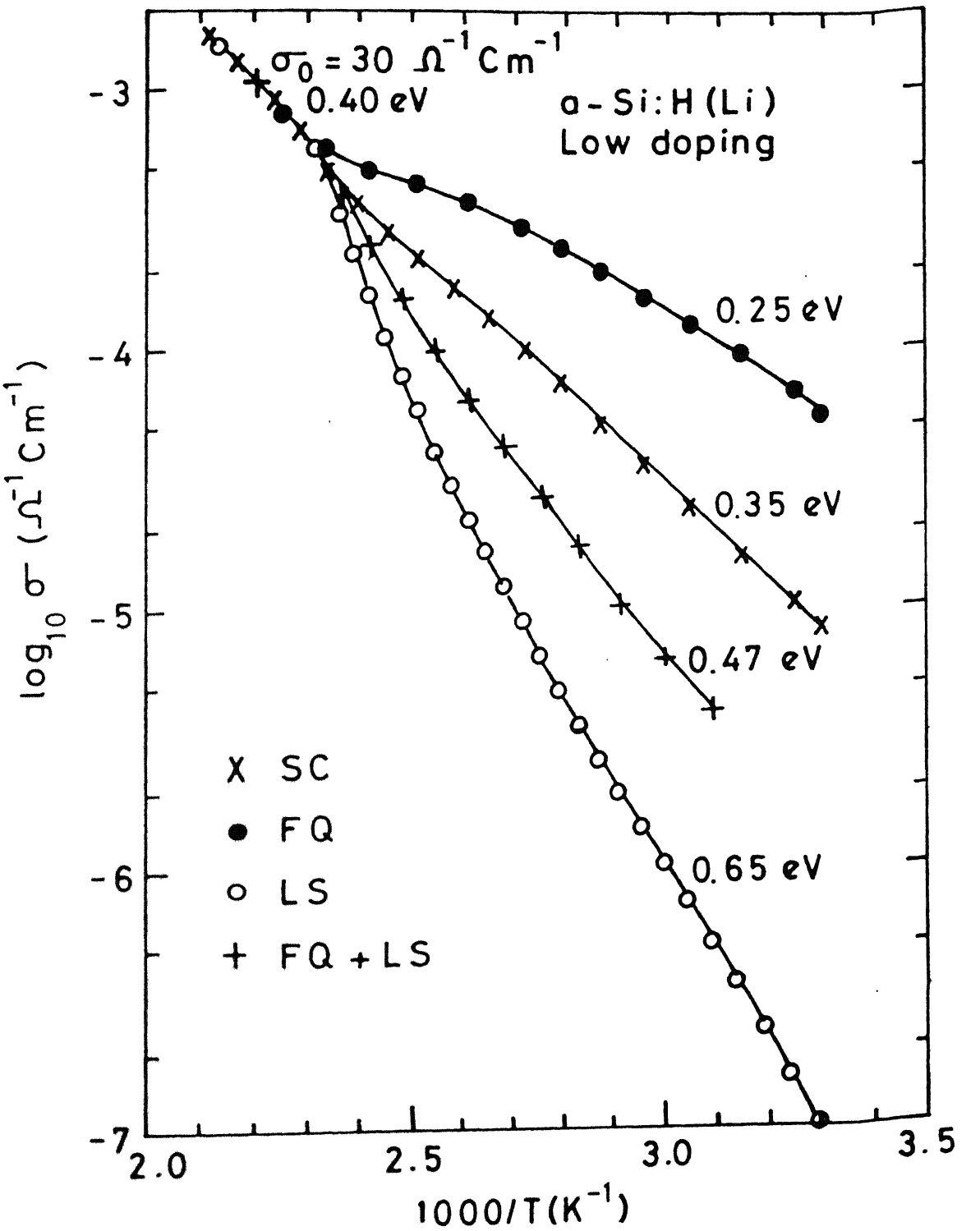

Figure 5.13: $\log \sigma$ vs. $1/T$ for low doped a-Si:H(Li) in SC, FQ, LS and FQ+LS states. Light soaking is done with LO white light for 10^4 s.

Table 5.4: Effect of light soaking on a-Si:H(Li) in fast quenched state. For comparison, σ in LS state is also given.

Details of light soaking	Before light soaking				After light soaking			Ratio
	State	$\sigma(i)$ $\times 10^{-5}$	$\sigma_{ph}(f)$ $\times 10^{-4}$	γ	$\sigma(i)$ $\times 10^{-7}$	$\sigma_{ph}(f)$ $\times 10^{-4}$	γ	$\frac{\sigma(i)}{\sigma(f)}$
5.5×10^4, white light $G \approx 10$	SC	1	6	0.35	0.25	1.36	0.77	400
	FQ	7.5	7.2		0.24	0.4	1.61	1875
7200 sec, red light $G \approx 5$	SC	1	2.7	0.36	39	2.25	0.40	2.56
	FQ	6.25	3.5	0.30	235	2.75	0.33	2.66
10^4 sec white light $G \approx 10$	SC	0.85			1.2			70
	FQ	~~0.625~~ 6.25			20			62
Note :	All σ values are in the units of $\Omega^{-1}cm^{-1}$ and G is the intensity of light in mW/cm^2							

whereas, upon light soaking in FQ state, σ decreases from $6.25 \times 10^{-6}\Omega^{-1}cm^{-1}$ to $1 \times 10^{-6}\Omega^{-1}cm^{-1}$. The activation energy in FQ+LS state is also different than that in LS state. However, it is interesting to note that FQ+LS state also meets the equilibrium $\sigma(T)$ curve in slow cooled state at the same T as observed for FQ or LS states. Similar changes in σ and σ_{ph} have been observed for other light soaking conditions and are summarized in Table 5.4. For small exposures, light soaking decreases σ by nearly the same factor irrespective of the initial state ie, SC or FQ states. The difference in FQ+LS state and LS state is more for small exposures and decreases as the exposure time is increased.

For a-Si:H films with high lithium concentration, light soaking in SC state (for 2h from heat filtered HI light) decreases $\sigma(300K)$ from $3 \times 10^{-3}\Omega^{-1}cm^{-1}$ to $1.5 \times 10^{-3}\Omega^{-1}cm^{-1}$, whereas, in the FQ state, $\sigma(300K)$ decreases from $6 \times 10^{-3}\Omega^{-1}cm^{-1}$ to

$3.0 \times 10^{-3} \Omega^{-1} cm^{-1}$ after light soaking. A decrease in σ_{ph} by the same ratio is observed in this case also. The results are shown in Table 5.1.

For P-doped a-Si:H films, no effect of light soaking on σ is observed irrespective of the initial state of the films (see Table 5.1).

For undoped a-Si:H films, no effect of FQ is observed on σ. However, σ_{ph} decreases after fast quenching. Table 5.1 shows that light soaking in SC state decreases σ_{ph} from $6.5 \times 10^{-5} \Omega^{-1} cm^{-1}$ to $9.9 \times 10^{-6} \Omega^{-1} cm^{-1}$. When these films are light soaked in FQ state, σ_{ph} decreases from $5.5 \times 10^{-5} \Omega^{-1} cm^{-1}$ to $9.25 \times 10^{-6} \Omega^{-1} cm^{-1}$.

These results show that electronic properties of a-Si:H e.g., σ after light soaking depend upon initial state of the samples.

5.4.4 Isothermal Relaxation

All the metastable states, created by fast quenching and light soaking relax back to the original slow cooled state following a stretched exponential as given by Eq. (3.8). The relaxation measurements are done at a fixed tempearture and normalized conductivity is obtained using Eq. (4.6). In the following section, we present our results on isothermal relaxation from FQ as well as LS states for a-Si:H(Li).

5.4.4.a Relaxation from Fast Quenched State

As is evident from Figs. 5.14 and 5.15, similar to a-Si:H(P), for a-Si:H(Li)films also σ in FQ state also approaches the slow cooled state following a stretched exponential after fast quenching them from high temperature $\approx 470K$). The stretching parameter β increases with the relaxation temperature (Fig. 5.17) and attains a value of ≈ 1 for $T \approx 400K$ in case of low lithium concentration. The relaxation time τ is thermally activated (Fig. 5.16) with $E_\tau = 0.95 \pm 0.2eV$ and $0.6 \pm 0.1eV$ for low and high concentration of lithium respectively. It is also evident from this figure that τ is small for heavily doped films as compared to the films with low Li concentrations.

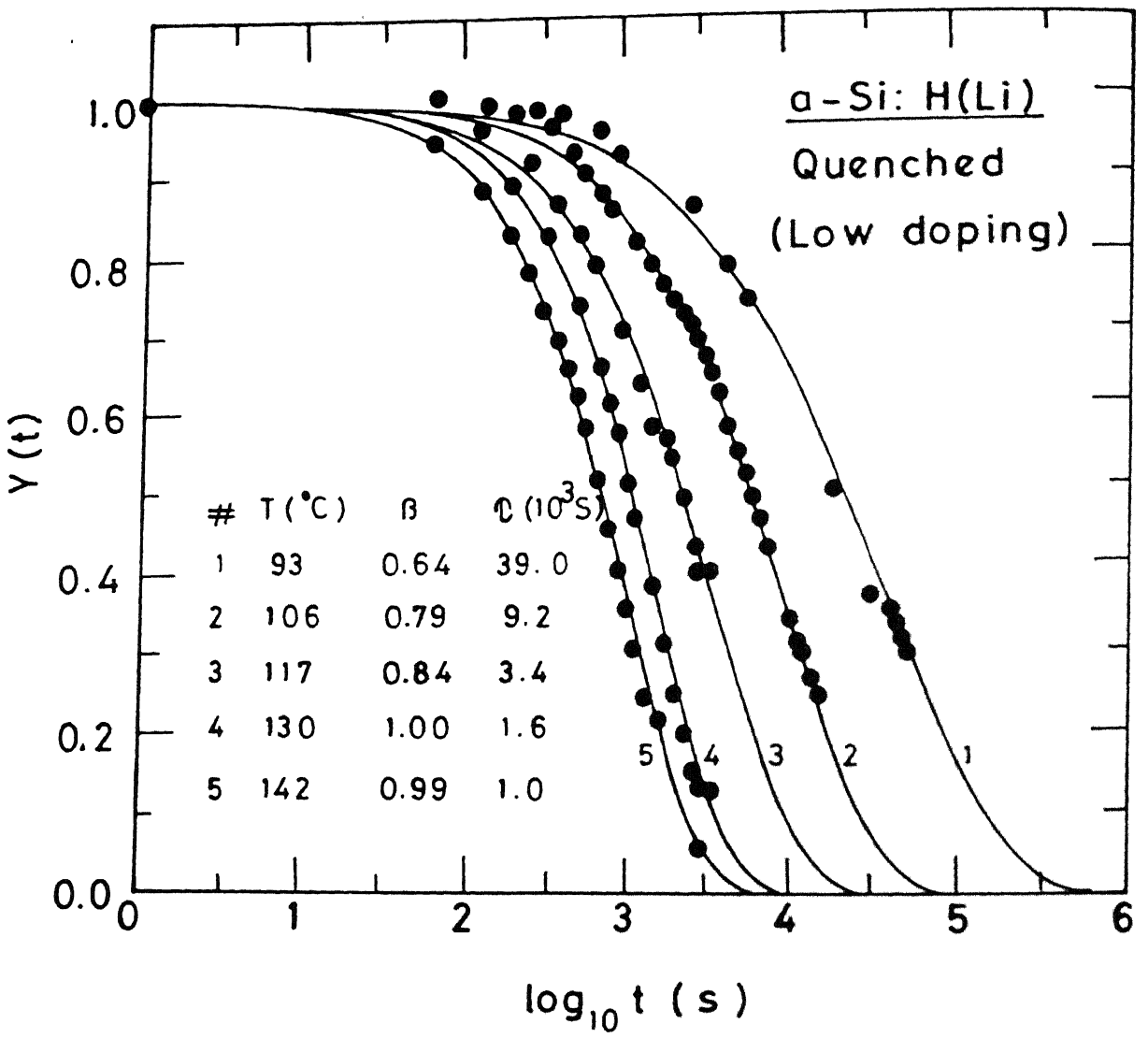

Figure 5.14: Normalised conductivity $Y(t)$ vs. $\log(t)$ for relaxation from FQ state for a low doped a-Si:H(Li) at different temperatures. Points are actual data, line is fit to the Eq. (3.8). The corresponding fit parameters β and τ are also shown.

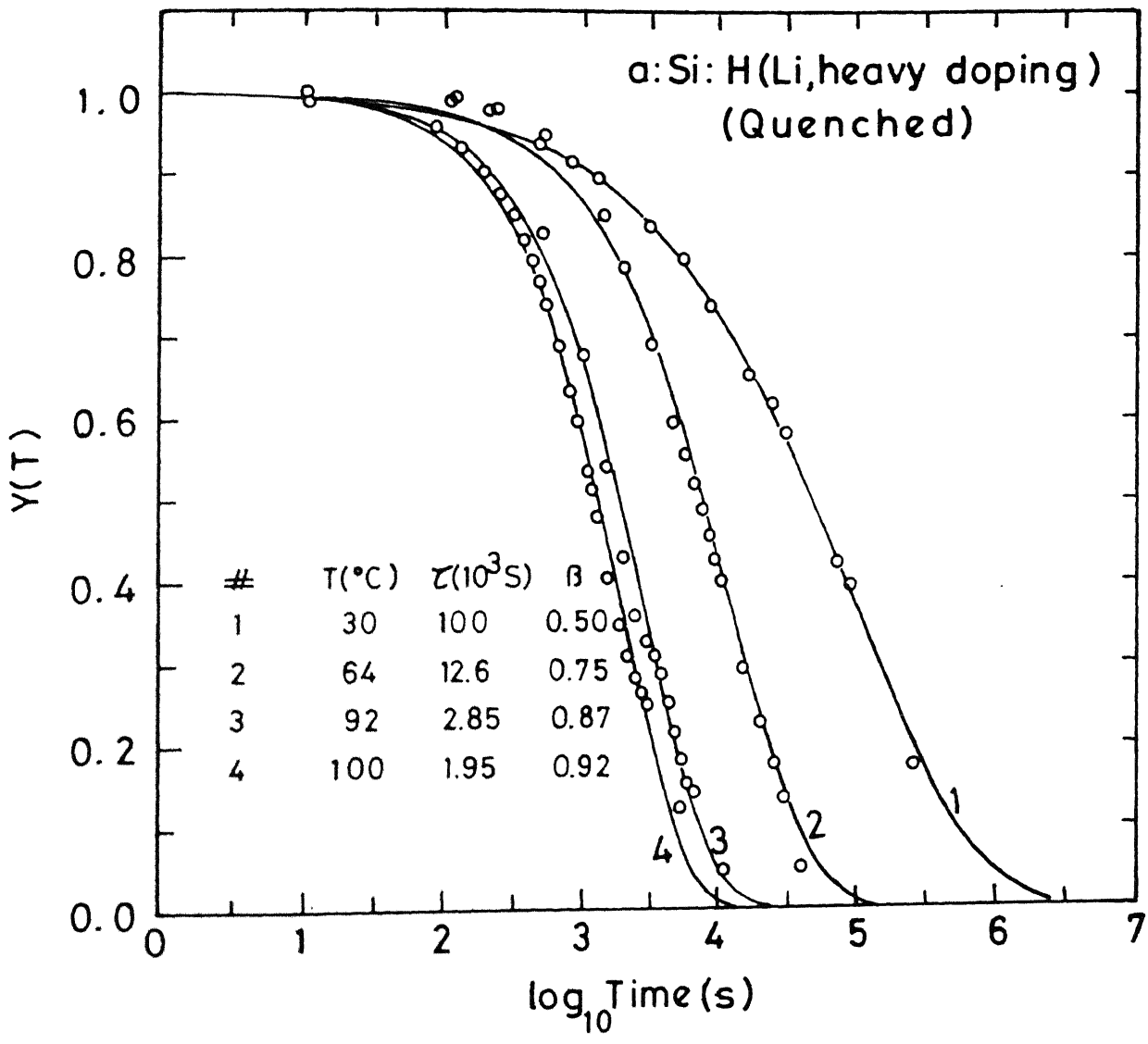

Figure 5.15: Normalised conductivity $Y(t)$ vs. $\log(t)$ for relaxation from FQ state for a heavily doped a-Si:H(Li) at different temperatures. Points are actual data, line is fit to the Eq.(3.8). The corresponding fit parameters β and τ are also shown.

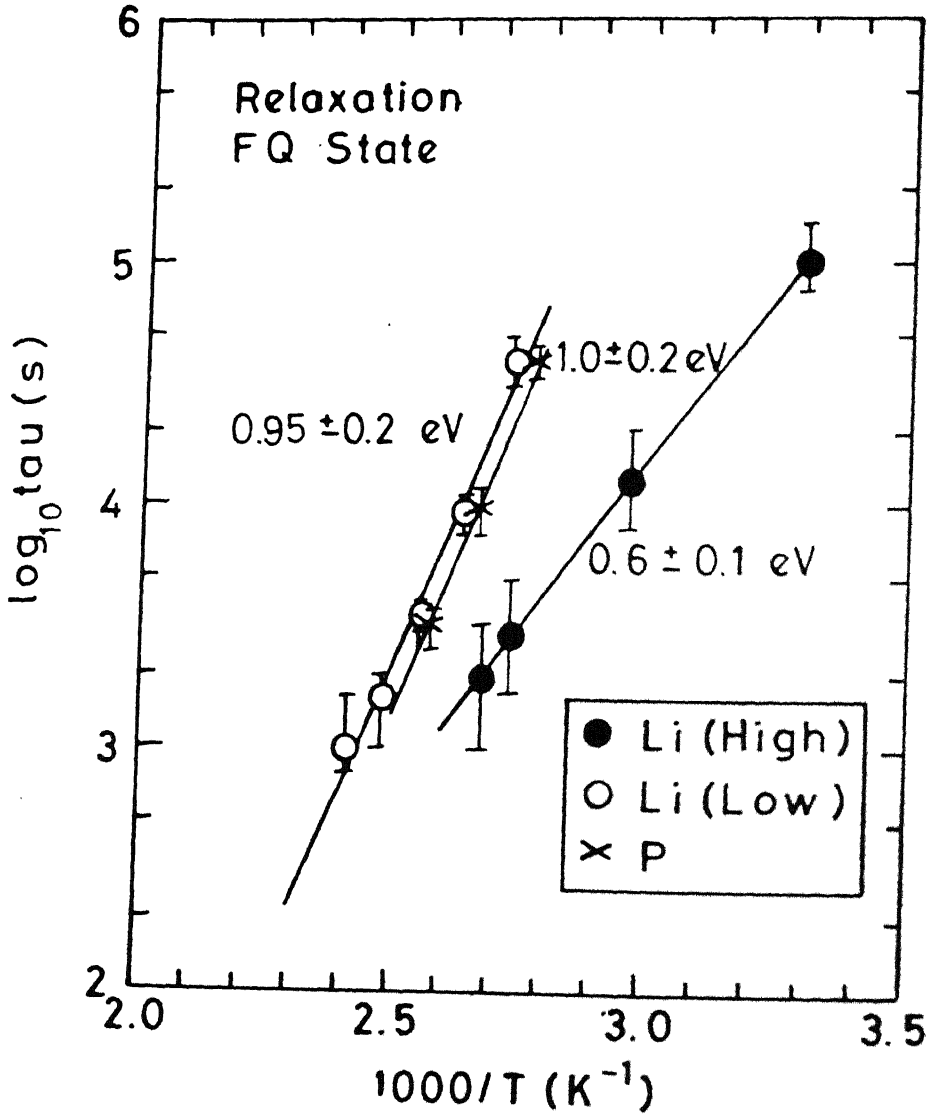

Figure 5.16: $\log \tau$ vs. $1/T$ a-Si:H(Li) for relaxation from FQ state at different temperatures.

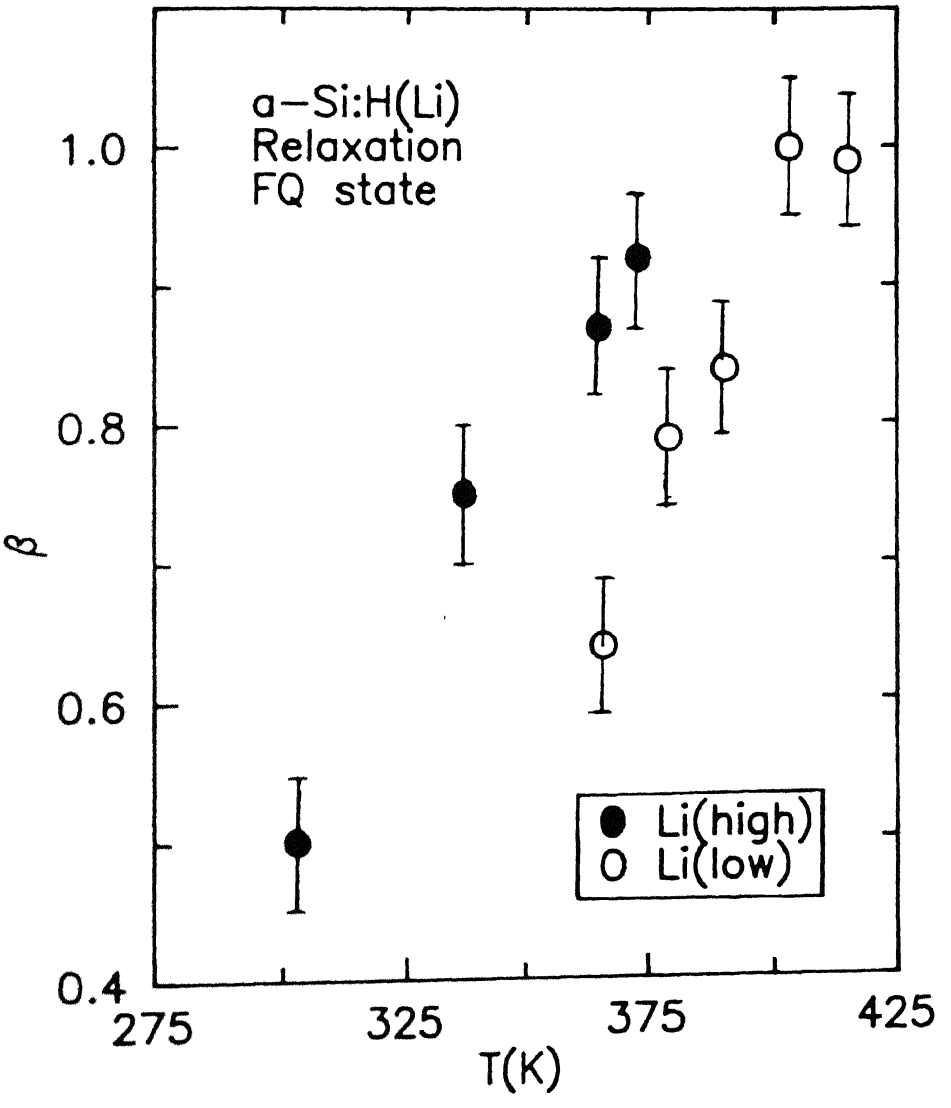

Figure 5.17: β vs. $1/T$ for a-Si:H(Li) for relaxation from FQ state

Table 5.5: Parameters β and τ as a function of temperature for relaxation from FQ state for a-Si:H(P) and a-Si:H(Li).

Sample	$T(^oC)$	β	$\tau(sec)$	$\nu(sec^{-1})$	$E_\tau(eV)$
a-Si:H(P)	86	0.60	3.93×10^4	3×10^9	1.0 ± 0.2
# 11	102	0.76	9.58×10^3		
	116	0.86	3.15×10^3		
a-Si:H(Li)	93	0.64	3.9×10^4	1.1×10^9	0.95 ± 0.2
(low)	106	0.79	9.2×10^3		
	117	0.84	3.4×10^3		
	130	1.0	1.6×10^3		
	142	0.99	1.0×10^3		
a-Si:H(Li)	30	0.50	1×10^5	1.2×10^4	0.6 ± 0.1
(high)	64	0.75	1.26×10^4		
	92	0.87	2.85×10^3		
	100	0.92	1.95×10^3		

We have summarized, in Table 5.5, the value of β and τ for P-doped and Li-doped a-Si:H for relaxation from FQ state.

5.4.4.b Relaxation from Light Soaked State

Isothermal relaxation curves for the two lithium doped films after light soaking are plotted in Figs. 5.18 and 5.19. For low lithium concentration, light soaking is done for 15 hours with LO light, while for high doping case, heat filtered HI light for 2 hours is used. The details of light soaking are described in chapter 4. It is evident from these figures that in both the cases the relaxation follows a stretched exponential time dependence. The relaxation time (τ), for both the dopings is thermally activated as shown in the Fig. 5.20 and its value depends upon the doping concentration. The activation energies for relaxation (E_τ) for the two doping cases are $1.45 \pm 0.2eV$ and $2.0 \pm 0.3eV$ respectively. Fig. 5.21 shows the temperature dependence of β. The

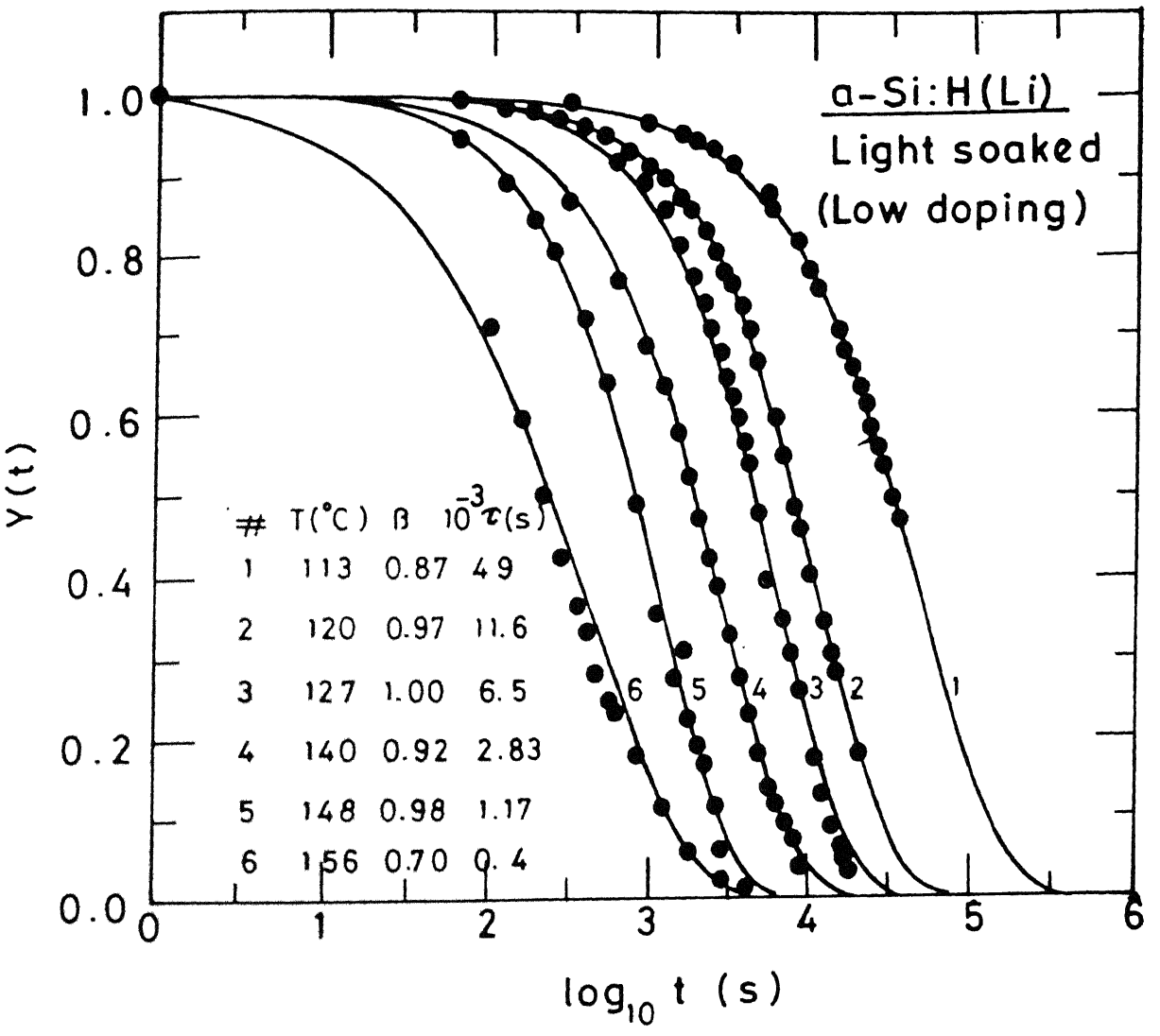

Figure 5.18: Normalised conductivity $Y(t)$ vs. $\log(t)$ for relaxation from LS state for a low doped a-Si:H(Li) at different temperatures. Points are actual data, line is fit to the Eq.(3.8). The corresponding fit parameters β and τ are also shown.

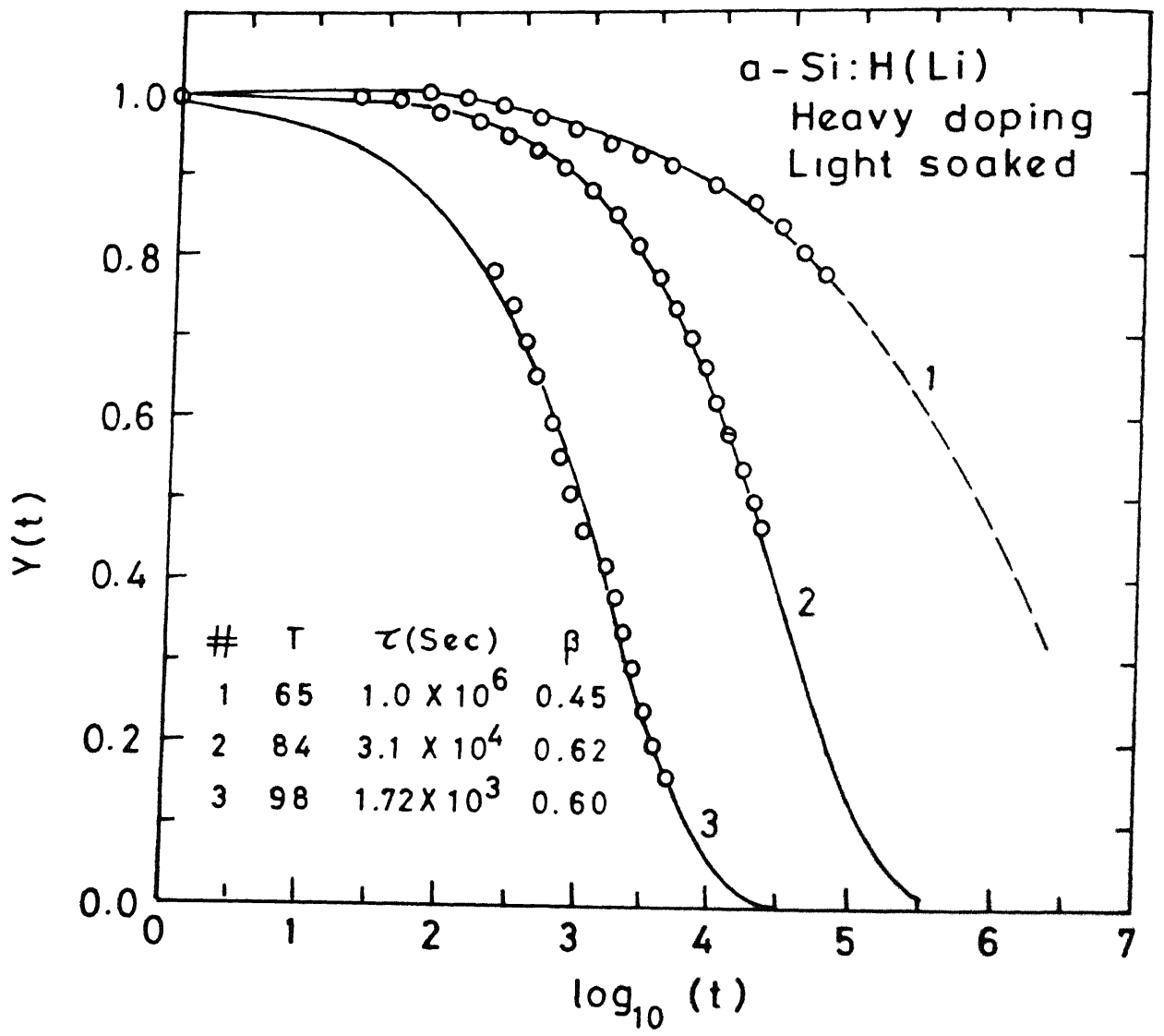

Figure 5.19: Normalised conductivity $Y(t)$ vs. $\log(t)$ for relaxation from LS state for a heavily doped a-Si:H(Li) at different temperatures. Points are actual data, line is fit to the Eq.(3.8). The corresponding fit parameters β and τ are also shown.

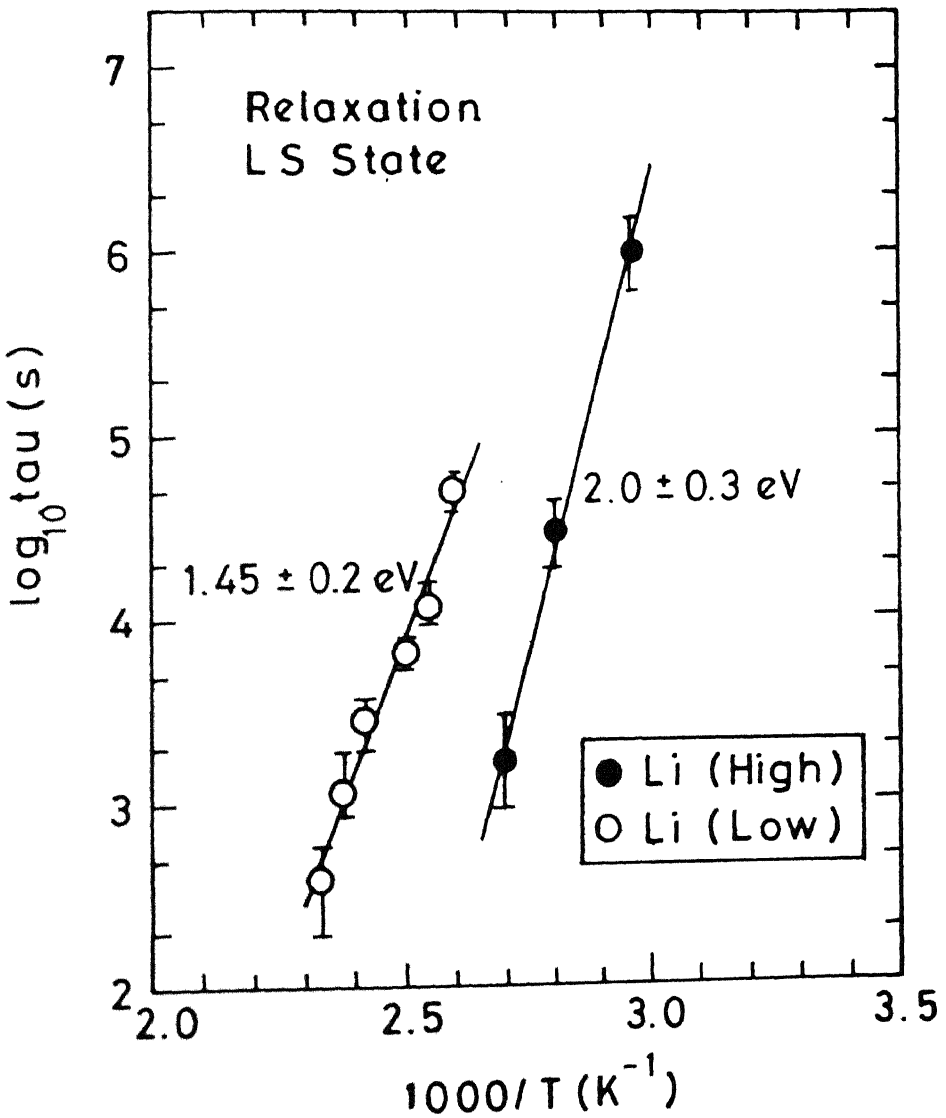

Figure 5.20: $\log \tau$ vs. $1/T$ for a-Si:H(Li) for relaxation from LS state at different temperatures.

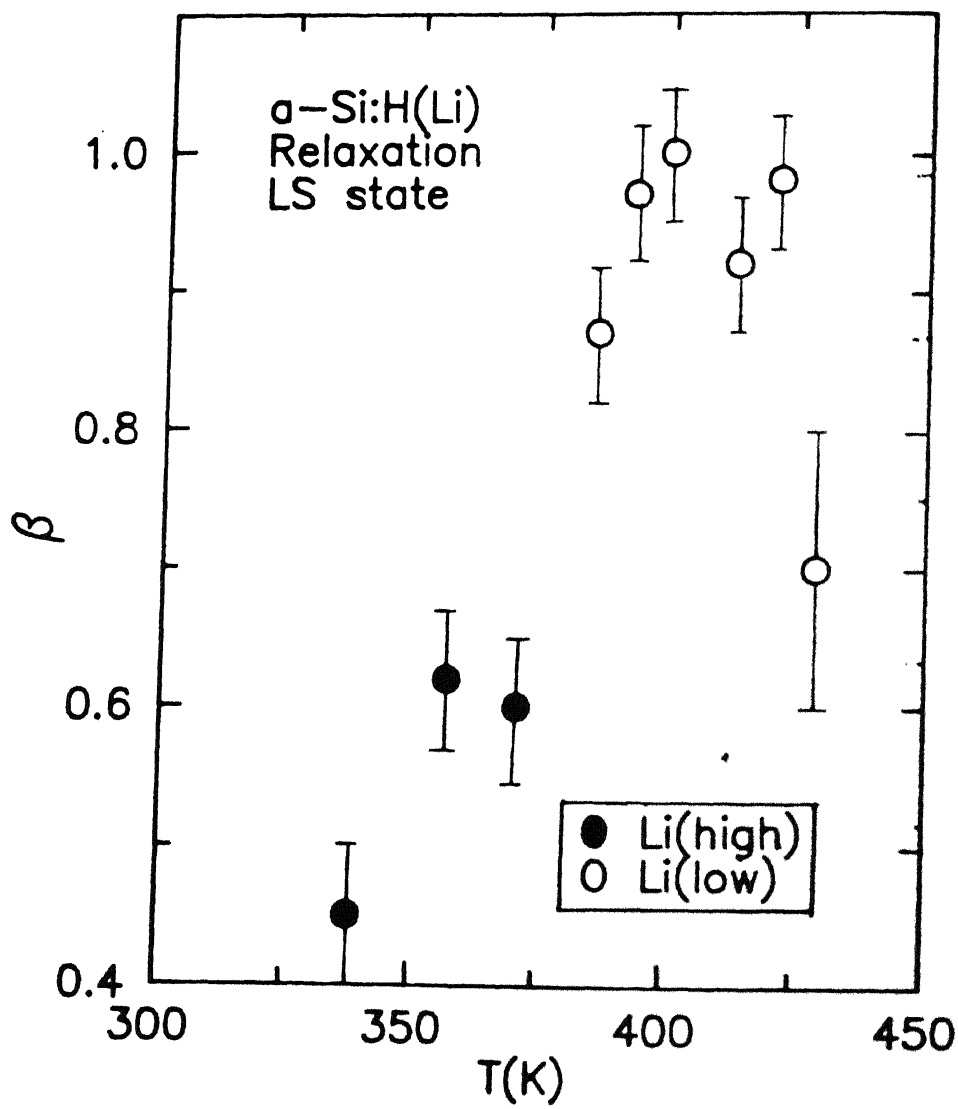

Figure 5.21: β vs. $1/T$ for a-Si:H(Li) for relaxation from LS state

Table 5.6: Parameters β and τ as a function of temperature for relaxation from LS state for a-Si:H(Li).

Sample	$T(^oC)$	β	$\tau(sec)$	$\nu(sec^{-1})$	$E_\tau(eV)$
a-Si:H(Li)	113	0.87	4.9×10^4	1.5×10^{14}	1.45 ± 0.2
(low)	120	0.97	1.16×10^4		
	127	1.00	6.5×10^3		
	140	0.92	2.83×10^3		
	148	0.98	1.17×10^3		
	157	0.70	4.0×10^2		
a-Si:H(Li)	65	0.45	1×10^6	$\approx 10^{21}$	2.0 ± 0.3
(high)	84	0.62	3.14×10^4		
	98	0.60	1.72×10^3		

values of β and τ for the relaxation from LS state are also summarized in Table 5.6.

5.4.4.c Relaxation from FQ+LS state

Fig. 5.22 shows decay of conductance at $\approx 340K$ as a function of time for a-Si:H film doped heavily with lithium in FQ+LS state. We have discussed in Section 5.4.3, that light soaking a heavily doped a-Si:H film in fast quenched state resulted in a conducting state, which is similar to the slow cooled state. However, we observe, that when these films are allowed to relax isothermally at an intermediate temperature, where rate of relaxation from LS and FQ are very different, we observe that conductivity decrease as time increases. A similar decrease in σ has been observed for recovery from FQ state. The conductivity σ approaches a saturated value after a few hours, but no sign of any increase in σ is observed as expected for the recovery from LS state. It is to be noted that τ(LS) is much higher at $340K$ as compared to τ(FQ). These results will be discussed in the next chapter.

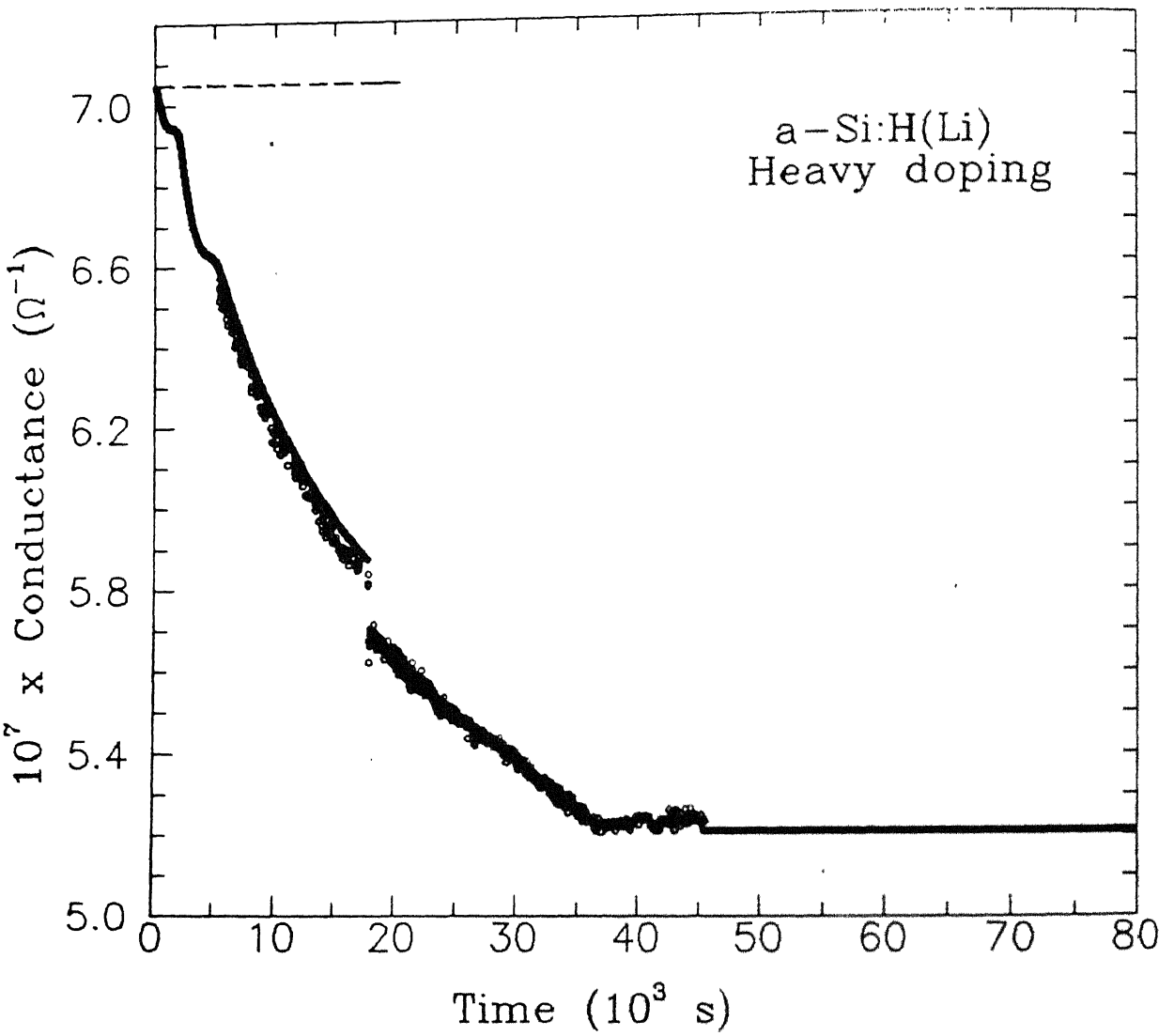

Figure 5.22: Conductance vs. time for relaxation from FQ+LS state at 340K for heavily doped a-Si:H(Li). A discontinuity in the curve is due to power fluctuations. Horizontal line shows the conductance in SC state.

5.4.4.d Errors in β, τ and E_τ

Since the relaxation data are fitted to a stretched exponential of the form given by Eq. 5.2, some error in the fit parameters β and τ is expected. The possible sources of error are the standard deviations in curve fitting and the error in determination of $Y(t)$.

A possible source of error in $Y(t)$ is due to an error in $\sigma(0)$ arising from the choice of $t = 0$. For the study of relaxation kinetics, the sample in metastable state is brought from room temperature to the measurement temperature in $10-20min.$ and the temperature is stabilized to an accuracy of $\pm 1K$. Since relaxation takes place at each temperature, there may be an error in determination of $t = 0$ and $\sigma(0)$. We have changed $t = 0$, and $\sigma(0)$ within reasonable limits and calculated the error in β and τ. These errors are shown by the vertical lines in $\log \tau$ vs. $1/T$ and β vs. $1/T$ curves reported here. In spite of all this, error bars are small enough to allow us to draw definite conclusions. The reason for this is

1. At low temperatures (T much below T_E), relaxation is slow and τ is large compared to the time taken in bringing the sample to the measurement temperature.

2. At high temperatures (T close to T_E), where relaxation is fast, one may expect large error bars. However, we see that for these temperatures, $\beta \approx 1$, i. e. , an exponential relaxation and thus τ will not be much affected by the choice of $t = 0$.

5.5 Thermopower

We have measured the thermopower of a-Si:H films doped with phosphorus and lithium in the slow cooled (annealed), light soaked and fast quenched states. In the following section, we present our results.

5.5.1 Phosphorus doped a-Si:H

Figs. 5.23 and 5.24 show the thermopower S as a function of temperature for the two phosphorus doped a-Si:H films in SC, FQ and LS states. It is clear from these figures that S for the phosphorus doped a-Si:H films is negative thus showing that electrons are the majority charge carriers.

5.5.1.a Slow Cooled State

Thermopower $S(300K)$ in SC state is $-1.08 \pm 0.01 mV/K$ and upon increasing the temperature the magnitude of S decreases. At $\approx 490K$, a kink is observed in the S vs. $1/T$ curve. The slope E_S below the kink temperature is $0.18 \pm 0.02eV$ and above the kink temperature it is $0.26 \pm 0.02eV$ (Fig. 5.23)

5.5.1.b Fast Quenched State

Upon fast quenching from $450K$, these films show a decrease in magnitude of S at $300K$. In the FQ state, $S(300K)$ is $-0.98 \pm 0.01 mV/K$ and $E_S = 0.12 \pm 0.02eV$. The S vs. $1/T$ curve obtained after FQ meets the corresponding curve in SC state at $\approx 395K$. Above this temperature only single curve is obtained for the two states (Fig. 5.23).

5.5.1.c Light Soaked State

Light soaking of these P-doped films with heat filtered HI light for 2h at $300K$ does not lead to any change in σ or S. Similar to the $\log \sigma$ vs. $1/T$ curve, the S vs. $1/T$ curve also remains intact upon LS. Fig. 5.23 shows that light soaking the films in FQ state also does not cause any change in σ or S vs. $1/T$ curve over the entire range of measurements.

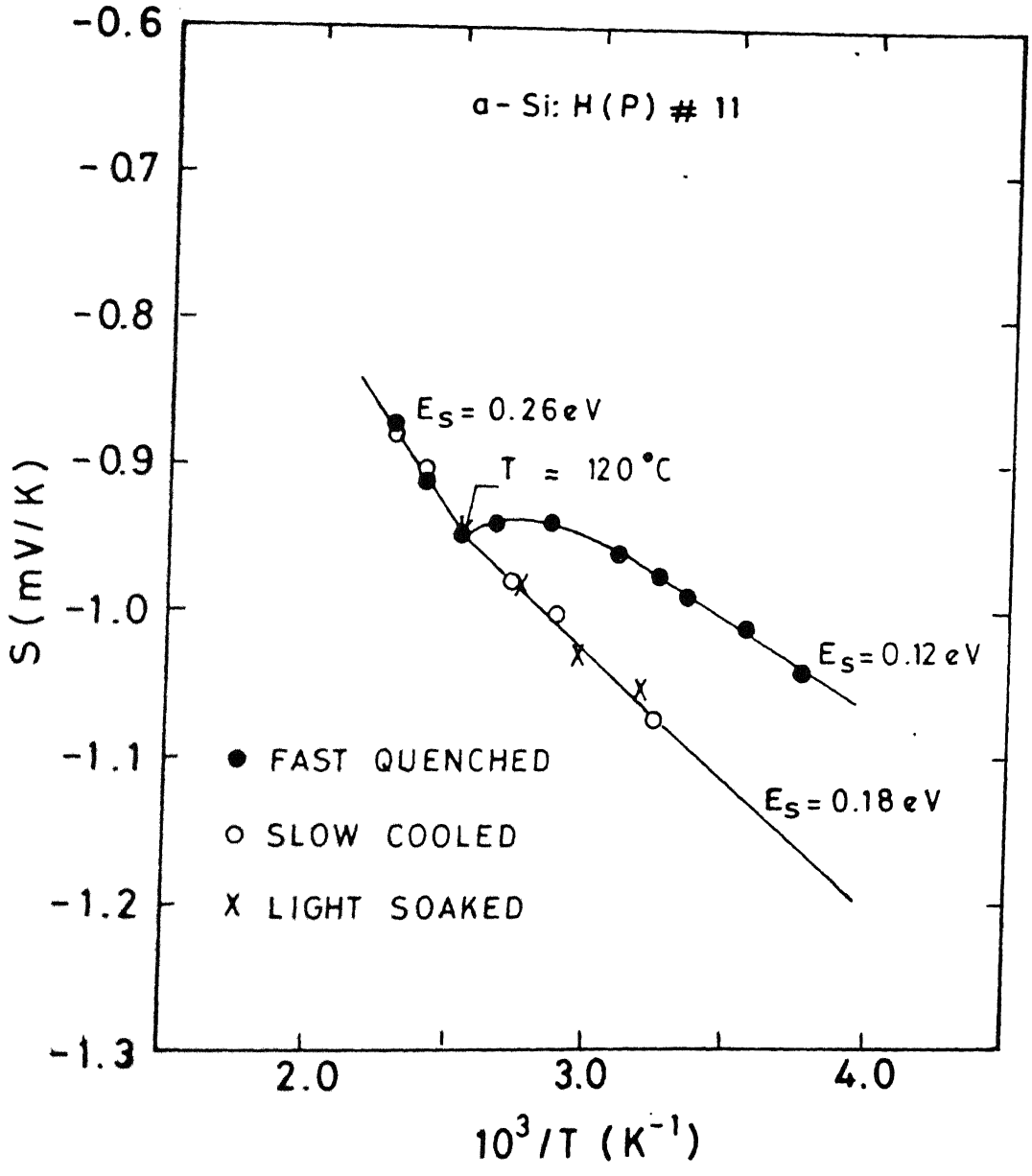

Figure 5.23: Thermopower S vs. $1/T$ for P-doped a-Si:H in SC, FQ and LS states.

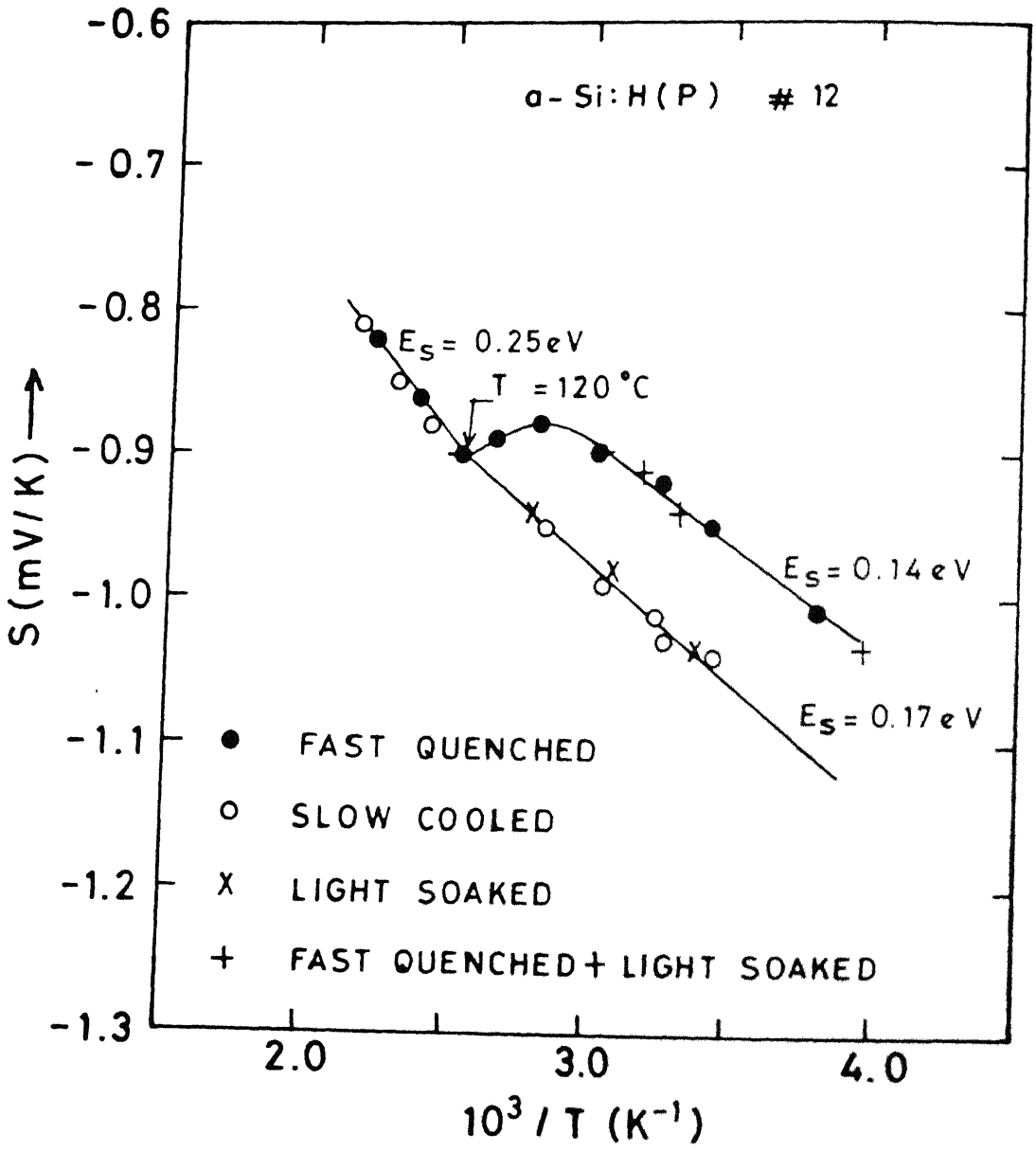

Figure 5.24: Thermopower S vs. $1/T$ for P-doped a-Si:H in SC, FQ and LS states.

Table 5.7: Thermopower S at 300K in SC, FQ and LS state for a-Si:H(P) and a-Si:H(Li).

Sample Name	State	S($\approx 300K$) mV K^{-1}	E_S eV	E_q eV	Q_0	E_S(eV) ($T > T_E$)
a-Si:H:P #11	SC	-1.08	0.18	0.1	≈ 8	0.25
	FQ	-0.99	0.12	0.1		
	LS	-1.08	0.18	0.1		
	FQ+LS	-0.98	0.12	0.1		
a-Si:H:P #12	SC	-1.03	0.17	0.07	≈ 8	0.25
	FQ	-0.93	0.14	0.07		
	LS	-1.02	0.17	0.07		
a-Si:H:Li (high)	SC	-1.0	0.14	≈ 0	≈ 5.8	
	FQ	-0.90	0.10	≈ 0	≈ 5.4	
	LS	-0.92	0.02	≈ 0.14	≈ 10	

Thermopower measurements for the P-doped a-Si:H films, with a slight difference in doping concentrations, show the qualitatively similar behaviour (Fig. 5.24). For these films, $S(300K)$ in SC state is $-1.02 \pm 0.01 mV/K$ and $E_S = 0.17 \pm 0.02 eV$ below kink temperature. These films also show a decrease in magnitude of $S(300K)$ and E_S after FQ, whereas LS does not effect the thermopower in this case also. Table 5.7 summarizes the thermopower results in SC, FQ and LS, and FQ+LS states.

5.5.2 Lithium Doped a-Si:H Films

Lithium doped a-Si:H films show a negative sign for thermopower S. Fig. 5.25 shows the S vs. $1/T$ plot for a heavily doped a-Si:H film in SC, FQ and LS states.

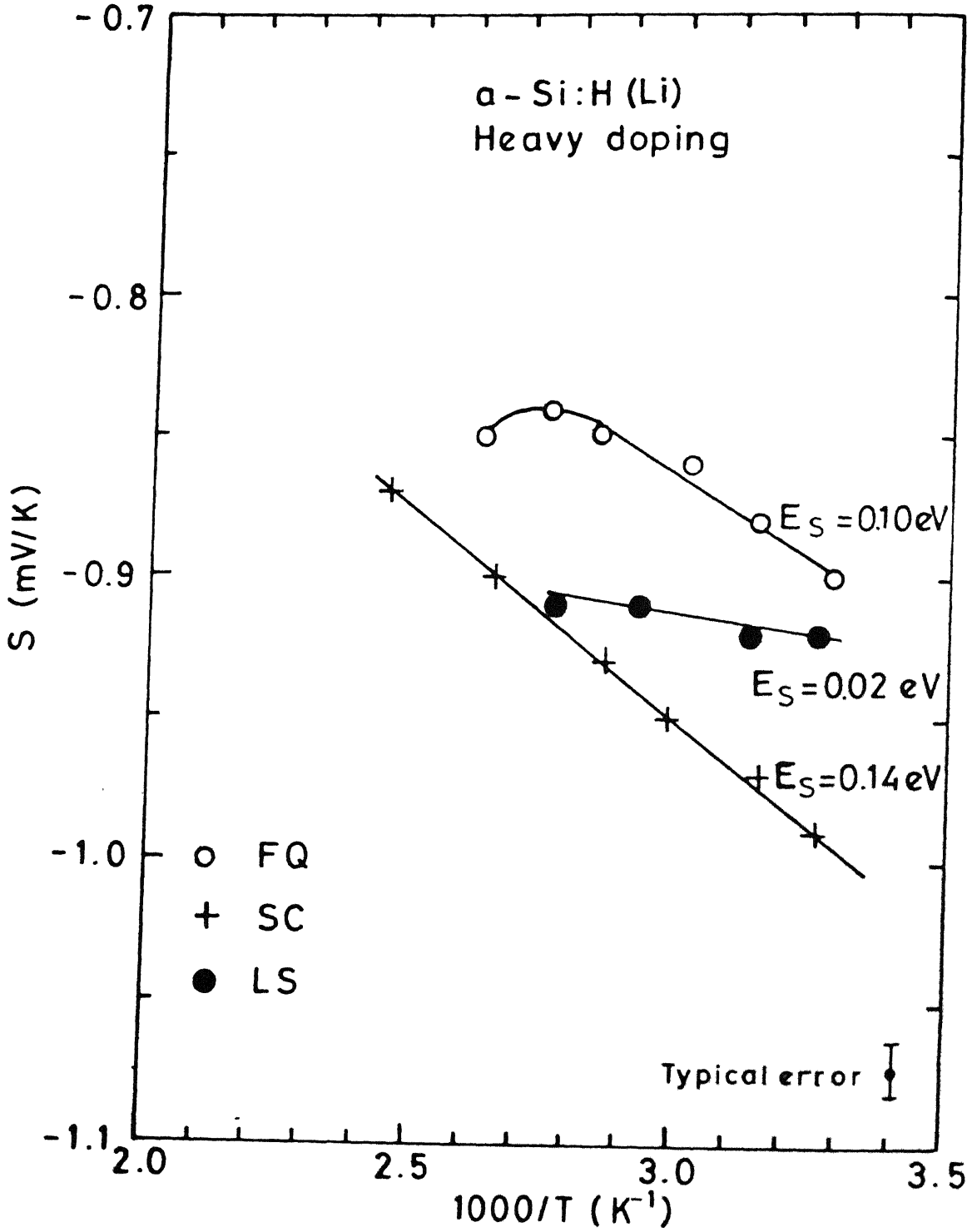

Figure 5.25: Thermopower S vs. $1/T$ for heavily doped a-Si:H(Li) in SC, FQ and LS states.

5.5.2.a Slow Cooled State

In SC state the S at $300K$ is $-1.0 \pm 0.01 mV/K$ and the slope E_S is $0.14 \pm 0.02 eV$, which is same as E_σ in SC state for these film. The magnitude of S decreases for these films when the temperature is increased.

5.5.2.b Fast Quenched State

Upon FQ from $470K$, a decrease in the magnitude of thermopower (S) is observed. $S(300K)$ in FQ state is $-0.90 \pm 0.01 mV/K$ and E_S is $0.10 \pm 0.02 eV$ and is same as the corresponding E_σ in FQ state for these films. This effect is similar to the one observed for the case of phosphorus doped a-Si:H films.

5.5.2.c Light Soaked State

Light soaking Li-doped a-Si:H films causes a decrease in σ and also a decrease in magnitude of S. After 2 hours of LS from heat filtered HI white light, $S(300K)$ changes to $-0.92 \pm 0.01 mV/K$ in LS state. A large decrease in E_S is also seen in LS state. It decreases from $0.10eV$ in SC state to $0.02eV$ in LS state. The value of E_S in LS state is much smaller than corresponding E_σ. Table 5.7 summarizes the thermopower results in SC, FQ and LS states for lithium doped films.

Chapter 6

Discussion

In Chapter 5, we have presented our results showing that a-Si:H films exhibit both thermal and light induced metastabilities near room temperature when they are cooled rapidly from a high temperature or exposed to strongly absorbing light. Fast quenching (FQ) results in an enhanced conductivity near room temperature of P-doped a-Si:H (a-Si:H(P)), whereas, Light soaking (LS) causes a decrease in conductivity (σ and σ_{ph}) of undoped a-Si:H. The metastable states so obtained are reversible and can be annealed at high temperatures. The high temperature state of the film is insensitive to the history of the sample and a-Si:H films seem to be in thermal equilibrium at these temperatures. Further, we have seen that the metastable states relax slowly and relaxation obeys a stretched exponential with a thermally activated relaxation time. These observations are similar to those reported by several other workers in the field [15,16]. In addition to the commonly studied undoped and P-doped a-Si:H, we have also studied the effect of thermal and light induced metastabilities on electrical properties of a-Si:H films doped with lithium (a-Si:H(Li)) to see if the metastable effects are similar in substitutionally doped (P-doped) [6] and interstitially doped [49] (Li-doped) a-Si:H. We observe that a-Si:H(Li) films exhibit effect of both fast quenching as well as light soaking on electrical properties and bear a close resemblance to a-Si:H(P).

The measurements of thermopower (S) and conductivity (σ) provide more insight into the conduction mechanism (Chapter 2). These measurements separate the effects on transport properties arising from a shift in position of Fermi level by external agencies, e.g., doping from those due to the inhomogeneities such a density fluctuations and a random distribution of charged centers [52]. We have measured thermopower of P-and Li doped a-Si:H in the annealed and slow cooled (SC), fast quenched (FQ) and light soaked (LS) states. The thermopower measurements in SC state are in qualitative agreement with the literature [52].

In the following, we try to understand the thermal and light induced metastabilities in a-Si:H in the light of existing models. We make an attempt to answer some of the interesting questions, e.g., whether the thermal induced metastability and light induced metastability have a common origin. Although both of these are studied in detail as summarized in Chapter 3, a clear picture is yet to emerge as to whether these effects are related to the creation of new (defect) states or a change in structure is also involved. The measurement of thermopower in the metastable states may help us understand, whether these metastabilities only affect the electronic structure (occupancy of density of states) of a-Si:H films or cause a change in atomic structure also (spatial variation of distribution of atoms). We are able to separate the effect due to the movement of the Fermi level from those arising from the change in the potential fluctuations. The annealing kinetics of the two metastable states has also been studied and compared.

Another interesting question is whether the substitutional doping by phosphorus during deposition [6] and interstitial doping by lithium after deposition [49] affect the properties of the a-Si:H films in a similar fashion and whether a common model can be used to explain the observed metastable behavior for the two types of doping. It is worth noting here that the lithium acts as an interstitial donor in a-Si:H films [49] and a similar correlation exists between the defect density and Fermi level position for P doped and Li doped a-Si:H films [149].

6.1 Metastabilities in Undoped and P-doped a-Si:H (Comparison with literature)

As described in Chapter 5, we have studied the thermal and light induced metastabilities in undoped and P-doped a-Si:H. Here we discuss our results in the light of the existing models for comparison with the literature.

6.1.1 Undoped a-Si:H

Fast quenching the undoped films from high temperatures ($200 - 225^0C$) does not show any significant effect on the σ of these films (Figs. 5.2, 5.3). However, a small decrease in σ_{ph} is observed for all the films, independent of preparation conditions (Table 5.1). A decrease in σ_{ph} suggests an increase in defect density (Si_3^0), however, the changes should be very small, as no measurable change in position of the E_f is observed. Similar decrease in σ_{ph} has also been observed by McMahon and Tsu [41]. The increase in defect density might be caused by the breaking of weak Si-Si bonds at high temperature, which gets frozen-in when a-Si:H is subjected to fast quenching [126]. At high temperatures, the hydrogen in a-Si:H moves and separates these newly created dangling bonds. When fast quenched, the structure cannot equilibrate with the cooling rate and a new structure with a higher defect density is frozen-in. The sub-gap absorption [40], SCLC [119] and ESR [129] also show an increase in defect density after fast quenching a-Si:H.

The decrease in dark and photo conductivity (σ and σ_{ph}) of undoped a-Si:H films upon light soaking is shown in Fig. 5.2, 5.3 and Table 5.1 The effect is in agreement with the results in literature [15] and can be explained by both weak-bond breaking [26] and charge trapping [28] models. As we have discussed in Section 3.1.1, both these models predict an increase in density of dangling bonds (Si_3^0) upon light soaking. These Si_3^0 act as trapping centers for the carriers and decrease the

σ and σ_{ph} of a-Si:H. Since these dangling bonds are located below Fermi level, an increase in their density causes the downward shift of the Fermi level, i.e., a higher E_σ, in agreement with the present observations. At low temperatures (near 300K), the thermal energy is lower than the energy needed to surmount the barrier between the metastable state and equilibrium state and the changes in electronic properties seem to be permanent.

6.1.2 P-doped a-Si:H

As shown in Figs 5.4 and 5.5, fast quenching results in an increase in σ of P-doped a-Si:H near room temperature. These results are similar to those reported in literature [16,51]. An increase in σ could be due to an increase in free carrier density or drift mobility. However, no measurable change in drift mobility is reported after fast quenching the a-Si:H(P) films [51]. This implies that the observed increase in σ is due to an increase in the density of free carriers. As has been discussed in Section 3.2.1, for a-Si:H(P), in thermal equilibrium

$$n_{bt} = P_4^+ - Si_3^- \tag{6.1}$$

where n_{bt}, P_4^+ and Si_3^- denote band tail carriers, ionized phosphorus donors and a negatively charged silicon dangling bond respectively. The σ of these films is related to n_{bt} as

$$\sigma = n_{bt}\, e\, \mu_d \tag{6.2}$$

Thus an increase in σ should be seen as an increase in n_{bt} upon fast quenching. The reported results in literature show an increase in n_{bt} as measured by charge sweep-out technique [16] and ESR [16,43] after fast quenching. Also, no measurable change in defect density has been reported so far suggesting an increase in donor density in the FQ state [44,82]. It appears that at high temperature, conversion of dopant atoms

from 3-fold coordination to 4-fold coordination takes place. This conversion might be associated with the movement of hydrogen at elevated temperatures. When fast quenched, a new structure corresponding to high temperature is frozen-in. Since the new state is characterized by a higher free carrier density, the Fermi level moves up towards the conduction band edge and a lower activation energy is observed.

The thermal equilibrium prevails for $T \geq T_E$ and thus the n_{bt} (and σ) is determined by the density of donors and dangling bonds. The Fermi level now lies in the minimum of the density of states (DOS) (see Fig. 3.3) and is nearly independent of temperature. σ is independent of cooling rate for $T \geq T_E$ and is only determined by the thermal equilibrium between donors and defect states [82].

There are a few reports in literature, which show a decrease in σ of a-Si:H(P) films upon light soaking but the effect is small and decreases as the doping concentration increases [15]. Dark conductivity (σ) of our a-Si:H(P) films does not change upon light soaking. It is believed that in the heavily doped films, the densities of photoinduced defects are too small to overcome the pinning of the Fermi level by the significantly larger densities of donors and defect states [150]. Also, the photoinduced breaking of weak Si-Si bonds may cause an increase in the density of charged donors (P_4^+) and dangling bonds (Si_3^-) [43]. Since P_4^+ lies above E_f and Si_3^- is below E_f, a simultaneous increase of both will result in a very small shift in the position of the Fermi level and hence cause a small or negligible change in electrical properties. The negligible difference between σ and σ_{ph} of these films also supports the presence of a high density of donors and defects in our P doped a-Si:H films.

6.1.2.a Isothermal Relaxation

We have seen in Section 5.3.3, that the metastable state introduced by fast quenching a-Si:H films relaxes slowly following a stretched exponential (Eq. (3.8)) and a thermally activated relaxation time (Eq. 3.5)). The slow non-exponential relaxation of metastable state is similar to that observed in many glasses [29]. This can be

explained by the Hydrogen Glass model assuming that the a-Si:Hbehaves as hydrogen glass [16] and the dispersive nature of hydrogen diffusion constant ($D_H \propto t^{-\alpha}$) is responsible for the observed stretched exponential time dependence. The dispersive nature is due to the random walk of hydrogen atoms through an exponential distribution $\exp\{-E/kT_o\}$ of trapping sites.

As is evident from Fig. (5.15), the activation energy E_τ for relaxation from FQ state is $\approx 1.0 \pm 0.2eV$. This value of E_τ is similar to the diffusion activation energy (E_{DH}) of hydrogen in P-doped films ($E_{DH} \approx 1.2 - 1.3eV$) [30] and thus supports Hydrogen Glass model (Sec.3.4) to be valid in this case. Kakalios *et al.* [82] also obtained a similar value of $E_\tau(0.95eV)$ by measuring the decay of excess charge carriers in the band tail states using charge sweep out technique for a-Si:H(P)after fast quenching [118]. It is, further, to be noted that the parameter β increases with temperature (Fig. 5.7) as expected in the Hydrogen Glass model.

The stretched exponential behaviour and a thermally activated τ can also be explained if defects are itself responsible for the metastabilities and thermal equilibration as suggested by Crandall [131]. However, we prefer the Hydrogen Glass model 3.4 as time dependence of D_H has been experimentally observed.

In summary, our results on undoped and P-doped a-Si:H are in agreement with the published work and can be explained as done in literature.

6.2 Metastabilities in Li-doped a-Si:H (Similarity with P-doped a-Si:H)

We have seen in Chapter 5 that σ of our Li doped a-Si:H films increases with increasing Li concentration. Furthermore, these films show both thermal and light induced metastabilities, when cooled rapidly from high temperatures ($\approx 470K$) or light soaked at room temperature ($\approx 300K$). The FQ and LS states are reversible and annealing at $\approx 450 - 470K$ results in the original equilibrium state. These

results are in qualitative agreement with literature for a-Si:H(P). In the following, we will see further similarities between P and Li in a-Si:H and try to explain these metastabilities in Li-doped a-Si:H.

As is evident from our $\sigma(T)$ measurements (Figs. 5.9 and 5.10) on a-Si:H(Li) films (Chapter 5), the σ of these films increases when fast quenched from high temperatures. The increase in σ is accompanied by a decrease in activation energy (E_σ). The sub gap absorption measurements on these films do not show any change after fast quenching thus ruling out the possibility of any significant change in density of dangling bonds [151]. It is expected that the observed changes in σ and E_σ are due to the changes in the occupancy of states above Fermi level. Our Li doped a-Si:H films behave in a qualitatively similar manner to P-doped a-Si:H, when subjected to fast quenching from high temperature and $\sigma(T)$ curve in the fast quenched state meets the equilibrium curve at elevated temperature T_E. For $T \geq T_E$, $\sigma(T)$ is independent of the history of the material. T_E is found to vary with concentration of Li in a-Si:H films from $170°C$ for films with low Li concentrations to $120°C$ for high concentrations of Li. The thermal induced metastability in these films may be explained in a manner similar to that used for a-Si:H(P). The thermal equilibrium model (Sections 3.2.1, 3.4) predicts that the density of occupied band tail states will be given as

$$n_{bt} = Li^+ - Si_3^- \tag{6.3}$$

Upon fast quenching, the density of active interstitial lithium (Li^+) will increase, which donates electrons to the conduction band tail. The extra charge in the band tail thus causes the E_f to move up into the band tail region towards the conduction band edge and the state is characterized by a lower activation energy. Above T_E, thermal equilibrium prevails and the $\sigma(T)$ is independent of the history of the film.

The metastable state after FQ relax following a stretched exponential (see Figs. 5.14, 5.15). These observations are similar to a-Si:H(P) and many other glass [29]. Because of the similarity, we can think of a-Si:H(Li) as a Hydrogen Glass, as has

already been proposed for a-Si:H(P) [30]. The properties of a-Si:H below T_E depend upon the rate of cooling from $T \geq T_E$. T_E in this case is equivalent to the glass transition temperature, where the properties of glass (like specific volume) depend upon the rate of cooling near T_g [29]. An analogy with the glass can further be seen in Fig. 5.11, where the quenching from different temperature (T_q) results in a different conducting state near room temperature. Since T_g is not unique, the quenching from higher temperature is equivalent to higher cooling rates and thus results in to a larger room temperature conductivity. However, not much difference is observed in E_σ as T_q is increased any further. This may be due to the fact that E_f has to move in to an exponentially rising density of states region and hence large changes are observed initially. Further increase in T_q causes relative smaller changes.

Light soaking results in a lower dark and photoconductivity (see Figs. 5.9 and 5.10; Table 5.1) of lithium doped a-Si:H films. The effect is large for the films with low Li concentrations. For low doped a-Si:H(Li), LS causes a decrease in $\sigma(300K)$ by about $\approx$ 3 orders of magnitude, whereas, for high Li concentrations, $\sigma(300K)$ decreases to half of its value in the slow cooled state (these results are in a nearly saturated state). These results are in qualitative agreement with those reported for a-Si:H(P) [15] and can be explained using similar arguments as proposed for a-Si:H(Li) films. For low doped a-Si:H(Li)films, the density of states in slow cooled state is $\approx 2.5 \times 10^{17} cm^{-3}$ and is not too high. Thus a large effect of LS is seen on σ and σ_{ph}. In the heavily doped films, the density of photocreated defects is too small to overcome the pinning of the Fermi level by the significantly larger density of donors and defect states [152] and a smaller effect of LS is observed on σ and σ_{ph}. The small difference between σ and σ_{ph} for heavily doped a-Si:H(Li) also predicts a larger defect density in these films.

From Fig.5.13 and Table 5.4, it is clear that the σ in the light soaked state depends upon the initial state of the films. The conductivity σ after light soaking in the initial slow cooled state of the samples is different than that for the initial fast

quenched state. For short exposures, the relative changes in σ are similar, irrespective of the initial state, although, the final state is different. These results are consistent with the proposition that thermal and light induced metastabilities are independent of each other [45].

An increase in density of states after LS is observed for a-Si:H(Li) also [151]. The similarity with a-Si:H(P) suggests a simultaneous increase in donor and defect density upon light soaking a-Si:H(Li) [43]. As the intensity or duration of light exposure is increased, more weak Si-Si bonds break, resulting in a rapid increase in donor and defect density in the beginning and a lower value of σ and σ_{ph} is observed (see Fig. 5.12). However, saturation sets in for long exposures and high intensities as the defect density becomes very high and the Fermi level is pinned.

6.2.1 Isothermal Relaxation

The fast quenched and the light soaked metastable states relax slowly (Figs. 5.14, 5.15, 5.18 and 5.19) following a stretched exponential (Eq. 3.8) and a thermally activated relaxation time τ (Eq. 3.5), as shown in Figs. (5.16) and (5.20).

Now, we will discuss how the temperature dependence of the parameters τ and β in the LS and FQ states can be explained by Hydrogen Glass model (Section 3.4).

6.2.1.a Temperature dependence of τ

We observe that the relaxation time τ depends upon the Li concentration in a-Si:H films and the metastable state. In the following, we discuss, how τ varies with temperature and also with doping concentrations.

Relaxation from fast quenched (FQ) state

It is clear from Fig. 5.16 that E_τ for relaxation from FQ state for the two lithium concentrations is nearly the same ($0.6 \pm 0.1eV$ for high and $0.95 \pm 0.2eV$ for low Li) as that for a-Si:H(P) ($1.0 \pm 0.2eV$). Furthermore, τ decreases with increasing lithium

concentrations. Similar doping dependence of τ is reported for the relaxation of FQ state in P-doped a-Si:H [122]. These results can be explained by Hydrogen Glass model 3.4, if D_H is thermally activated in lithium doped a-Si:H also (for P-doped and undoped a-Si:H the activation energy of D_H is $\approx 1.2 - 1.5eV$) and is higher for higher lithium concentrations ($D_H \propto 1/\tau$) [153]. Since no results on measurements of D_H on Li doped a-Si:H are available, we can not be sure of this hypothesis, at present. However, since D_H has been measured on P-doped films and has been found to increase with increasing doping concentrations, a similar behaviour may be expected for Li-doped films also.

Relaxation from light soaked (LS) state

As is evident from Fig. 5.20, the relaxation time τ for light soaked state in lithium doped films is also thermally activated. The activation energy E_τ for the two concentrations of lithium are nearly the same within the error limits ($1.45 \pm 0.2eV$ for low and $2.0 \pm 0.3eV$ for high concentrations of Li). A thermally activated relaxation has also been observed for relaxation of undoped a-Si:H from LS state. Further, τ is more for films with lower concentration of Li. Thus, it is possible to explain the doping dependence of τ in terms of Hydrogen Glass model, as in the FQ state. However, since the measured value of E_τ and τ are different for FQ and LS states, the hydrogen diffusion parameters have to be different for the two cases. We shall discuss this point later when we compare the relaxation of LS and FQ states.

Relaxation from FQ + LS state

We have seen in Fig. 5.22, that although the $\sigma(T)$ in the FQ + LS state is similar to that in SC state for a heavily doped a-Si:H(Li), at 340K, σ decreases with time. This is consistent with the proposition that thermal and light induced states are independent of each other, and since LS state relaxes slowly as compared to the FQ state, a decrease in σ is observed when measured as a function of time.

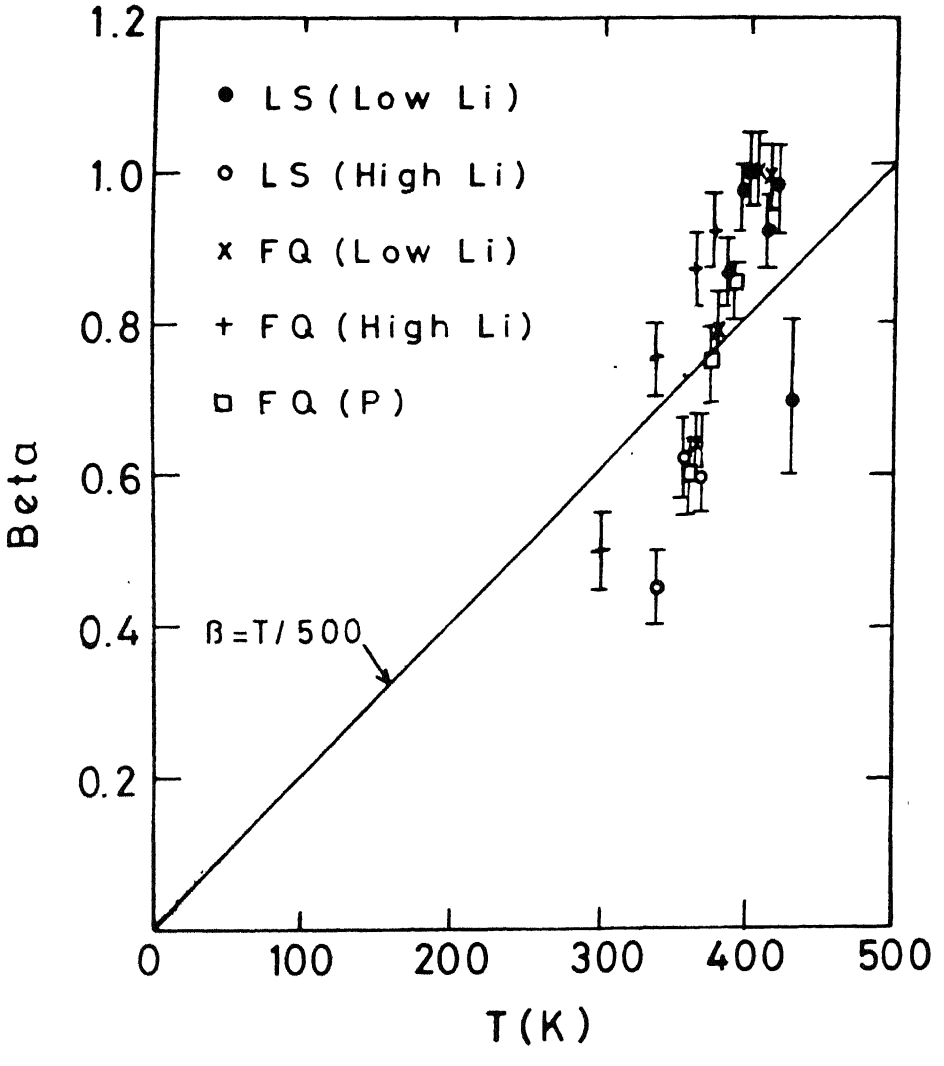

Figure 6.1: Stretching parameter β as a function of measurement temperature for relaxation from FQ and LS states.

6.2.1.b Temperature dependence of β

For relaxation from FQ state, β is found to increase with temperature for Li doped a-Si:H (Fig. 5.17). The behaviour is consistent with the reported results for P-doped a-Si:H. However, for relaxation from LS state in lithium doped films, β is nearly independent of temperature in the measurement temperature range (Fig. 5.21). For low lithium concentration, $\beta \approx 1$, whereas, for high Li concentration, $\beta \approx 0.6$. A decrease in β is also observed at $\approx 430K$ for low concentrations, which is different from the commonly observed trend (β increasing with temperature) and the origin of this is not clear at present.

It seems difficult to fit these values to $\beta = T/T_o$ for individual sample as expected from Hydrogen Glass model [30]. We note that our temperature range is limited and the number of data points for each case is rather small, therefore it is not clear at present whether the disagreement noted above are significant. However, if we plot β *vs* T for all the relaxations, as shown in Fig. 6.1, we find a reasonably good fit $\beta = T/T_o$ with $T_o = 500K$. This value of T_o is close to the reported value ($600K$) for a-Si:H(Li) [30].

Thus, we conclude that the metastabilities in Li-doped a-Si:H are similar to those observed in P-doped a-Si:H.

6.3 Thermopower Measurements in Annealed and Metastable States

As discussed in the Chapter 2, for electron in the conduction band, conductivity σ and thermopower S, are given as:

$$\sigma = \sigma_0 \exp\left(-\frac{E_c - E_f}{kT}\right) = \sigma_o \exp\left(-\frac{E_\sigma}{kT}\right) \tag{6.4}$$

and

$$S = -\left(\frac{k}{e}\right)\left[\frac{(E_c - E_f)}{kT} + A\right] = -\left(\frac{k}{e}\right)\left[\frac{E_S}{kT} + A\right] \tag{6.5}$$

It is observed that both $\log\sigma$ vs. $1/T$ and S vs. $1/T$ in general, exhibit a kink and often their slopes (E_σ and E_S) are not equal. We have discussed in chapter 2 that the nonlinear statistical shift of Fermi level can explain the kink. The difference between E_σ and E_S may arise [69] if

1. electrons and holes, both contribute to the conduction,
2. mobility edges are not sharp,
3. mobility is thermally activated or
4. potential fluctuations are present in the material [52].

However, the presence of potential fluctuations due to density fluctuations, growth inhomogeneities or charge centers is the more likely reason for the observed difference between E_σ and E_S (see Section 2.3). A function Q defined as

$$Q = \ln\sigma + \frac{e\,S}{K} \tag{6.6}$$

is independent of Fermi level and thus separates the effects on transport properties arising due to the statistical shift of Fermi level from those due to the structural disorder giving rise to potential fluctuations. Absence of any kink in $Q(T)$ is a signature of the nonlinear shift of the Fermi level and a non-zero slope E_Q of $Q(T)$, where

$$Q = Q_0 - \frac{E_Q}{kT} \tag{6.7}$$

is attributed to the presence of potential fluctuations. Overhof and Beyer [72] showed that the slope E_Q is related to the width Δ of potential fluctuations arising due to the random distribution of charge centers in a-Si:H. In the following, we will discuss our results on thermopower in annealed and slow cooled state as well as in metastable states for P-doped and Li doped a-Si:H. Thermopower in undoped a-Si:H could not be measured because of their high resistance.

6.3.1 P-doped a-Si:H

Results on thermopower measurements in SC, FQ and LS states are discussed in this section.

6.3.1.a Slow Cooled State

Results on thermopower measurements on two P-doped a-Si:H films for $250K \leq T \leq 400K$ are shown in Figs. (5.23) and (5.24). It is evident, from these figures that the two films are qualitatively similar. We will discuss only one of them in the following.

In the slow cooled (SC) state, near room temperature the magnitude of S is $1.08 \pm 0.01 mV/K$ and the slope E_S is $0.18 \pm 0.01 eV$. These values are in good agreement with those reported by Beyer *et al.* [52]. From these figures, it is apparent that like $\log \sigma$ vs. $1/T$ curves (Fig. 5.4 and 5.5), S vs. $1/T$ curves also show a kink near $400K$. Above the kink temperature, the value of both $E_\sigma(0.34eV)$ and $E_S(0.26eV)$ are higher than the respective values at low temperature. It is also apparent that E_S is lower than E_σ for low as well as in the high temperature range.

Following Overhof and Beyer [72], we plotted the function Q defined by Eq.(6.6) as a function of inverse temperature in Figs. (6.2 and 6.3). It is evident that, Q vs. $1/T$ does not have any kink and has a single slope in the measurement temperature range ($300 \leq T \leq 450K$). This may imply that the kink is due to the non linear shift of the Fermi level. This non linear shift may arise as the density of state distribution is not symmetric above and below the Fermi level in a-Si:H (see for e.g., Fig. 3.3).

Now we turn our attention to the difference in the slopes of $\sigma(T)$ and $S(T)$. As expected from the expression for σ and S (Eqs. (6.4) and (6.5)), E_σ and E_S should have the same value, i.e., $E_\sigma = E_S = E_c - E_f$. However, we find that, for both the samples $E_\sigma > E_S$. As discussed in the Chapter 2, the presence of the long range potential fluctuations are the most likely cause for our experimental results.

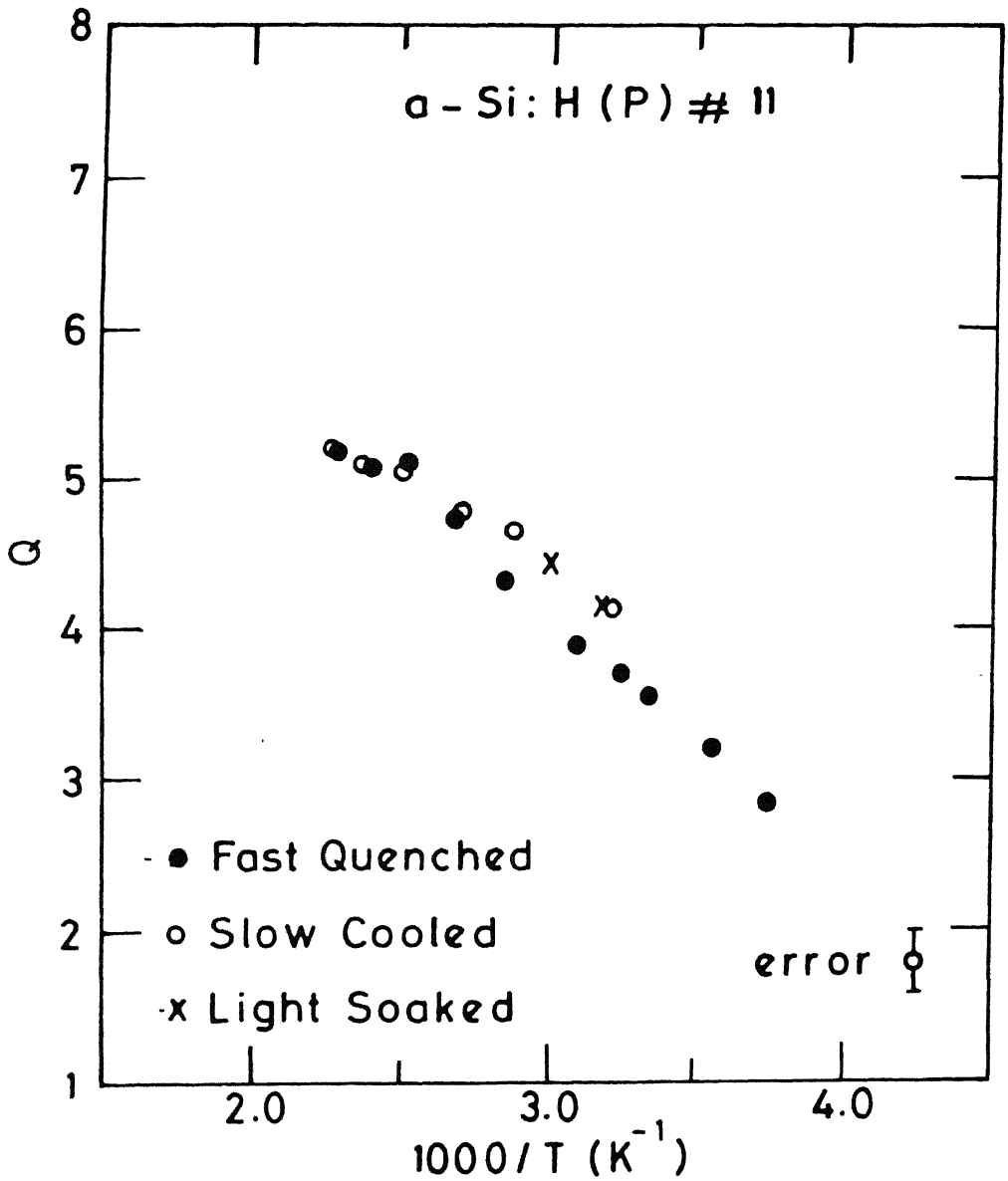

Figure 6.2: Q vs. $1/T$ for a-Si:H(P) in SC, FQ and LS states.

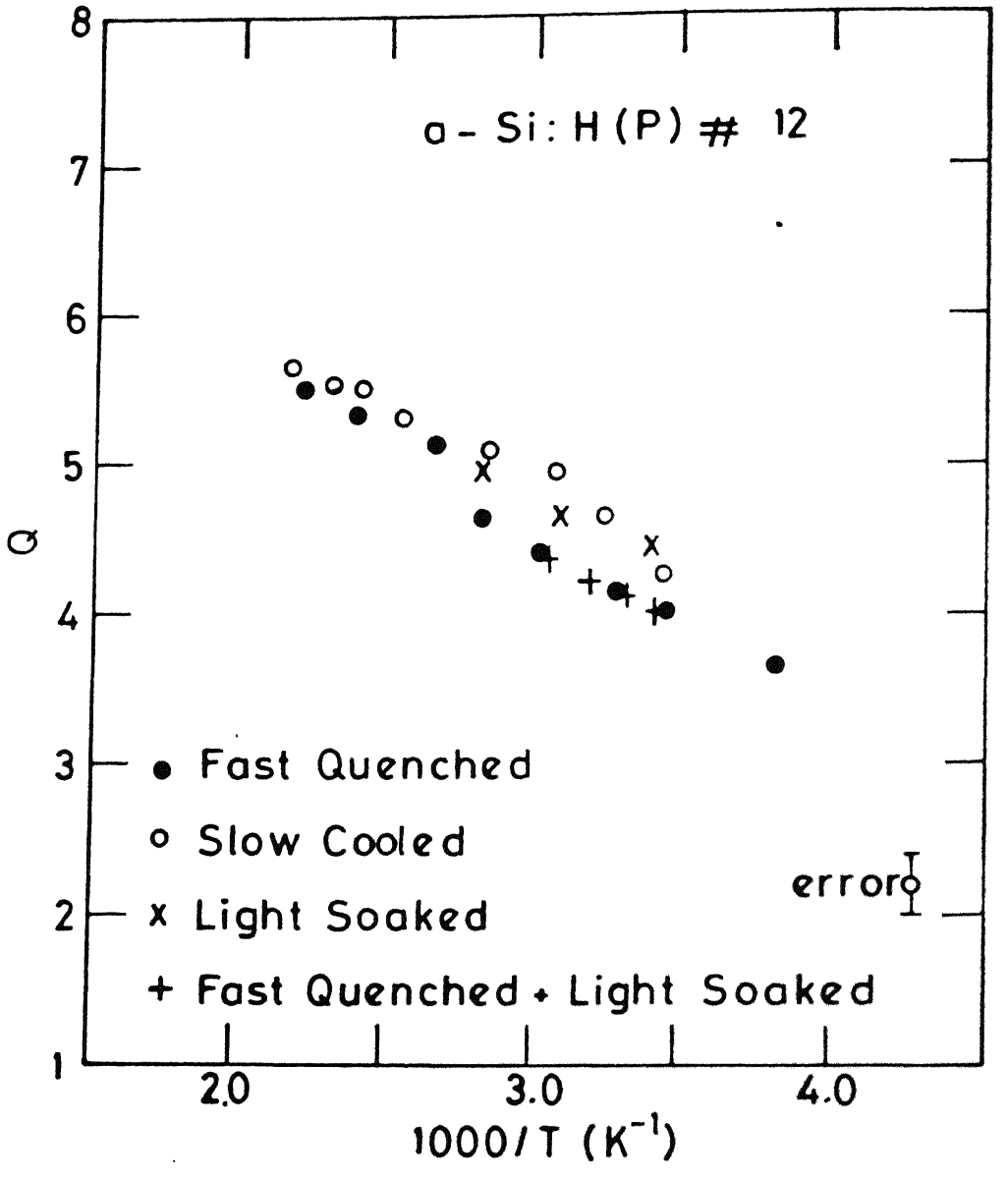

Figure 6.3: Q vs. $1/T$ for a-Si:H(P) in SC, FQ and LS states.

Several other experimental results are also in favour of the potential fluctuations as the underlying reason for the observed difference between E_σ and E_S in these films. We observe a slope of $E_Q \approx 0.07 \pm 0.02eV$ P doped a-Si:H films, which is similar to the values observed by Beyer *et al.* $(0.05 \leq E_Q \leq 0.20eV)$ [52].

6.3.1.b Fast Quenched State

Upon fast quenching these films from $450K$ at a rate of $\approx 500K/min.$, we observe a decrease in magnitude of S (see Fig. 5.23 and 5.24). The value S at $300K$ in this state is $-0.98 \pm 0.01mV/K$ (see Table 5.7 also). A decrease in E_S is also observed after FQ, which changes to $0.12 \pm 0.01eV$. We have earlier pointed out (Sec. 6.1.2), that quenching results in an increase in σ accompanied by a smaller activation energy E_σ (Figs. 5.4 and 5.5), i.e., E_f moves upward towards E_c. Smaller values of S and E_S in FQ state are also consistent with this. In the fast quenched state, S vs $1/T$ curve has a downward kink at $T \approx 360K$ and meets the corresponding curve in the slow cooled state at $\approx 395K$ (Figs. 5.23 and 5.24). Above $395K$, the S vs $1/T$ is same in both fast quenched and slow cooled state. This is somewhat smaller than $T_E(425K)$ observed in $\sigma(T)$ curves. We discuss this point later in this section.

It is interesting to note here that although quenching changes both E_σ and E_S, the difference $E_\sigma - E_S$ is the same as in case of slow cooling, for all the samples. Further, a plot of Q vs $1/T$ in Fig. 6.2 and 6.3 shows that the function Q is almost unchanged after fast quenching these P-doped films. It may, therefore, imply that fast quenching does not change the potential fluctuations. Reported experimental results suggest that the fast quenching results in an increased number of band tail carriers n_{bt} (and σ) without any measurable change in density of states distribution below Fermi level [82,45]. However, a very small change in the density of P_4^+ upon fast quenching may account for the observed metastability, as shown below. In thermal equilibrium, n_{bt}, P_4^+ and Si_3^- are related by Eq.(6.1). It is reported that $n_{bt} \ll P_4^+$ and Si_3^- (according to the doping model, each ionized dopant give rise to a charged

dangling bond in the gap). Thus a commonly observed 2-fold increase in σ or n_{bt} after fast quenching is due to less than 10% increase in density of P_4^+. Since P_4^+ increases, it may appear that potential fluctuations also increase in the fast quenched state, however, the increase in P_4^+ is too small to change the potential fluctuations significantly.(since $\Delta \propto (N_c^2/n_f)^{1/4}$, Eq. (2.25), where N_c is the concentration of charge centers, i. e. , P_4^+ and Si_3^- and n_f is free carrier density). The effect of these additional charge centers will further be screened by an increased density of free carriers in the fast quenched state. For a 2–fold increase in n_f and a 10% increase in N_c, $\Delta(FQ) \approx 0.85\Delta(SC)$. Thus, the net effect of fast quenching is simply a shift of Fermi level without any detectable change in potential fluctuations.

If we look at $S(T)$ and $\sigma(T)$ curves more carefully, we find that in the fast quenched state, $S(T)$ curve meets the corresponding curve in the slow cooled state at a lower temperature ($\approx 395K$) as compared to the $\sigma(T)$ curve where T_k is $\approx 425K$. The reason for this may be that S(T) measurements take a longer time and the metastable state, which is a function of both temperature and time relaxes during measurements. If the relaxation is taken in to account, observed E_S will be smaller than the true value, i.e. , relaxation will result in a larger difference between E_σ and E_S. Since the observed value of Δ does not change, it may be concluded that quenching does not change the potential fluctuations, notwithstanding the uncertainty in the experimental procedure, as described above.

6.3.1.c Light Soaked State

No effect of light soaking on $S(T)$ is observed in our P-doped a-Si:H films. These films do not show any change in $\sigma(T)$ also, when exposed to light (Table 5.1). It is often seen that the effect of light soaking is small in heavily doped films, but a-Si:H films with low doping concentrations have been reported to show an appreciable change on electrical properties. For low doped films, light soaking causes a decrease in σ accompanied by an increase in E_σ and density of states below E_f. Hauschildt *et al.*

[154] have reported an increase in magnitude of S and its slope E_S upon light soaking the low P-doped films. The increase in E_σ and E_S is such that the difference $E_\sigma - E_S$ also increases from $0.09eV$ in slow cooled state to $0.21eV$ in light soaked state. These changes in E_σ and E_Q after light soaking are in opposite direction to that observed as a result of increasing doping concentration. This clearly shows that the increase in E_Q upon illumination is not due to the shift of Fermi level, but due to a change in current path. Hauschildt *et al.* [154] argued that a homogeneous distribution of charge centers cannot account for such a large change in E_Q after exposure to light. However, the inhomogeneous distribution of charge centers, which may arise due to the structural inhomogeneities in these films [33,34], can give rise to large potential fluctuations. It is reported that hydrogen is distributed non-uniformly in a-Si:H, in a dilute monohydride phase and a clustered hydride phase [33]. The variation in hydrogen concentration may cause a spatial variation of the gap energy, which will give rise to fluctuating mobility edges [35]. This variation in gap energy in space may result in some preferential sites for creation and recombination of photogenerated carriers, which in turn may increase the heterogeneities in the material. Hence an enhancement in the magnitude of the potential fluctuations is observed.

It is further observed that when light is shone on these films in fast quenched state (higher conducting state), $\sigma(T)$ and $S(T)$ do not change. The main reason of it could be that although in the fast quenched state, conductivity is higher due to high free carrier concentration, the DOS does not show any observable change in FQ state, when measured by ICTS [45,44] and subgap absorption [82]. Since the DOS in this case is similar to that in the slow cooled state and is high enough, light soaking has no effect and the results can be explained easily as in case of light soaking in the slow cooled state.

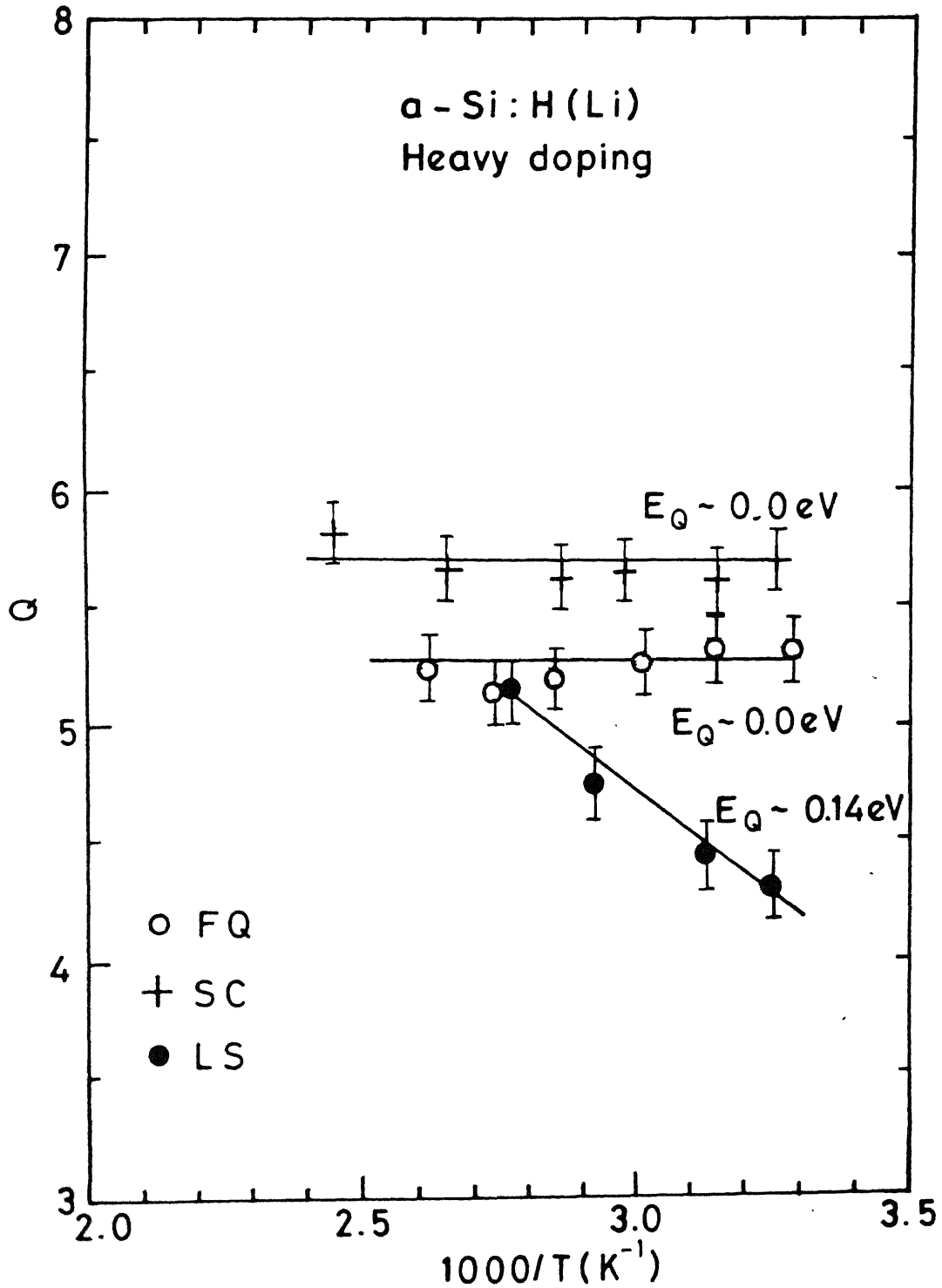

Figure 6.4: Q vs. $1/T$ a-Si:H(Li) in SC,FQ and LS states.

6.3.2.c Light Soaked State

Upon light soaking, lithium doped films show a change in both σ and S. It is observed that both the magnitude of S and E_S decrease in the light soaked state. An appreciable change in Q vs. $1/T$ is also observed and E_Q is now $0.14 \pm 0.02eV$ as compared to the $0.0 \pm 0.02eV$ in the SC and FQ states. The increase in E_Q implies that the potential fluctuations have increased in these films as a consequence of light soaking. As suggested by Stutzmann [43] for P-doping, in a-Si:H(Li)also, light may result in an enhanced dopant and defect density with smaller free carrier density, which increases the potential fluctuations. The increase in dopant and defect concentrations will cause a small shift in Fermi level, which is indeed observed (E_σ changes from $0.14eV$ to $0.15eV$, see Fig. 5.10). We have mentioned while discussing the light soaking in P-doped films that a-Si:H films grow inhomogeneously with varying hydrogen concentration. These growth inhomogeneities give rise to the large fluctuations of mobility edges, which are further enhanced after light exposure. In Li doped a-Si:H films, in addition to hydrogen, lithium is also present. SIMS studies show that lithium is not uniformly distributed and is more on the surface and interface. The presence of active lithium will add to the density of charged centers.

Since FQ and LS metastable states relax with time for $T < T_F$ at each temperature, one may enquire the effect of relaxation on S and E_Q. The observed E_S may be different from the actual E_S because the sample in FQ or LS state relaxes at each temperature at a different rate. We note however, that the actual E_S can only be higher than the measured E_S in the FQ or LS metastable state, since the relaxation is faster at high temperature. Since $E_Q = E_\sigma - E_S$ is a measure of potential fluctuations, the measured E_Q is the upper limit of the potential fluctuations. In FQ state, $E_Q = 0$, for a-Si:H(Li), and there is no room to decrease it any further. Therefore, the measured E_Q is very close to the actual value. In LS state, relaxation is slower than the FQ state, hence, the measured E_Q should even be closer to the actual value as compared to the FQ state.

These discussions show that our σ and S results can be explained by assuming the presence of long range potential fluctuations. Further, we see that the FQ does not change the magnitude of the potential fluctuations in a-Si:H, whereas, LS increase their magnitude.

6.4 Comparison of Thermal and Light Induced Metastable States

So far we have discussed the thermal and light induced metastabilities in undoped, P-doped and Li-doped a-Si:H. The two metastable effects seems to be different as the change in σ in case of FQ is in the reverse direction to that in case of LS state. We have seen in the above discussion that there are differences in other properties also. However, there are certain similarities between the two effects. In the following, we discuss, these similarities and differences and the effect of fast quenching and light soaking on the structure of Li doped a-Si:H.

These discussions show that our σ and S results can be explained by assuming the presence of long range potential fluctuations. Further, we see that the FQ does not change the magnitude of the potential fluctuations in a-Si:H, whereas, LS increase their magnitude.

6.4.1 Similarities between FQ and LS states

It is interesting to note that the $\ln\sigma$ vs. $1/T$ in the SC, FQ and LS states meet at the common temperature T_E (Figs. 5.9, 5.10, which is a characteristic of the sample. It, therefore, appears that the two metastable states (FQ and LS states) have a common origin. Further, both of these relax following a stretched exponential (Figs.

5.14, 5.15, 5.18 and 5.19), which can be related to the diffusion of hydrogen in a-Si:H. The common T_E and the stretched exponential relaxation may suggest that a common microscopic mechanism may be operative in both the cases.

6.4.2 Differences Between FQ and LS States

In spite of a common equilibration temperature T_E for the FQ and LS states, there are several differences between the two metastable states. We discuss, these differences in the following sections.

6.4.2.a E_τ for relaxation from FQ and LS states

Figs. 6.5 and 6.5 show the $\log \tau$ vs. $1/T$ curves for the recovery from FQ and LS states for the two lithium doped a-Si:H films. For both doping concentrations, the LS state relaxes slower than the FQ state. Let us first see, if Hydrogen Glass model can explain the difference. It is proposed [129] that the time dependence of D_H is related to the shape of valence band tail distribution. If it is true, then one expects a faster relaxation of LS state, as light soaking causes an increase in disorder and thus a higher slope of valence band tail state. This is in contrary to the experimental observations. Since relaxation time τ is thought to be inversely proportional to the hydrogen diffusion constant [155], the different annealing rates for FQ and LS suggest that D_H is different in FQ and LS states. It has been reported [47] that for P-doped a-Si:H films also, relaxation times are longer for LS state. Deng and Fritzsche [156] also reported that when doped a-Si:H films are fast quenched after a short light exposure at high temperature, the metastable state so obtained is different with higher equilibration temperature than the one observed without light exposure. It is suggested that light causes the formation of donor-defect complexes, which are difficult to anneal [156]. Various transport and density of states measurements suggest that light soaking results in an increase in both, the density of donors above E_f and density of dangling bond below E_f, with a decrease in density of free carriers,

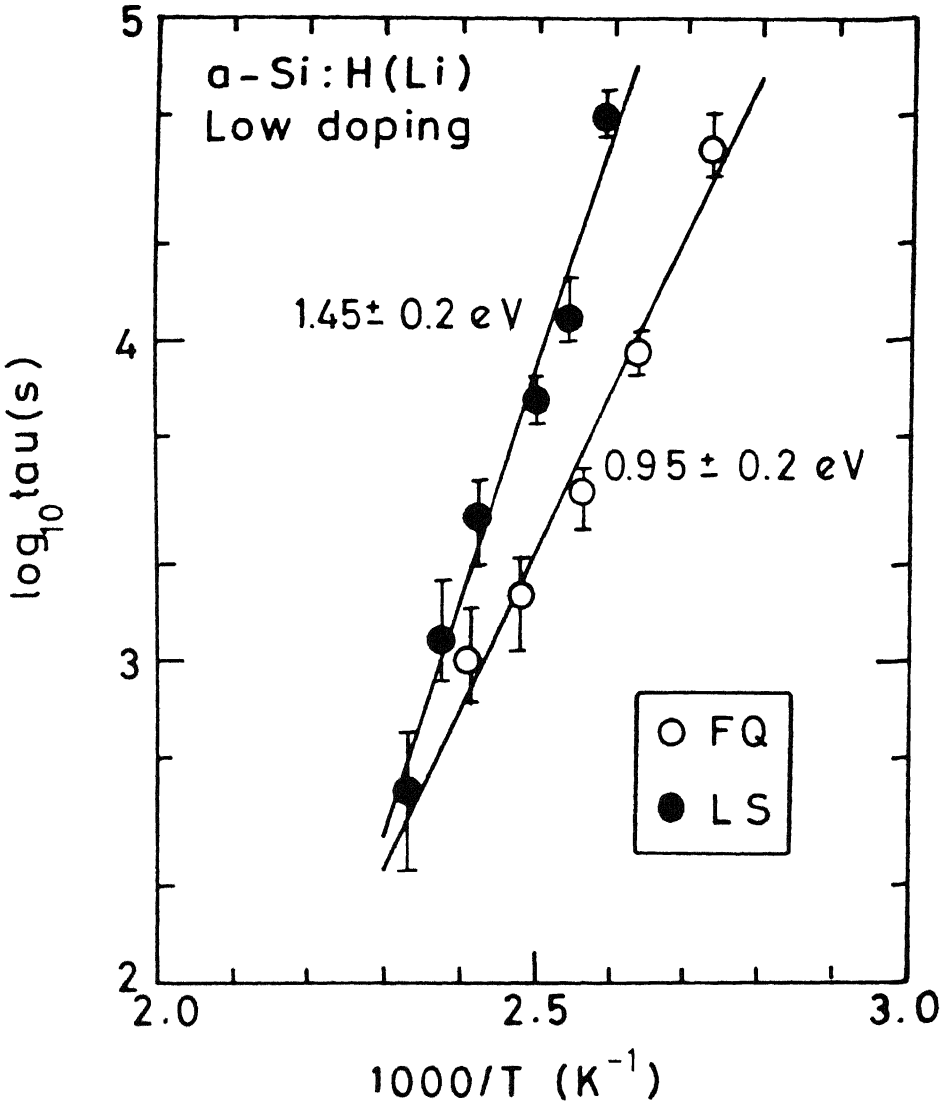

Figure 6.5: $\log \tau$ vs. $1/T$ for relaxation from FQ and LS states for low doped a-Si:H(Li).

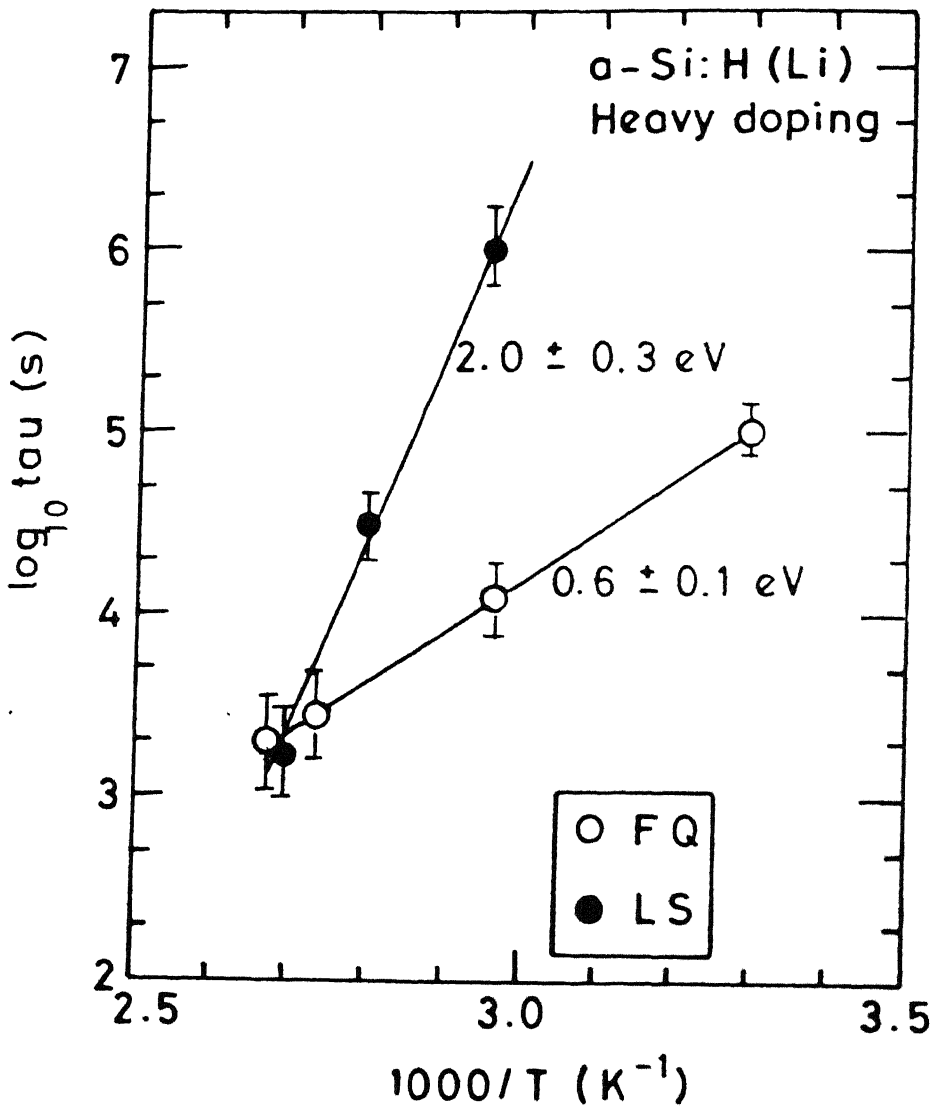

Figure 6.6: $\log \tau$ vs. $1/T$ for relaxation from FQ and LS states for heavily doped a-Si:H(Li).

while FQ increase the density of donors and free carriers above E_f without changing the density of dangling bonds. A difference in the density of states in case of FQ and LS suggests that the two states are not similar and thus may anneal at different rates. These results, therefore can be explained by the movement of hydrogen, if D_H is more in FQ than in LS state.

We find that E_τ is nearly the same for different Li concentrations. This is understandable since SIMS results also show that E_{DH} is independent of dopant and doping concentrations. However, E_τ values are different for relaxation from FQ and LS states. For FQ states, the E_τ is lower ($0.6 \pm 0.1eV$ and $0.95 \pm 0.2eV$) as compared to LS state ($1.4 \pm 0.2eV$ and $2.0 \pm 0.3eV$). Although a range of activation energies ($0.6 \leq E_\tau \leq 2.0eV$) are reported [131] for different samples, for a given sample, Hydrogen Glass model predicts the same value of E_τ for LS and FQ states, since all the metastable defects arise from a single pool of hydrogen, controlling the recovery kinetics. For differently prepared samples, variation in E_τ may be related to the distribution of H bonding energies, defect formation energies and valence band tail states [129]. Thus in Hydrogen Glass model it appears difficult to understand the different E_τ for FQ and LS states.

So far we have tried to apply only Hydrogen Glass model (Sec. 3.4) to explain our results. Another model called Defect Controlled Relaxation (DCR) model (Sec. 3.5.2) has been proposed by Crandall [131]. We now discuss how this model can also be used to explain our results. The model (Sec. 3.5.2) assumes that the relaxation of metastable state is governed by the defects itself. The annealed and metastable states are separated by potential barriers. The stretched exponential, in this model, arises from an exponential distribution of barrier energies due to the structural disorder in amorphous material.

The difference in E_τ for FQ and LS states can be explained using DCR model (Sec. 3.5.2) [131]. If the slow cooled state and metastable state are separated by a barrier as required in DCR model, different metastable states can be denoted by

different barrier energies and thus may have different E_τ. A distribution in annealing energies has also been suggested by Gleskova *et al.* [157]. These authors [157] have observed that the metastable defects in a-Si:H anneal with different E_τ, when annealing is done in dark or under illumination. The E_τ is $1.56 \pm 0.2eV$ for recovery in dark, which changes to $0.91 \pm 0.2eV$ under illumination.

Although, the two models are quite different physically, they both predict similar results, *viz.*both predict the stretched exponential and a thermally activated relaxation time. The reason for this may be that the disorder in a-Si:H is the main determinant of the form of relaxation in each model [131]. Although Crandall has suggested ways to distinguish between them, it is difficult to say which model is preferable in our case.

6.4.2.b The Meyer-Neldel Relation : Relation between ν and E_τ

It is interesting to note that ν and E_τ for our samples obey a Meyer-Neldel (M-N) type relationship [158], in agreement with the published work [130,131]. Fig. 6.7 shows the $\ln \nu$ vs. E_τ plot for doped and undoped a-Si:H in various metastable states as compiled by Crandall [131] from the literature. Also, shown are our results for relaxation from FQ and LS states for P-doped and Li-doped a-Si:H. As is evident from the Fig. 6.7, our results agree with the published work, and follow

$$\nu = \nu_0 \exp(E_\tau / E_0)$$

Jackson [130] has suggested a connection between the M-N relation and multiple trapping transport of hydrogen. The M-N relation between ν and E_τ is due to the dispersive diffusion of hydrogen in a-Si:H [130]. It is further shown [130] that the parameters ν_o and E_o can be related to the energy distribution of trapping sites and microscopic transport properties.

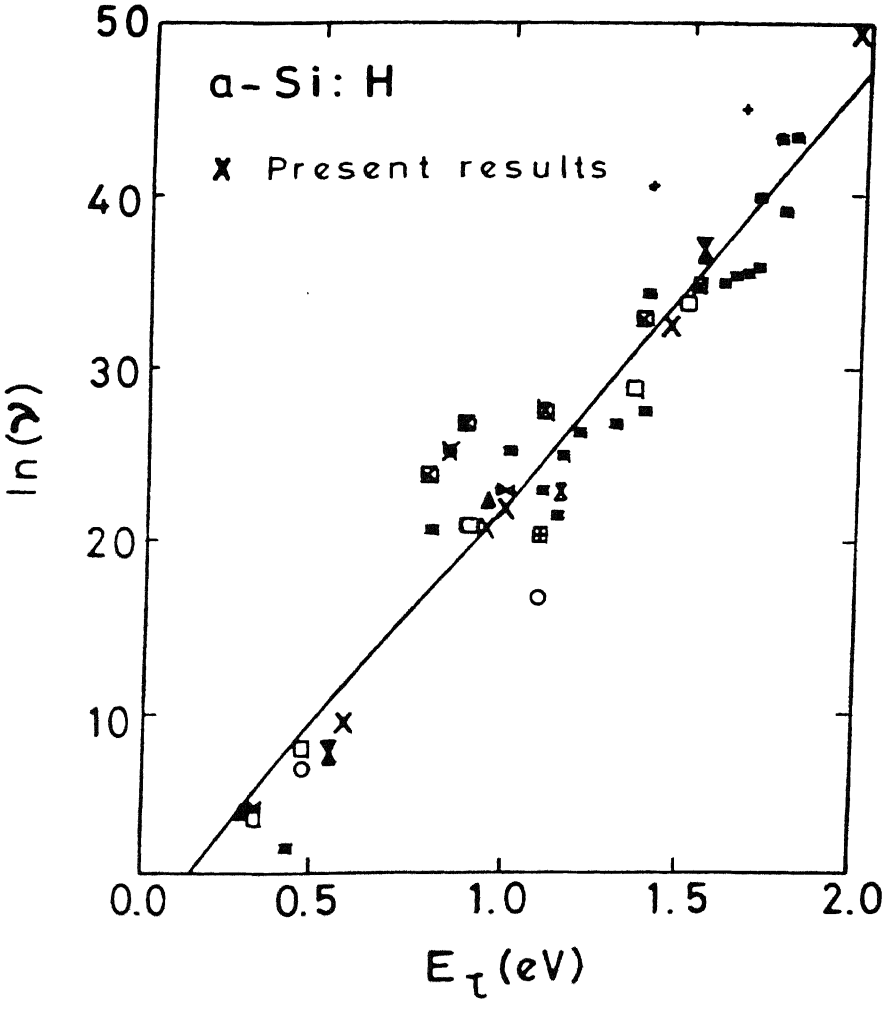

Figure 6.7: $\log \nu$ vs. E_τ for relaxation from metastable states (after Crandall). $\times$ denotes our data.

On the other hand, Crandall [131] has considered the defect controlled model (Section 3.5.2) with a distribution of barrier energies and shown that the model predicts M-N relation between ν and E_τ.

Although the M-N relationship is observed by other thermally activated processes (see Section 6.4.2.e), its origin is not very clear. These results seem to reflect disorder in a-Si:H as the underlying cause for this relationship [131].

6.4.2.c Change in Potential Fluctuations in FQ and LS states

We have seen in Section 6.3, while describing our results on thermopower in SC, FQ and LS states, that FQ does not change the potential fluctuation in the a-Si:H, whereas, light soaking enhances them significantly. Let us discuss these further.

Our results show that the potential fluctuations in a-Si:H(Li) are negligible in the annealed and slow cooled state, since the slope E_Q is almost zero. One might argue that the presence of conduction electrons tend to screen the potential fluctuations present. It may be further argued that since after FQ, the number of these electrons increases, the screening is more and hence the slope E_Q remains zero. Thus, it appears that our assertion that FQ does not affect the potential fluctuations might not be fully justified. Here we would like to point out that in our P-doped a-Si:H also, E_Q does not change after FQ. Since E_Q is not zero in P-doped a-Si:H, the above argument given for a-Si:H(Li) about screening does not apply. Although further experiments are necessary to prove our point, the similarities in the behaviour of P-doped and Li-doped a-Si:H suggest that FQ does not change potential fluctuations in a-Si:H(Li) also.

In case of light soaking, the number of free carriers decreases, and one might again argue that the observed increase in E_Q is due to the reduced screening of the potential fluctuations. However, the decrease in free carriers density is too small to account for the observed increase in E_Q (using (2.25)). The observed decrease in free carrier density along with increase in density of charge carriers will increase the

magnitude of potential fluctuations by a factor of 2 only. (In LS state, σ is half of its value in SC state and hence for an increase in density of charge centers by a factor of two, we get $\Delta(LS) = 1.7 \times \Delta(SC)$), whereas, we observe an increase of about one order of magnitude in Δ in LS state. It is thus concluded that increase in magnitude of potential fluctuations after light soaking is not only due to an increase in density of charge centers or a decrease in free carrier density, but some structural changes are also associated with light soaking. This may also be the cause of the higher activation energy for relaxation from the LS state.

6.4.2.d Light Induced Structural Changes in a-Si:H

The difference in E_τ between FQ and LS states can be explained by Hydrogen Glass model only if diffusion constant of hydrogen in the two metastable states is different. It is reported that hydrogen is distributed inhomogeneously in a-Si:H, in a dilute Si-H phase and a clustered phase with 5-7 H atoms. Light soaking effects are believed to be related to the Si-H bond clusters [39]. This may cause a further heterogeneous distribution of hydrogen. It is thus possible that LS is associated with a change in structure resulting in an enhanced potential fluctuations and a higher barrier for hydrogen diffusion.

A decrease in drift mobility of electrons and increase in band tail slopes has also been reported as a result of light soaking [50,159]. Light soaking increases the number of charged defects which modifies the transport edge [159]. This might result in increased potential fluctuations, thereby reducing the mobility of electrons at the transport edge. These changes are similar to those observed upon increasing the doping concentrations in these films. It has been observed that the heavily doped films have a higher value of E_Q, which can be due to an increased number of charged centers as well as due to higher disorder. These observations are in favour of larger potential fluctuations as a result of light soaking.

It is also possible that the observed difference in E_τ between LS and FQ states is caused by the presence of lithium. The microscopic H diffusion is found to be different in clustered and dilute H phase in a-Si:H [37] and thus it is likely that H diffusion coefficient is modified by the presence of Li in these films. Our SIMS results (Fig. 4.2) show that in the as deposited sample, lithium concentration is large on the film surface and is nearly uniform in the bulk of the material. Similar results are reported by Winer and Street [48]. It is proposed that at high temperature ($\approx 500K$), in-diffusion of Li produces an (presumably) uniform Li concentration in a-Si:H consistent with the solubility at this temperature. When cooled back to $300K$, the Li concentration lies above the solubility limit and excess Li diffuses towards the interface, resulting in a non-uniform distribution of Li.

It is found that lithium is ≈ 3 orders of magnitude more mobile than hydrogen in a-Si:H films and it is quite probable that diffusion coefficient of lithium also changes in presence of light, similar to that of hydrogen [160]. The overall effect of both hydrogen and lithium related defects and their changes in presence of light may cause strong potential fluctuations resulting in a change in $\sigma(T)$ and $S(T)$.

In the case of the relaxation from fast quenched state, the value of E_τ is small. Following the argument of lithium precipitation at the interfaces near room temperature [48], we expect that when these films are fast quenched from high temperatures, the frozen-in structure is likely to have a more uniform distribution of lithium than LS state. This may provide a smaller barrier for hydrogen diffusion and thus a smaller activation energy is seen for relaxation from fast quenched state.

6.4.2.e Relationship Between σ_0 and E_σ : Meyer–Neldel Rule

Fig. 6.8 shows the $\log \sigma_0$ vs. E_σ curve for all a-Si:H films (undoped, P-doped and Li-doped) in slow cooled and metastable state (both thermal and light induced). It is evident that all the points are scattered around a straight line

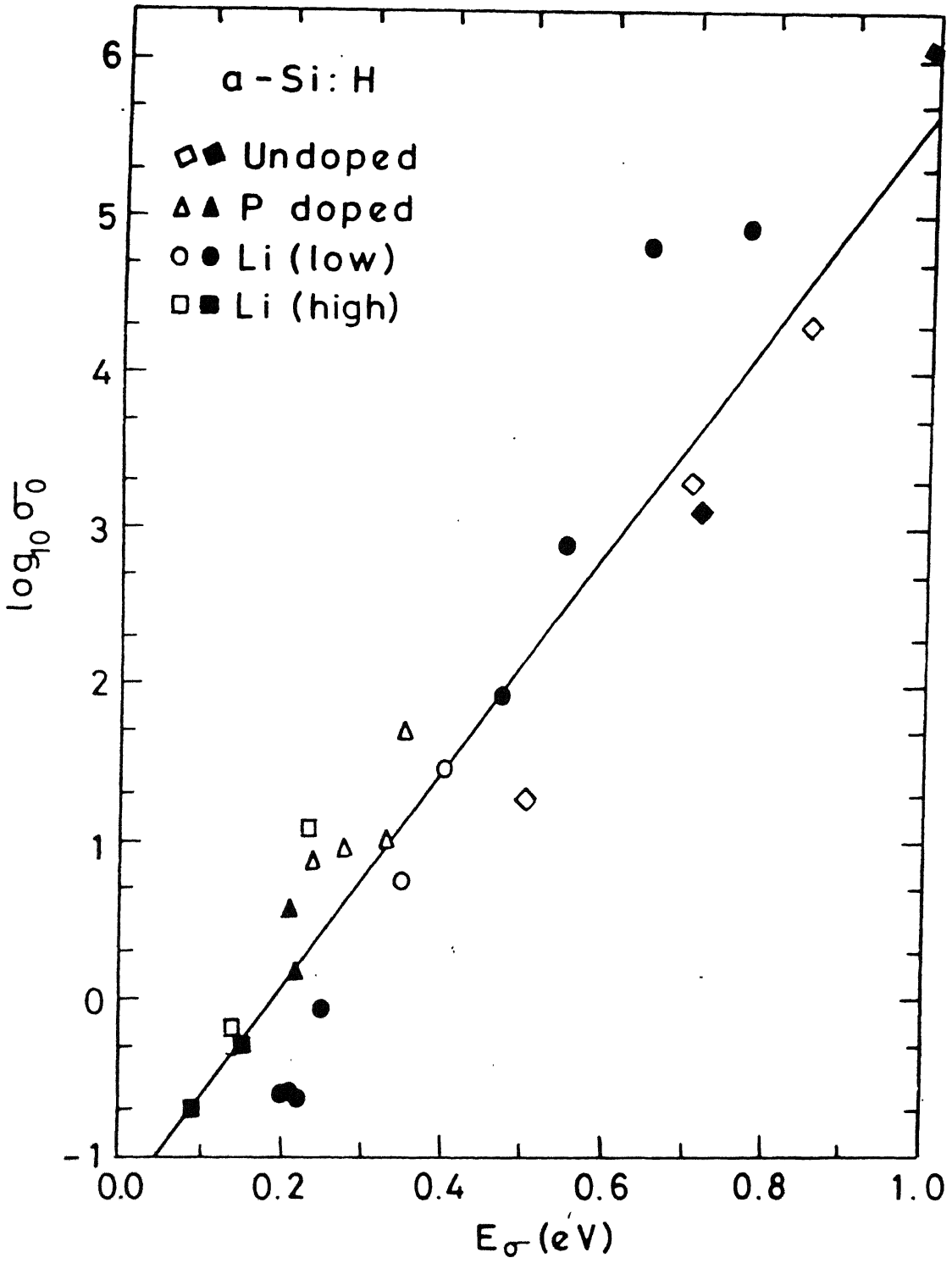

Figure 6.8: $\log \sigma_0$ vs. E_σ for a-Si:H films in slow cooled (empty symbols) and metastable (filled symbols) states.

$$\log \sigma_0 = \log \sigma_{00} + E_\sigma / E_0$$

with $\sigma_{00} = 0.05\,\Omega^{-1}\,cm^{-1}$ and $E_0 \approx 0.05eV$ and obey the empirical Meyer-Neldel (M-N) rule [158]. Similar relationship is reported for undoped, doped and compensated a-Si:H films in the slow cooled state [52]. The M-N rule has been attributed to the following

1. the presence of heterogeneities [161]
2. the temperature dependence of Fermi level [162–164]
3. the temperature dependence of mobility edges [165].

It has been shown that temperature dependence of mobility edge cannot account for the M-N rule [166]. The temperature dependence of Fermi level, however, seems to be responsible for the observed M-N rule [163,164]. The large variation of σ_o is ascribed to the effects that do not alter the transport path [52]. Our results on conductivity and thermopower in slow cooled and metastable states suggest that the function $Q(T)$ does not change upon the fast quenching. However, after light soaking the Li-doped a-Si:H, potential fluctuations change. The M-N rule in this case can be ascribed due to the temperature dependence of Fermi level and the density of states distribution which control the position of E_f.

It has been observed that the steady state photoconductivity σ_{ph} is not a single valued function of dangling bond defect concentration [104]. The decrease in σ_{ph} of a-Si:H is much more by the light exposure than by the same number of native defects as that produced by the light exposure [105]. Further, the experimental observations such as an increase in Si-H stretching mode at wave number $2000cm^{-1}$ [53], a reversible shift of about 0.1eV of the Si 2p X–ray photoelectron spectroscopy to lower binding energy [106], changes in 1/f noise spectrum of a-Si:H [107] and in proton NMR dipolar spin lattice relaxation time [108] also can not be explained by a simple increase in dangling bond defects but require some additional changes in structure of a-Si:H upon light soaking.

A change in structure upon FQ has not been directly observed so far. However, it is possible that these are too small to be detected easily. Furthermore, it is also possible that the distribution and bonding of hydrogen after fast quenching may be different from that obtained after light soaking.

From the above discussion, it is clear that fast quenching and light soaking affect the properties of a-Si:H differently. Fast quenching does not change the magnitude of potential fluctuations in the material and the observed changes in the electrical properties are due to a shift in E_f arising from a change in occupancy of the density of states. Light soaking, in addition to a change in the density of states, changes the magnitude of potential fluctuations. Higher activation energy for relaxation from LS state may be associated with the change in potential fluctuations. Furthermore, the M-N relationship between ν vs. E_τ and σ_o vs E_σ suggest that these metastabilities do not a)lter the transport path and are related to disorder in a-Si:H.

Chapter 7

Conclusions

The aim of the present study is to understand the thermal and light induced metastabilities in a-Si:H. So far numerous studies have been done, but the origin of these still remains unclear. After fast quenching or light soaking, the original state can not be recovered by IR quenching but only annealing at elevated temperatures brings the original state back. This suggests that some atomic movement and structural changes are associated with these metastabilities.

We have investigated the effect of fast quenching (FQ) and light soaking (LS) on conductivity (σ) and thermopower (S) of Li doped a-Si:H films (a-Si:H(Li)). In addition to a-Si:H(Li), we have also studied these metastabilities in undoped and P-doped a-Si:H (a-Si:H(P)).

Our results show that the effect of these metastabilities on a-Si:H(P) and a-Si:H(Li) are qualitatively similar. Further, we observe that the heterogeneities play an important role and that the fast quenching and light soaking affect a-Si:H in different ways. In particular, we find that FQ does not change the magnitude of the long range potential fluctuations, whereas, LS enhances them. In the following, we summarize briefly our results and indicate how we arrive at these and other conclusions.

In undoped a-Si:H, we observe that light soaking decreases the dark and photoconductivity (σ and σ_{ph}). The decrease in σ is accompanied by an increase in the activation energy (E_σ). Upon fast quenching, undoped a-Si:H films do not show any appreciable change in σ, however, a small decrease in σ_{ph} is observed. The changes are reversible and annealing at elevated temperatures brings the original state back. A decrease in σ_{ph} after FQ and LS, suggests that density of defects (Si_3^0) have increased in both the cases. However, the changes introduced by fast quenching are negligibly small. The results are in good agreement with the published work [10,41] and can be explained by any of the several models proposed by others (For details on some of these, please see Sec. 3.1.1). A possible mechanism for the increase in the density of Si_3^0 is the breaking of weak Si–Si bonds (Sec. 3.1.1.a). Since Si atoms are unlikely to move, it is believed that the stabilization of these defects is assisted by the movement of hydrogen [26,129].

In case of a-Si:H(P), we observe an increase in σ below the equilibration temperature T_E upon fast quenching. However, for $T \geq T_E$, $\sigma(T)$ is unique. The isothermal relaxation studies from FQ state show that the relaxation follows a stretched exponential and is thermally activated. The behaviour resembles the properties of a glass [29], where T_E plays the role of the glass transition temperature T_g. The metastabilities and thermal equilibrium in these films can be explained by the dispersive diffusion of hydrogen in a-Si:H (Hydrogen Glass Model, Sec. 3.4) [30]. These observations also agree with the reports in the literature [16].

Thermopower (S) measurements on a-Si:H(P) show that the conduction is by the electrons in the extended band. We find that E_σ and E_S (E_S is the slope of S vs. $1/T$ curve) are different. Analysis of the data, following Overhof and Beyer [72] indicates that the presence of the long range potential fluctuations in these films can explain our results. The potential fluctuations may be present because of the heterogeneities [56], such as, inhomogeneous distribution of hydrogen and charged donors. The slope E_Q of Q vs. $1/T$ is a measure of the potential fluctuations [72].

The function $Q = \ln\sigma + eS/k$ is independent of the position of the Fermi level and thus a change in σ or S due to the position of E_f is not reflected in $Q(T)$. However, any change in structure giving rise to the long range potential fluctuations will reveal itself in Q [52].

A change in S and E_S in FQ state is observed for the P-doped samples under the present investigation, however, no change in Q or E_Q ($E_Q = E_\sigma - E_S$) is found. The results suggest that fast quenching does not change the potential fluctuations in a-Si:H(P).

Our P-doped films do not show any measurable change in σ or S when subjected to light soaking. Reports in literature, however, find a decrease in σ and S after light soaking is reported for a-Si:H films with low P concentrations [154]. It may appear that the absence of any effect of light soaking on our a-Si:H(P) is at variance with the published work. However, we note that the effect decreases with the increasing doping concentrations [150] and has been associated with a higher defect density in heavily doped films. Therefore, small differences in the preparation conditions, which might yield films with different density of states, may account for this apparent discrepancy.

Now we summarize our findings on lithium doped a-Si:H films, which exhibit both thermal and light induced metastabilities. Fast quenching from high temperatures increases conductivity of these films below T_E. The metastable state, so obtained, relaxes back to the annealed state following a stretched exponential and a thermally activated relaxation time τ. For $T \geq T_E$, $\sigma(T)$ is unique and these films appear to be in thermal equilibrium. These observations are in qualitative agreement with the P-doped a-Si:H. When these films are light soaked, a new metastable state with a lower conductivity is obtained. The LS state is reversible and can be annealed at high temperatures. A similar light soaking effect is reported in literature for a-Si:H(P) [15]. The metastable state obtained after light soaking also relaxes following a stretched exponential. Both thermal and light induced changes decrease as Li concentration is increased. Further, the relaxation time $\tau(T)$ and equilibrium

temperature T depend upon the Li concentrations. T_E is lower for a-Si:H films with higher concentration of lithium. These observations show that the thermal induced and the light induced effects in a-Si:H(Li) are similar to a-Si:H(P). This suggests that the models used to understand the thermal and light induced metastabilities in a-Si:H(P) can also explain our results on a-Si:H(Li).

Let us now compare the FQ and LS metastablities. A notable observation for our lithium doped a-Si:H is that T_E is same for all the metastable states. Further, both FQ and LS states relax following a stretched exponential. At first sight, these observations may tempt one to believe that all the metastable states are equivalent and a similar mechanism may be operative in all cases. However, a closer look shows that the parameters β, τ are different for the relaxation from FQ and LS states. Further, the light soaked state relaxes slowly with a higher activation energy E_τ as compared to the FQ state. The thermal induced metastability has been explained in terms of the Hydrogen Glass model [30], which involves movement of hydrogen in a rigid Si matrix. It has been proposed that light soaking causes breaking of weak bonds, but movement of hydrogen to the appropriate sites makes these changes difficult to anneal near room temperature [26]. If movement of hydrogen is taken to be responsible for both fast quenching and light soaking effects, it is difficult to reconcile the observed difference between E_τ values for the two cases. In particular, the higher value of E_τ for the LS state suggests that higher barriers are encountered during relaxation from the LS state than from the FQ state. Therefore, even if the two metastabilities are caused by the movement of hydrogen, the structural and electronic changes in case of FQ must differ from those in case of LS. This is also supported by the observation that in our a-Si:H(Li) films FQ increases σ, whereas, LS decreases it.

The difference between FQ and LS states is quite pronounced in the thermopower (S) measurements also. $S(T)$ changes after fast quenching and light soaking. For a-Si:H(Li), Q does not change upon fast quenching and is the same as in the slow

cooled state. The slope E_Q is nearly zero in both SC and FQ states. On the other hand, light soaking causes an increase in E_Q. These results suggest that in a-Si:H(Li), fast quenching does not change the magnitude of the potential fluctuations, whereas, light soaking enhances them. We know that hydrogen is distributed non-uniformly in a-Si:H in dilute and clustered phases [167], which may result in a spatial variation of the gap giving rise to the potential fluctuations in the material. When these films are exposed to light, the trapping and recombination kinetics in the two phases will be different. The photoexcited electron and holes tend to drift to the regions where mobility gap is narrower and more recombination may occur in these regions [168]. This may increase the inhomogeneities of the defect centers which in turn may enhance the potential fluctuations. Thus light soaking appears to be related to the inhomogeneities present in a-Si:H.

Further, light soaking seems to be able to change the long range potential fluctuations significantly. This is consistent with the suggestions by Fritzsce [54], who proposed photoinduced changes in structure of a-Si:H in addition to the dangling bonds, in order to explain several experimental observations, which are not correlated with the concentration of the dangling bond defects.

Unsolved Problems and Scope for Future work

Amorphous semiconductors can exist in several disordered configurations, which have almost similar free energies but are separated by energy barriers. Application of external perturbations, e.g., light soaking or thermal quenching from a high temperature might induce transitions from one metastable state to another. In this sense, all disordered materials are likely to show the type of metastabilities, discussed here. Indeed, chalcogenide glasses show a shift of absorption edge [169] and also a change in conductivity upon light soaking. A change in structure of chalcogenides after exposing them to light is also reported [170]. However, no effects of fast quenching on the electronic properties of chalcogenide glasses have been reported, so far.

Our preliminary investigations on a-Ge Se bulk glasses and thin films [171] indicate that the thermal induced metastability is absent in these glasses. This is surprising, since the quenching effect in a-Si:H is explained in terms of Hydrogen Glass model (Sec. 3.4), the effect seems to be absent in these glasses, where glass transition is easily observed. This may mean that one needs a mobile species (e.g. hydrogen in a-Si:H) in a rigid network (e.g. Si), in order to see quenching effects. In any case, further investigations in this direction are needed to confirm the validity of the Hydrogen Glass model.

Our studies show that the hydrogen plays an important role in the observed metastabilities in a-Si:H. Also, the role played by hydrogen is amply illustrated by the various studies. One may therefore ask whether the instabilities can be reduced or eliminated, if hydrogen is replaced by some other less diffusive bond terminator [172]. Investigations on amorphous silicon films with fluorine replacing hydrogen may answer this question [173]. It is not clear whether the hydrogen in the dilute or clustered phase is responsible for the metastabilities and thermal equilibration behaviour.

It has been reported that the hydrogen diffusion constant increases in presence of light [160]. However, no report is available, which illustrates whether the enhanced hydrogen diffusion during light soaking will be different in the two phases and result in a more inhomogeneous distribution of hydrogen. By exposing a-Si:H films to different dosages of ion bombardment, it may be possible to obtain films with different disorder but the same hydrogen and doping concentrations. Study of these films might be useful in understanding the role of disorder in these metastabilities.

More experiments are desirable to verify our claim that LS changes the long range potential fluctuations, whereas, FQ does not. For this it will be necessary to find other ways of measuring potential fluctuations in a-Si:H. The observed differences between CPM and PDS [174] might arise from these potential fluctuations [175]. However,

more theoretical and experimental work is needed to correlate this differenceto the potential fluctuations both qualitatively and quantitatively.

A stretched exponential time dependence of light induced defect creation has been assigned to the movement of hydrogen [26]. It is proposed [109] that the illumination only triggers the breakage of weak Si–Si bonds in the neighbourhood of Si–H–Si bonds. This process requires only 0.04eV energy. Hydrogen hops from one site to another and the process continues [109]. If it is so, a source of this energy, for e.g. the ultrasonic beam, will also lead to a similar behaviour and should be experimentally observable.

It is proposed that a part of energy released during the recombination process creates the dangling bonds. The rest of it is dissipated locally and may give rise to the other photoinduced structural changes [54]. the above hypothesis can be checked if the similar structural changes are observed by supplying a high energy to the sample. which does not cause the effusion of hydrogen or creation of the dangling bonds, for e.g. a very short laser pulse, whose energy matches the vibrational mode and hence does not create an electron-hole pair or dangling bonds [54].

Clearly, a lot of exciting physics concerning these metastabilities remains to be explored, both experimentally as well as theoretically.

Bibl iography

[1] A. catalano, R.R. Arya, B. Fieselimann, B. Goldstein, and J. Newtone. *J. Non Cryst. Solids*, **115**, (1989), 14.

[2] P. G. LeComber. *J. Non Cryst. Solids*, **115**, (1989), 1.

[3] N. F. Mott and E. A. Davis. *Electronic Process in Non-Crystalline Materials*, Chapter 2 and 6. (Clarendon Press, Oxford, 2 edition, 1979).

[4] M.H. Cohen, H. Fritzsche, and S.R. Ovshinsky. *Phys. Rev. Lett.*, **22**, (1969), 1065.

[5] W. E. Spear and P. G. LeComber. *J. Non Cryst. Solids*, **8–10**, (1972), 727.

[6] W. E. Spear and P. G. LeComber. *Solid State Commn.*, **17**, (1975), 1193.

[7] W.E. Spear and P.G. LeComber. *Philos. Mag.*, **33**,(1976), 935.

[8] R. A. Street. *Phys. Rev. Lett.*, **49**, (1982) 1187.

[9] H. Overhof and P. Thomas. *Electronic Transport in Hydrogenated Amorphous Semiconductors*, volume 114. (Springer–Verlag, Berlin, 1989).

[10] D. L.Staebler and C. R. Wronski. *Appl. Phys. Lett.*, **31**, (1977), 292.

[11] U. Voget-Grote, W. Kummerle, R. Fischer, and J. Stuke. *Philos. Mag.*, **B 41**, (1980), 127.

[12] U. Schneider and B. Schroder. Amorphous silicon and related materials. in Fritzsche [176], page 687.

[13] R. A. Street, D. K. Biegelson, and J. Stuke. *Philos. Mag.*, **B 40**, (1979), 451.

[14] R. A. Street, J. Kakalios, and T. M. Hayes. *Phys. Rev.*, **B 34**, (1986), 3030.

[15] D. L.Staebler and C. R. Wronski. *J. Appl. Phys.*, **51**, (1980), 3262.

[16] R. A. Street, J. Kakalios, C. C. Tsai, and T. M. Hayes. *Phys. Rev.*, **B 35**, (1987), 1316.

[17] D. G. Ast and M. H. Brodsky. in *Proc. of the 14th Intl. Conf. on the Physics of Semiconductors*, ed. B. L. H. Wilson, (Inst. Phy. Conf. Ser. No. 43, IOP Bristol, 1979), 1159.

[18] S. M. Pietruszko. *J. Non Cryst. Solids*, **164–166**, (1993), 255.

[19] M. Vanecek, J. Fric, R. S. Crandall, and A. H. Mahan. *J. Non Cryst. Solids*, **164–166**, (1993), 335.

[20] R. Meaudre, M. Meaudre, and J. Chanel. *Phys. Rev.*, **B 43**, (1991), 9792.

[21] A.K. Sinha, P. Agarwal, S. Kumar, S.C. Agarwal, P.N. Dixit, O.S. Panwar, T. Seth, and R. Bhattacharya. in Lal [178], page 595.

[22] D. He, F. Zhang, W. Chen, and G. Ganguly. *J. Non Cryst. Solids*, **137–138**, (1991), 657.

[23] K. Eberhardt, M. Heintze, and G. H. Bauer. *J. Non Cryst. Solids*, **137–138**, (1991), 187.

[24] J. I. Pankove and J. E. Berkeyheiser. *Appl. Phys. Lett.*, **37**, (1980), 705.

[25] M. Stutzmann. *Philos. Mag.*, **B 56**, (1987), 63.

[26] M. Stutzmann, W. B. Jackson, and C. C. Tsai. *Phys. Rev.*, **B 32**, (1985), 23.

[27] Z. E. Smith and S. Wagner. *Phys. Rev.* **B 32**, (1985), 5510.

[28] D. Adler. *Solar Cells*, **9**, (1983), 133.

[29] S. R. Elliot. *Physics of Amorphous Materials*, (Longman Scientific and Technical, UK, 2 edition, 1990).

[30] J. Kakalios and W. B. Jackson. Amorphous silicon and related materials. in Fritzsche [176], page 207.

[31] L. Battezzati, F. Demichelis, C. F. Pirri, A. Tagliaferro, and E. Tresso. *J. Non Cryst. Solids*, **137–138**, (1991), 87.

[32] S. Matsuo, H. Nasu, C. Akamatsu, R. Hayshi, T. Imura, and Y. Osaka. *Jap. J. Appl. Phys.*, **27**, (1988), L132.

[33] R. A. Reimer, R. W. Vaughan, and J. C. Knights. *Phys. Rev. Lett.*, **44**, (1980), 193.

[34] K.K. Gleason, M.A. Petrich, and J.A. Reimer. *Phys. Rev.*, **B 36**, (1987), 3259.

[35] M.H. Brodsky. *Solid State Commun.*, **36**, (1980), 55.

[36] H. Fritzsche. *J. Non Cryst. Solids*, **6**, (1971), 49.

[37] P. Hari, P. C. Taylor, and R. A. Street. *J. Non Cryst. Solids*, **164–166**, (1993), 313.

[38] R. A. Street, C. C. Tsai, J. Kakalios, and W. B. Jackson. *Philos. Mag.*, **B 56**, (1987), 305.

[39] M. Kondo and K. Morigaki. *J. Non Cryst. Solids*, **137–138**, (1991), 247.

[40] Z. E. Smith, S. Aljishi, D. Slobodin, V. Chu, S. Wagner, P. M. Lenahan, R. R. Arya, and M. S. Bennett. *Phys. Rev. Lett.*, **57**, (1987), 2450.

[41] T. J. McMahon and R. Tsu. *Appl. Phys. Lett.*, **51**, (1987), 412.

[42] J. Kakalios and R.A. Street. *AIP Conference Proceedings*, **157**, (1987), 179.

[43] M. Stutzmann. *Phys. Rev.*, **B 35**, (1987), 9735.

[44] H. Okushi, R. Banerjee, T. Furai, and K. Tanaka. *J. Non Cryst. Solids*, **114**, (1989), 669.

[45] H. Okushi, R. Banerjee, and K. Tanaka. Amorphous silicon and related materials. in Fritzsche [176], page 657.

[46] T. M. Leen, J. D. Cohen, and A. V. Gelatos. *Mat. Res. Soc. Symp. Proc.*, **192**, (1990),707.

[47] R. Konenkamp and E. Wild. *J. Non Cryst. Solids*, **137–138**, (1991), 239.

[48] K. Winer and R. A. Street. *J. Appl. Phys.*, **65**, (1989), 2272.

[49] W. Beyer and R. Fischer. *Appl. Phys. Lett.*, **31**, (1977), 850.

[50] J. Takada and H. Fritzsche. *Phys. Rev.*, **B 36**, (1987), 1706.

[51] J. Takada and H. Fritzsche. *Phys. Rev.*, **B 36**, (1987), 1710.

[52] W. Beyer and H. Overhof. in Pankove [177], pages 258–305.

[53] Y. Zhao, D. Zhang, G. Kong, G. Pan, and X. Liao. *Phys. Rev. Lett.*, **74**, (1995), 558.

[54] H. Fritzsche. *Solid State Commn.*, **94**, (1995), 953.

[55] P. Nagels. in *Amorphous Semiconductors*, ed. M. H. Brodsky, (Springer Verlag, Berlin, 1979), 113-158.

[56] H. Fritzsche. *Solid State Commun.*, **9**, (1971), 1813.

[57] P. G. LeComber, D.I. Jones, and W. E. Spear. *Philos. Mag.*, **35**, (1977), 1173.

[58] M. Roilos. *Philos. Mag.*, **B 38**, (1978), 477.

[59] D.K.C. MacDonald. *Thermoelectricity.* (John-Wiley & Sons, New York, 1962).

[60] W. Beyer, A. Medeisis, and H. Mell. *Commun. Phy*, **2**, (1977), 21.

[61] W. E. Spear, D. Allan, P. G. LeComber, and A. Ghaith. *Philos. Mag.*, **B 42**, (1980), 419.

[62] D. A. Anderson and W. Paul. *Philos. Mag.*, **B 44**, (1981), 187.

[63] W. Beyer, H. Mell, and H. Overhof. In W. E. Spear, editor, *Proc. of 7 international Conference on Amorphous and Liquid Semiconductor*, CICL 1977, (1977), 328.

[64] D. A. Jones, P. G. LeComber, and W. E. Spear. *Philos. Mag.*, **36**, (1977), 541.

[65] D. A. Anderson and W. Paul. *Philos. Mag.*, **B 45**, (1982), 1.

[66] C. Tsang and R. A. Street. *Phys. Rev.*, **B 19**, (1979), 3027.

[67] H. Fritzsche. *Solar Energy Mater.*, **3**, (1980), 447.

[68] R. A. Street. *J. Non Cryst. Solids*, **77–78**, (1985), 1.

[69] R. A. Street. *Hydrogenated Amorphous Silicon.* (Cambridge University Press, 1991).

[70] G. Dohler. *Phys. Rev.*, **B 19**, (1979), 2083.

[71] W. Beyer, R. Fischer, and H. Overhof. *Philos. Mag.*, **B 39**, (1979), 205.

[72] H. Overhof and W. Beyer. *Philos. Mag.*, **B 43**, (1981), 433.

[73] H. Overhof and W. Beyer. *Philos. Mag.*, **B 47**, (1983), 377.

[74] J. C. Knights and R. A. Reimer. *Appl. Phys. Lett.*, **35**, (1979), 244.

[75] D. M. Goldie, W. E. Spear, and E. Z. Liu. *Philos. Mag.*, **B 62**, (1990), 509.

[76] J. A. Howard and R. A. Street. *Phys. Rev.*, **B 44**, (1991), 7935.

[77] J. M. Marshall, R. A. Street, and M. J. Thomson. *Phys. Rev.*, **B 29**, (1984), 2331.

[78] N. Hata and A. Matsuda. *J. Non Cryst. Solids*, **164–166**, (1993), 187.

[79] E. Andrianova, J. Gerdiskaya, Y. Roizin, and V. Sviridov. *J. Non Cryst. Solids*, **137–138**, (1991), 79.

[80] E. Esar. *J. Appl. Phys.*, **59**, (1986), 3508.

[81] D. Redfield. *Appl. Phys. Lett.*, **48**, (1986), 846.

[82] J. Kakalios and R. A. Street. in Fritzsche [176], page 165.

[83] W. M. Pontushka, W. E. Carlos, P. C. Taylor, and R. W. Griffith. *Phys. Rev.*, **B 25**, (1982), 4362.

[84] S. Guha, J. Yang, W. Czubatyi, S. J. Hudgens, and M. Hack. *Appl. Phys. Lett.*, **42**, (1982), 589.

[85] H. Pfleiderer, W. Kusian, and W. Krauhler. *Solid State Commun.*, **49**, (1984), 493.

[86] H. R. Park, J.Z. Liu, and S. Wagner. *Appl. Phys. Lett.*, **55**, (1989), 265.

[87] A. Skunamich, N. M. Johnson, and W. B. Jackson. *Phys. Rev.*, **B 31**, (1985), 2263.

[88] J. Kocka, M. Vanecek, J. Stuchlik, O. Stika, I. Kubelik, and A. Triska. in *Proc. of Intl. Conf. Amorphous Semiconductors*, ed. R. Grigorovici, (Bucharest, Romania, 1982) 150.

[89] F. Schauer and J. Kocka. *Philos. Mag.*, **B 52**, (1985), 125.

[90] D. S. Mishra. *Ph.D. Thesis.* I.I.T., Kanpur, 1984, (Unpublished).

[91] H. Dersch, J. Stuke, and J. Beichler. *Appl. Phys. Lett.*, **37**, (1980), 456.

[92] M. Tanielian, N.B. Goodman, and H. Fritzsche. *J. Phys. Colloq. Orsay, France*, **42(Suppl. 10)**, (1981), C4–375.

[93] S. Kumar and S. C. Agarwal. *Philos. Mag.*, **B 49**, (1984), 453.

[94] B. Aker and H. Fritzsche. *J. Appl. Phys.*, **54**, (1983), 6628.

[95] K. Zellama, J. D. Cohen, and T. Walsh. *J. Non Cryst. Solids*, **77–78**, (1985), 381.

[96] A. Glade, J. Beichler, and H. Mell. *J. Non Cryst. Solids*, **77–78**, (1985), 397.

[97] S. Guha, C. Y. Huang, and S. J. Hudgens. *Phys. Rev.*, **B 29**, (1984), 5995.

[98] S. Guha, C. Y. Huang, S. J. Hudgens, and J. S. Payson. *J. Non Cryst. Solids*, **66**, (1984), 65.

[99] S. Guha. *J. Non Cryst. Solids*, **77–78**, (1985), 1451.

[100] D. Han and H. Fritzsche. *J. Non Cryst. Solids*, **59–60**, (1983), 397.

[101] K. Morigaki and F. Yonezawa. *J. Non Cryst. Solids*, **164–166**, (1993), 215.

[102] H. Hikita, K. Takeda, Y. Kimura, H. Yokomichi, and K. Morigaki. *J. Non Cryst. Solids*, **164–166**, (1993), 219.

[103] K. Shepard, Z. E. Smith, S. Aljishi, and S. Wagner. *Mat. Res. Soc. Symp. Proc.*, **118**, (1988), 147.

[104] P. Strandins and H. Fritzsche. *Philos. Mag.*, **B 69**, (1994), 121.

[105] M. Tran, H. Fritzsche, and P. Strandins. *Mat. Res. Soc. Symp. Proc.*, **297**, (1993), 195.

[106] D.P. Masson, A. Ouhlal, and A. Yelon. *J. Non Cryst. Solids*, In Press, 1995.

[107] J. Fan and J. Kakalios. *Philos. Mag.*, **B 69**, (1994), 595.

[108] P. Hari, P. C. Taylor, and R. A. Street. *Mat. Res. Soc. Symp. Proc.*, **336**, (1994), page 329.

[109] R.Prasad. Private Communication.

[110] G. Mullar, S. Kalbitizer, and H. Mansperger. *Appl. Phys.*, **A 39**, (1986), 243.

[111] G. Mullar. *Appl. Phys.*, **A 45**, (1988), 41.

[112] H. M. Branz and M. Silver. *Mat. Res. Soc. Symp. Proc.*, **192**, (1990), 261.

[113] T. Shimuzu. *J. Non Cryst. Solids*, **164–166**, (1993), 163.

[114] T. Shimizu, M. Kumeda, A. Morimoto, H. Yokomichi, and N. Ishii. *J. Non Cryst. Solids*, **77–78**, (1985), 377.

[115] N. Isoya, S. Yamasaki, H. Okushi, A. Matsuda, and K. Tanaka. *Phys. Rev.*, **B 47**, (1993), 7013.

[116] Q. Zhang, M. Kumeda, and T. Shimizu. *Jpn. J. Appl. Phys.*, **32**, (1993), L371.

[117] T. Shimuzu, M. Matsumoto, M. Yoshita, M. Iwami, A. Morimoto, and M. Kumeda. *J. Non Cryst. Solids*, **137–138**, (1991), 391.

[118] R. A. Street. *Philos. Mag.*, **B 60**, (1989), 213.

[119] S.C. Agarwal, J.S. Payson, and S. Guha. *Phys. Rev.*, **B 36**, (1987), 9348.

[120] R. Meaudre, P. Jenson, and M. Meaudre. *Phys. Rev.*, **B 38**, (1988), 12499.

[121] S. Kumar, P.N. Dixit, O.S. Panwar, T. Seth, and R. Bhattacharya. in Lal [178], page 598.

[122] R. A. Street, M. Hack, and W. B. Jackson. *Phys. Rev.*, **B 37**, (1988), 4209.

[123] J. Kakalios and R. A. Street. *J. Non Cryst. Solids*, **97–98**, (1987), 767.

[124] M. Meaudre and R. Meaudre. *Phys. Rev.*, **B 45**, (1992), 4524.

[125] R. A. Street, J. Kakalios, and M. Hack. *Phys. Rev*, **B 38**, (1988), 5603.

[126] Z E. Smith and S. Wagner. *Phys. Rev.*, **B 32**, (1985), 5510.

[127] W. B. Jackson and J. Kakalios. *Phys. Rev.*, **B 37**, (1988), 1020.

[128] M. Meaudre, R. Meaudre, and P. Jenson. *J. Non Cryst. Solids*, **122**, (1990), 312.

[129] R. A. Street and K. Winer. *Phys. Rev.*, **B 40**, (1989), 6236.

[130] W. B. Jackson. *Phys. Rev.*, **B 38**, (1988), 3595.

[131] R. S. Crandell. *Phys. Rev.*, **B 43**, (1991), 4057.

[132] J. Kakalios, R. A. Street, and W. B. Jackson. *Phys. Rev. Lett.*, **59**, (1987), 1037.

[133] D. E. Carlson and C. W. Magee. *Appl. Phys. Lett.*, **33**, (1978), 81.

[134] H. Scher and E.W. Montroll. *Phys. Rev.*, **B 12**, (1975), 2455.

[135] M. Shlesinger and E.W. Montroll. *Proc. of Natl. Acad. Sci. (USA)*, (1984), 1280.

[136] R. Meaudre and M. Meaudre. *Phys. Rev.*, **B 45**, (1992), 12134.

[137] M. Stutzmann. *Appl. Phys. Lett.*, **56**, (1990), 2313.

[138] D. Redfield and R. H. Bube. *Appl. Phys. Lett.*, **54**, (1989), 1037.

[139] D. Redfield and R. H. Bube. *J. Appl. Phys.*, **66**, (1989), 820.

[140] D. Redfield. *Appl. Phys. Lett.*, **54**, (1989), 398.

[141] S. R. Dhariwal and B. M. Deoraj. *J. Appl. Phys.*, **71**, (1992), 4196.

[142] I. Abdulhalim. *J. Appl. Phys.*, **77**, (1995), 1897.

[143] G. Schumm. *Appl. Phys. Lett.*, **66**, (1995), 2706.

[144] A. Matsuda and N.Hata. In K. Tanaka, editor, *Glow-Discharge Hydrogenated Amorphous Silicon*, (KTK Scientific Publishers, Tokyo, 1989), 9-38.

[145] Shailendra Kumar. *Ph.D. Thesis.* I.I.T., Kanpur, 1984, (Unpublished).

[146] R. Swanpole. *J.Phys.*, **E 16**, (1983), 1214.

[147] J. Tauc. In J. Tauc, editor, *Amorphous and Liquid Semiconductors*, Chapter 4. (Plenum Press, New York, 1974).

[148] Pankaj Khandelwal. M.tech. thesis. I.I.T., Kanpur, 1994, (Unpublished).

[149] K. Pierz, W. Fuh, and H. Mell. *J. Non Cryst. Solids*, **114**, (1989), 651.

[150] C.R. Wronski. in Pankove [177], pages 347–374.

[151] Anil K. Sinha. I.I.T. Kanpur, Private Communication.

[152] C. R. Wronski and R. Daniel. *Phys. Rev.*, **B 23**, (1980), 794.

[153] W. B. Jackson and J. Kakalios. Amorphous silicon and related materials. In Fritzsche [176], page 247.

[154] D. Hauschildt, W. Fuhs, and H. Mell. *Phys. Stat. Solidi*, **B 111**, (1982), 171.

[155] W.B. Jackson, J.M. Marshall, and D.M. Moyer. *Phys. Rev.*, **B 39**, (1989), 1164.

[156] X.-M. Deng and H. Fritzsche. *Phys. Rev.*, **B 36**, (1987), 9738.

[157] H. Gleskova, M. Nakata, and S. Wagner. *Mat. Res. Soc. Symp. Proc.*, **336**, (1994), 245.

[158] W. Meyer and H. Neldel. *Z. Tech. Phys.*, **12**, (1937), 588.

[159] H. Antoniadis, Q. Wang, E.A. Schiff, and S. Guha. *Mat. Res. Soc. Symp. Proc.*, **219**, (1992), 33.

[160] P. V. Santos, N. M. Johnson, and R. A. Street. *Phys. Rev. Lett.*, **67**, (1991), 2686.

[161] H. Fritzsche and M. Taniellian. in *AIP Conference Proceedings* (1981), eds. D. K. Biegelsen and J. C. Knights, p318.

[162] W. Beyer and H. Overhof. *J. Non Cryst. Solids*, **59–60**, (1983) 301.

[163] K. L. Narsimhan. *Pramana: J. Phys.*, **34**, (1990), 561.

[164] X. Wang, Y. Bar-Yam, D. Adler, and J. D. Joannopoulos. *Phys. Rev.*, **B 38**, (1988), 1601.

[165] W. E. Spear, D. Allan, P. G. LeComber, and A. Ghaith. *J. Non Cryst. Solids*, **35–36**, (1980), 357.

[166] D. R. Bapat, K.L. Narsimhan, and R. Kuchibotla. *Philos. Mag.*, **B 56**, (1987), 71.

[167] J.A. Reimer, R.W. Vaughan, and J.C.Knights. *Phys. Rev.*, **B 23**, (1981), 2567.

[168] S.C. Agarwal. *Bull. of Mater. Science*, In press, 1995.

[169] G. Pfeiller, M.A. Paesler, and S.C. Agarwal. *J. Non Cryst. Solids*, **130**, (1991), 111.

[170] S. Rajgopalan, K.S. Harshvardhan, L.K. Malhotra, and K.L. Chopra. *J. Non Cryst. Solids*, **50**, (1982), 29.

[171] P. Agarwal, S.C. Agarwal, E. Bhattacharya, S. Kumar, and A. Kumar. *Indian J. of Pure and Appl. Phys.*, **31**, (1993), 367.

[172] H. Fritzsche. in *Physics and Application of Semiconductors* ed. F. Demichelis, (World Scientific, Singapore, 1988).

[173] A. Madan, S.R. Ovshinsky, and E.Benn. *Philos. Mag.*, **B 40**, (1977), 259.

[174] Z E. Smith, V. Chu, K. Shepard, D. Slobodin, J. Kolodzey, S. Wagner, and T.L. Chu. *Appl. Phys. Lett.*, **50**, (1987), 1521.

[175] S.C. Agarwal. Private Communication.

[176] H. Fritzsche, editor. *Amorphous Silicon and Related Materials*, volume 1A. (World Scientific, Singapore, 1989).

[177] J. I. Pankove, editor. *Semiconductors and Semimetals: Hydrogenated Amorphous Silicon*, volume 21 C. (Academic Press Inc., 1984).

[178] Krishan Lal, editor. *Proc. of 7th International Conf. on Phys. of Semicond. Devices.* (Narosha Publishing House, New Delni, 1993).

List of Publications

In Journals

1. **Search For Thermal Metastability in Chalcogenide Glasses.**
   Pratima Agarwal, S. C. Agarwal, E. Bhattacharya, S. Kumar, and A. Kumar. Indian Jour. of Pure and Applied Physics. **31**, (1993) 367-370

In Conferences

1. **Search for Thermal Metastability in Chalcogenide Glasses.**
   Pratima Agarwal, S. C. Agarwal, E. Bhattacharya, S. Kumar, and A. Kumar, 2^{nd} *National Workshop on Disorderd Systems. H. B. T. I. Kanpur* (Dec 1991).
2. **Thermal Metastability in Ion-Bombarded a-Si:H.**
   Pratima Agarwal, S. C. Agarwal, E. Bhattacharya, and P. N. Dixit. S. S. F Symposium (DAE) **34C**, (1991) 222, BHU Varanasi.
3. **Ambipolar Diffusion Length in Amorphous Hydrogenated Silicon**
   E. Bhattacharya, G. Ravindra Kumar, and Pratima agarwal. 6^{th} *Interna tional Photovoltaic Science and Engineering conference*, New Delhi, India (1992) 355.
4. **Metastabilities in Lithium Doped a-Si:H.**
   P. Agarwal, S. K. Tripathi, S. Kumar, and S. C. Agarwal. 15^{th} *International Conference on Amorphous Semiconductors (ICAS-15 Cambridge, U. K.* , (1993), (Accepted).
5. **Effect of Quenching on Thermo-Electric Power of a-Si:H.**
   Pratima Agarwal, P. Manoravi, P. N. Dixit, S. Kumar, and S. C. Agarwal. 7^{th} *International Conference on Physics of Semiconducto Devices* ed. Krishan Lal, New Delhi, India. (1993) 604.
6. **Metastabilities in Undoped a-Si_x:Ge_{1-x}:H Alloys.**
   A. K. Sinha, P. Agarwal, S. Kumar, S. C. Agarwal, P. N. Dixit, O. S. Panwa T. Seth, and R. N. Bhattacharya. *ibid.* (1993) 595.

7. **Thermal and Light Induced Metastabilities in Lithium Doped a-Si:H.**
   Pratima Agarwal, S. K. Tripathi, S. Kumar, and S. C. Agarwal, *S. S. P. Symposium (DAE)*, **36C**, (1993) 84. BARC Bombay.

8. **Comparison of Metastabilities in Substitutionally and Interstitially doped a-Si:H.**
   Anil K. Sinha, Pratima Agarwal, S. Kumar and S. C. Agarwal *Meeting on Recent Developments in Solid State Materials Related to Devices*, (Mar.1994), Univ. of Roorkee, Roorkee (U. P.)

9. **Metastable Changes in Conductivity and Thermopower of a-Si:H(Li).**
   Pratima Agarwal, S. K. Tripathi, S. Kumar and S. C. Agarwal *S. S. P. Symposium (DAE)*, **37C**, (1994). Univ. Of Raj. Jaipur.

10. **Comparison of Thermally Induced Metastabilities in Interstitially and Substitutionally Doped n-type a-Si:H.**
    Pratima Agarwal, S. K. Tripathi, S. Kumar and S. C. Agarwal *National Conference on Thin Film Processing and Applications* (Jan 23-24, 1995), P-25, S. V. University, Tirupati.

11. **Comparison of Thermal and Light Induced Metastabilities in Lithium Doped a-Si:H.**
    Pratima Agarwal, Satyendra Kumar and S. C. Agarwal
    16^{th} *International Conference on Amorphous Semiconductors (ICAS-16)* Kobe, Japan. (Sept. 1995), (Accepted, Paper submitted)

12. **Effect of Light Soaking on Fast Quenched a-Si:H.**
    Pratima Agarwal, S. K. Tripathi, S. Kumar and S. C. Agarwal
    8^{th} *International Conference on Physics of Semiconductor Devices* NPL New Delhi, India. (Dec.1995). (Accepted)

PHY-1995-D-AGA-THE